AD-A113 813 IIT RESEARCH INST CHICAGO IL F/G 13/9
WEAR AND CORROSION OF COMPONENTS UNDER STRESS AND SUBJECTED TO --ETC(U)
FEB 82 K Y KIM, S BHATTACHARYYA N62269-79-C-0702
UNCLASSIFIED IITRI-M06060-8 NADC-79137-60 NL

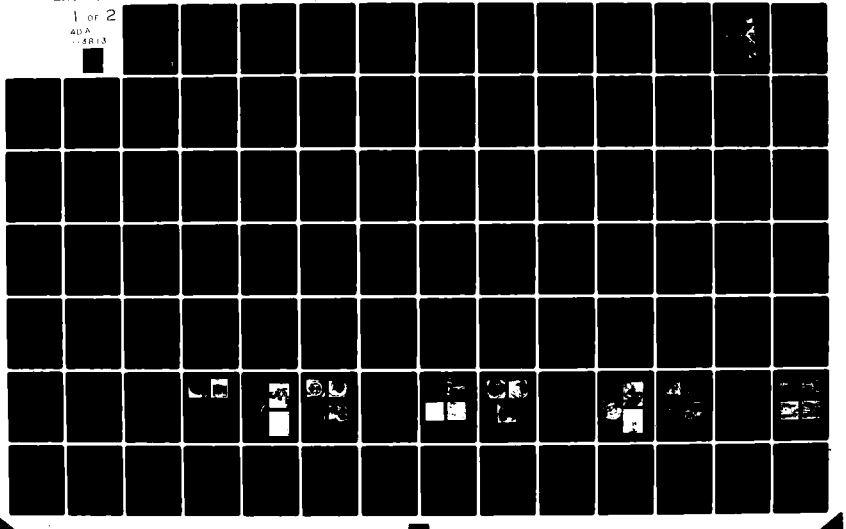

(12)

REPORT NO. NADC-79137-60

WEAR AND CORROSION OF COMPONENTS UNDER STRESS AND SUBJECTED TO MOTION

K. Y. KIM AND S. BHATTACHARYYA
I.I.T. RESEARCH INSTITUTE
10 West 35th Street
Chicago, Illinois 60616

5 February 1982

INTERIM REPORT
TASK AREA WR02201-001
Work Unit No. DG212

APPROVED FOR PUBLIC RELEASE; DISTRIBUTION UNLIMITED

Prepared for
NAVAL AIR DEVELOPMENT CENTER
Aircraft and Crew Systems Technology Directorate
Warminster, Pennsylvania 18974

NOTICES

REPORT NUMBERING SYSTEM – The numbering of technical project reports issued by the Naval Air Development Center is arranged for specific identification purposes. Each number consists of the Center acronym, the calendar year in which the number was assigned, the sequence number of the report within the specific calendar year, and the official 2-digit correspondence code of the Command Office or the Functional Directorate responsible for the report. For example: Report No. NADC-78015-20 indicates the fifteenth Center report for the year 1978, and prepared by the Systems Directorate. The numerical codes are as follows:

CODE	OFFICE OR DIRECTORATE
00	Commander, Naval Air Development Center
01	Technical Director, Naval Air Development Center
02	Comptroller
10	Directorate Command Projects
20	Systems Directorate
30	Sensors & Avionics Technology Directorate
40	Communication & Navigation Technology Directorate
50	Software Computer Directorate
60	Aircraft & Crew Systems Technology Directorate
70	Planning Assessment Resources
80	Engineering Support Group

PRODUCT ENDORSEMENT – The discussion or instructions concerning commercial products herein do not constitute an endorsement by the Government nor do they convey or imply the license or right to use such products.

APPROVED BY: J. R. Woods **DATE:** 2/5/82

J. R. WOODS
CDR, USN

UNCLASSIFIED

SECURITY CLASSIFICATION OF THIS PAGE (When Data Entered)

REPORT DOCUMENTATION PAGE	READ INSTRUCTIONS BEFORE COMPLETING FORM
1. REPORT NUMBER: NADC-79137-60	2. GOVT ACCESSION NO.: AD-A113 813
3. RECIPIENT'S CATALOG NUMBER:	
4. TITLE (and Subtitle): Wear and Corrosion of Components Under Stress and Subjected to Motion	5. TYPE OF REPORT & PERIOD COVERED: Interim 14 Sept. 1979-14 Sept. 1981
	6. PERFORMING ORG. REPORT NUMBER: IITRI-M06060-8
7. AUTHOR(s): K. Y. Kim and S. Bhattacharyya	8. CONTRACT OR GRANT NUMBER(s): N62269-79-C-0702
9. PERFORMING ORGANIZATION NAME AND ADDRESS: IIT Research Institute, 10 West 35 Street, Chicago, IL 60616	10. PROGRAM ELEMENT, PROJECT, TASK AREA & WORK UNIT NUMBERS: TASK AREA WR02201-001, Work Unit No. DG212
11. CONTROLLING OFFICE NAME AND ADDRESS: Naval Air Development Center, Aircraft & Crew Systems Technology Directorate, Warminster, PA 18974	12. REPORT DATE: 5 February 1982
	13. NUMBER OF PAGES: 99
14. MONITORING AGENCY NAME & ADDRESS(if different from Controlling Office)	15. SECURITY CLASS. (of this report): UNCLASSIFIED
	15a. DECLASSIFICATION/DOWNGRADING SCHEDULE

16. DISTRIBUTION STATEMENT (of this Report)

Approved for public release; distribution unlimited.

17. DISTRIBUTION STATEMENT (of the abstract entered in Block 20, if different from Report)

18. SUPPLEMENTARY NOTES

19. KEY WORDS (Continue on reverse side if necessary and identify by block number)

Rubbing surfaces, wear, corrosion, electrochemical polarization, open-circuit potential, active, passive, M2, 52100, 304 SS, Armco Iron, NaCl, $Na_2Cr_2O_7$, Na_2MoO_4.

20. ABSTRACT (Continue on reverse side if necessary and identify by block number)

A "Dynamic Corrosion-Wear Cell" was developed to study the effects of both electrochemical and mechanical factors on the material degradation of bearing components applicable to Navy aircraft. Electrode polarization technique was used to evaluate corrosion behavior of the materials under stress and motion. M2 steel, 52100 steel, Armco iron, and 304 SS were evaluated in various electrolytes containing NaCl with corrosion inhibitors such as dichromates and molybdates. Corrosion current density, open-circuit potential, and wear loss were analyzed both statistically and phenomenologically.

DD FORM 1 JAN 73 1473 EDITION OF 1 NOV 65 IS OBSOLETE

UNCLASSIFIED

SECURITY CLASSIFICATION OF THIS PAGE (When Data Entered)

The effect of continuous wear on the corrosion process was very significant when a passive film was formed in air or in solution, but almost negligible otherwise. Generation of active metal surface by disruption of passive film under wear was mainly responsible for increase in corrosion current and the open-circuit potential shift. However, a small increase in corrosion current and negligible shift in the open-circuit potential were observed by surface roughening and structural deformation by frictional wear. Analytical scanning electron microscopy was used for metallurgical examination of the corrosion-wear surface morphology. Elemental maps of the materials passivated in NaCl solutions with $Na_2Cr_2O_7$ and Na_2MoO_4 showed that deposition of Cr and Mo was higher in the activated wear debris than at general wear scar areas. Surface roughness was measured to obtain additional insight into the observed phenomena.

Wear appears to control the anodic polarization process significantly, but not the cathodic polarization process. A kinetic mechanism occurring in corrosion-wear systems is suggested.

ABSTRACT

A "Dynamic Corrosion-Wear Cell" was developed to study the effects of both electrochemical and mechanical factors on the material degradation of bearing components applicable to Navy aircraft. Electrode polarization technique was used to evaluate corrosion behavior of the materials under stress and motion. M2 steel, 52100 steel, Armco iron, and 304 SS were evaluated in various electrolytes containing NaCl with corrosion inhibitors such as dichromates and molybdates. Corrosion current density, open-circuit potential, and wear loss were analyzed both statistically and phenomenologically.

The effect of continuous wear on the corrosion process was very significant when a passive film was formed in air or in solution, but almost negligible otherwise. Generation of active metal surface by disruption of passive film under wear was mainly responsible for increase in corrosion current and the open-circuit potential shift. However, a small increase in corrosion current and negligible shift in the open-circuit potential were observed from surface roughening and structural deformation by frictional wear. Analytical scanning electron microscopy was used for metallurgical examination of the corrosion-wear surface morphology. Elemental maps of the materials passivated in NaCl solutions with $Na_2Cr_2O_7$ and Na_2MoO_4 showed that deposition of Cr and Mo was higher in the activated wear debris than at general wear scar areas. Surface roughness was measured to obtain additional insight into the observed phenomena.

Wear appears to control the anodic polarization process significantly, but not the cathodic polarization process. A kinetic mechanism occurring in corrosion-wear systems is suggested.

FORWARD

This report was prepared by I.I.T. Research Institute (IITRI), Chicago, Illinois for the Materials Protection Branch of the Naval Air Development Center (NADC), Warminster, Pennsylvania under contract No. N62269-79-C-0702. Dr. Vinod S. Agarwala, Code 6062, (NADC) was the Project Engineer and Monitor.

The responsibility for carrying out this program was given to the Materials and Manufacturing Technology Division of the I.I.T Research Institute. Drs. S. Bhattacharyya and K. Y. Kim of IITRI were the principal and associate investigators, respectively, and also the authors of this report. Dr. V. S. Agarwala (NADC) also provided the technical guidance in this study.

This report was released by the authors in December 1981 and covers the work accomplished during the period of September 1979 through September 1981.

TABLE OF CONTENTS

LIST OF TABLES

1. INTRODUCTION

Wear and corrosion during service life can cause significant loss of reliability and unpredicted failure in critical components and load-bearing structures in Navy aircraft. This laboratory evaluation was directed toward an understanding and characterization of the combined damaging effects of wear and corrosion in Navy aircraft bearing materials subjected to simulated service conditions. Electrochemical techniques were used to separate the effect of corrosion from wear when the surfaces are subjected to relative motion under load. In addition, parallel immersion corrosion tests were performed. Corrosion and wear effects were analyzed with SEM and surface roughness measurements. A set of 12 tests were designed statistically and analyzed to obtain correlation between the test variables and the observed electrochemical effects.

2. CORROSION-WEAR EQUIPMENT

A "Dynamic Corrosion-Wear Cell" was designed to study both electrochemical and mechanical effects occurring in a corrosion-wear system. In this study, it was shown that the IITRI-designed corrosion-wear apparatus, shown in Fig. 1, is a suitable device for reproducible and efficient study of the combined effects of wear and corrosion. Figure 2 shows a schematic diagram of the corrosion-wear apparatus. This diagram illustrates the relationship between material, load, motion, and current path. The test apparatus consisted of an electrochemical cell, and a loading and driving system. The apparatus container (cell), made of clear plastic (H) was filled with electrolyte in which the working electrode (A) was immersed. A Luggin capillary tube (C), located near the moving working electrode, provided a salt-bridge to the reference electrode (not shown). Two platinum counter electrodes were used to polarize the working electrode. The acidity (or basicity) of the electrolyte was continuously monitored. A Teflon-coated magnetic bar was used for stirring in the electrolyte.

The two most important features of the wear-cell design were (1) the ability to insulate all internal metallic surfaces, other than the wear surface of the working electrode (sample) covered by the electrolyte, from the current supplied by the counter electrodes, and (2) the ability to conduct the impressed current through the rotating wear surface of the working electrode to the measuring device. As shown in Fig. 2, all the internal metallic surfaces except the contact area were coated. The cell current was conducted through a lead wire in contact with a pin on the holder (D). Through the hollow shaft, the lead wire conducted the cell current to the current-collecting device (F) outside the cell. Satisfactory, nonfluctuating current signals were obtained even at the 0.1 μA range.

The load was applied through the stationary pin electrode onto the rotating sample electrode using a precalibrated constant-tension spring. The motion was designed to simulate low-speed continuous motions, such as those experienced in the bearing systems of naval aircraft. The electric motor and speed reducer provided a stable motion of 0.9 to 44 rpm at constant torque. The equipment can be modified to incorporate oscillatory motion and torque measurement.

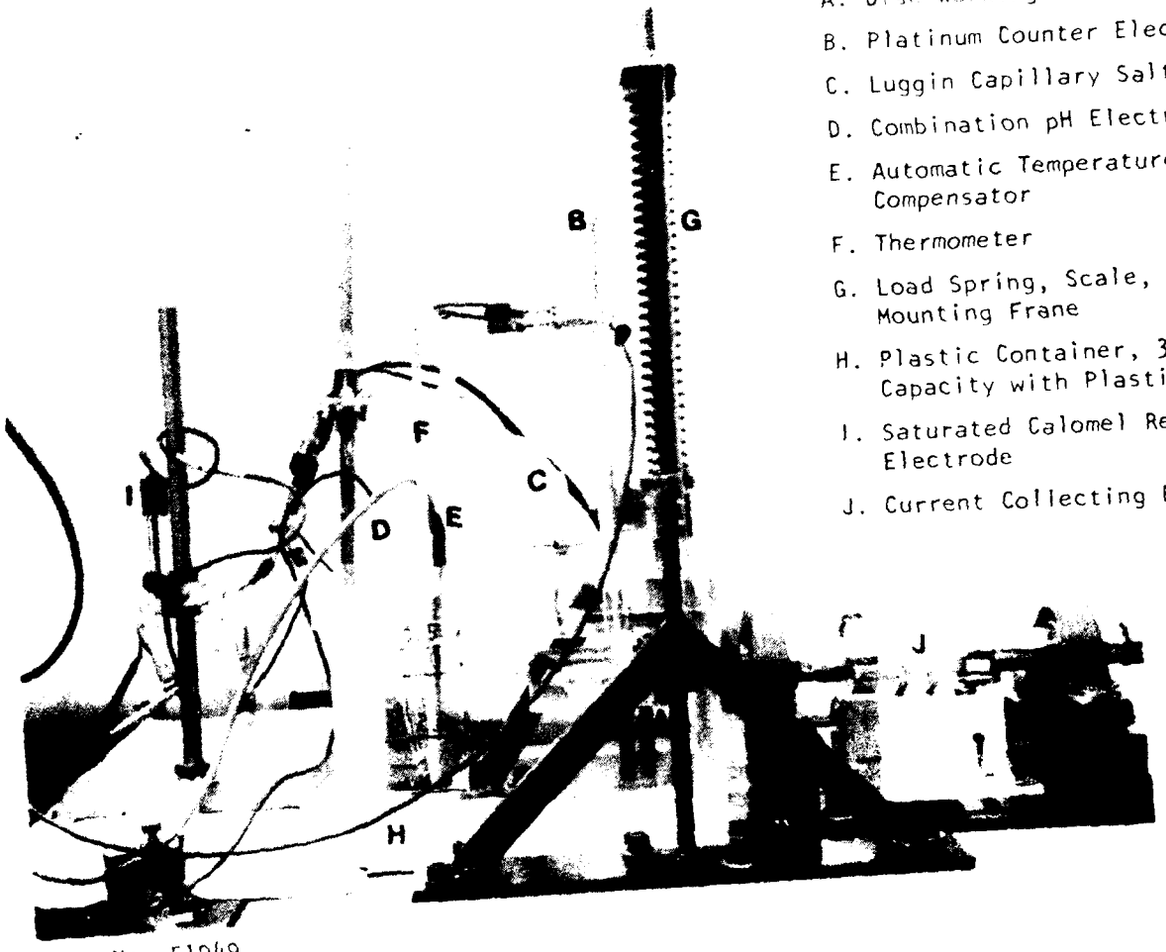

Neg. No. 51949

Figure 1. Dynamic corrosion-wear electrochemical test apparatus.

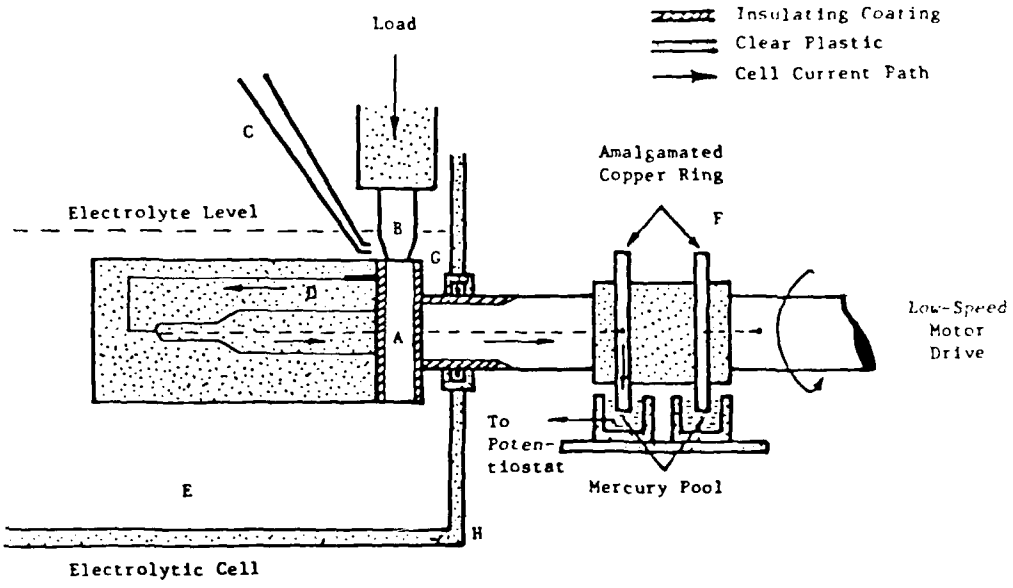

A. Lower Disc Electrode
B. Upper Pin Electrode
C. Salt Bridge to SCE
D. Current Collecting Pin in a Plastic Holder
E. Electrolyte with Stirrer and Temperature Compensator
F. Copper-plated Ring for Current Transmission
G. Epoxy-Resin-Covered Metallic Surface
H. Clear plastic

Figure 2. Schematic arrangement of dynamic electrochemical wear-corrosion apparatus.

3. DESIGN OF EXPERIMENTS

The basic objective of the study was to understand failure mechanisms in Navy aircraft load-bearing components and to use this knowledge to improve reliability in component performance. The overall objective included study of the following subjects:

1) Role of naval environment in corrosion-wear systems and naval aircraft bearing materials.

2) Mechanisms of corrosion under stress and motion.

3) Effect of additives in mitigating corrosion and wear.

4) Corrosion-wear surface characterization and development of relationship between observed phenomena and surface structural changes.

The test materials and principal system variables used in this program were as follows:

Material	-	M2 steel, 52100 steel, Armco iron, and 304 stainless steel
System Variables	-	NaCl concentration, solution pH, corrosion inhibitors and their concentration, environment, load, and speed.

Type M2 and 52100 steels are typical materials for load-bearing components. Armco iron was used for basic research; and 304 SS, for comparative study since it has a naturally occurring passive film on the surface.

Tests were conducted in NaCl solution with the different system variables mentioned above. The material evaluation was performed mainly through the electrode polarization measurement under wear. Separate immersion tests were performed to isolate the corrosive effect of environment. Scanning electron microscopy with EDX analysis was used for metallographic observations, and profilometer and Proficorder were incorporated for the study of surface roughness.

A logic diagram shown in Fig. 3 illustrates the preliminary basic approach to the corrosion-wear study with an attempt to separate the effects of corrosion and wear individually, and to examine the effect of one on the other. Since an effective study of wear was possible only when corrosion under no-wear condition was relatively low, control of corrosion rate to a reasonable range was systematically conducted by changing the condition of system variables. Material evaluation was initiated with 3.5% NaCl solution in ambient air since this concentration is known as average salinity in the ocean. In this solution, Type 304 SS was essentially passivated under no-wear condition due to the naturally occurring passive film on the surface, and was suitable for study of wear effect. However, M2, 52100 steels, and Armco iron corroded so severely that a systematic evaluation of wear effect on corrosion was almost impossible. Therefore, control of solution pH, reduction of NaCl concentration, addition of corrosion inhibitor, and control of electrolyte environment were applied separately, or in combination, to reduce the corrosion rate for an effective study of wear.

In most cases, it was found that the effect of wear on the corrosion process was significant when the material was passivated with either naturally occurring passive film or passive film forming in the electrolyte which was controlled by the above system variables. On the basis of test results obtained through electrochemical polarization, gravimetric analysis, scanning electron microscopy, and surface analysis, the factors most significantly affecting the corrosion-wear mechanisms were evaluated.

During the last 6 months of the study, a statistical design of experimental method based on a Plackett-Burman[1] design was incorporated to obtain a quantitative measure of the effectiveness of the most important variables controlling the corrosion-wear process with a minimum of testing. The six variables chosen were as follows:

[1] J. W. Dini and H. R. Johnson, "Use of Strategy of Experimentation in Gold Plating Studies," Plating and Surface Finishing, Vol. 68 (2), 1981, pp. 52-56.

Materials: M2, 52100 Steels, 304 SS, Armco Iron

System Variables: NaCl concentration, solution pH, inhibitor and its concentration, environment, load, speed, lubricant and its concentration.

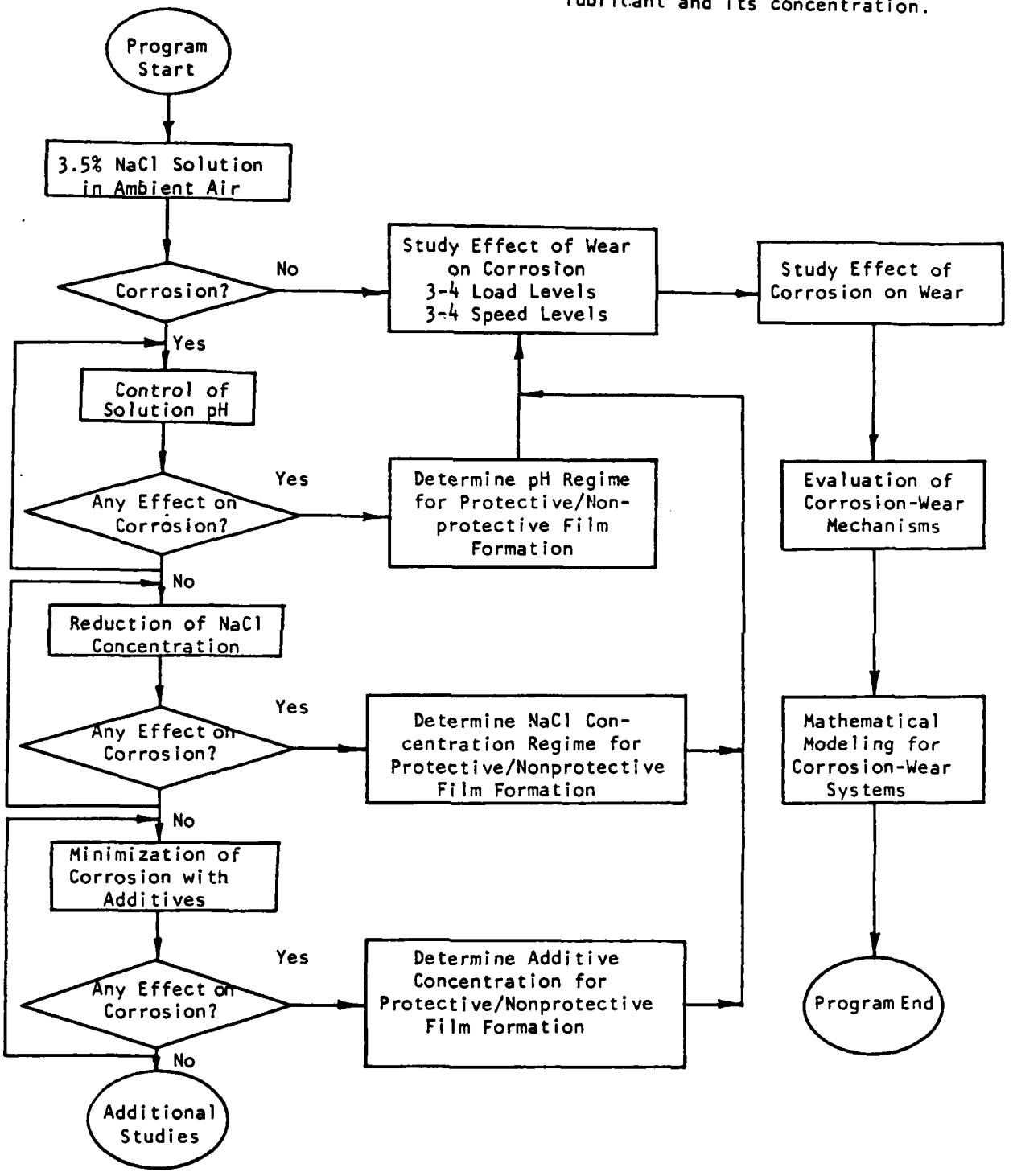

Figure 3. Logic flow diagram for an approach to corrosion-wear study.

Variables	(+)	(-)
X_1 = Material	52100	Armco iron
X_2 = Electrolyte	Passive	Active
X_3 = Load	High	Low
X_4 = Speed	High	Low
X_5 = Environment	Deaerated	Aerated
X_6 = Preexposure	4 hr	1 hr

The active type of electrolyte was 10 ppm NaCl solution without corrosion inhibitor whereas the passive type electrolyte was 10 ppm NaCl solution with 500 ppm $Na_2Cr_2O_7$ and 500 ppm Na_2MoO_4. The low and high levels of load and speed were chosen as 16 and 56 lb, and 1 and 10 rpm, respectively. The aerated environment refers to the electrolyte open to the ambient air, while the deaerated environment refers to the electrolyte purged with argon gas during the test period. Through this test method, the main factors affecting corrosion rate, open-circuit potential, and weight change were evaluated.

4. EXPERIMENTAL RESULTS AND DISCUSSION

4.1 IMMERSION TEST

Immersion tests were performed for a group of materials in NaCl solutions under various conditions. The materials tested were Armco iron, 304 SS, and Type M2, 52100, and 1020 steels (Table 1). The concentration of NaCl solution ranged 10 to 5000 ppm, and various corrosion inhibitors and buffer solutions were used to observe the passivation characteristics. Table A-1 of Appendix A summarizes the details of each test condition and test results. Two types of specimen geometry were used; one is cylindrical in shape (6.3 mm dia x 38.1 or 50.8 mm), and the other is a square coupon (25.4 x 25.4 x 9.5 mm, only for Armco iron).

The specimens were suspended with a nylon string in 200 ml (tests A1-A22) or 2000 ml (tests A23-A55) of the test solution containing various corrosion inhibitors or buffer solutions in such a way that the center of the specimen was about 2 cm below the waterline of the solution. All the experiments were performed at room temperature. Tests A1-A43 were conducted in open-air condition, while tests A44-A55 were conducted in deaerated condition by Ar purging. At the end of the experiment, the specimens were taken out of the solutions, carefully washed with distilled water and dried. The specimens were then cleaned using NACE standard solution (50 g/l of $SnCl_2$ and 20 g/l of $SbCl_3$ in conc. HCl). Exposure of a dummy sample to the cleaning solution (for calibration purpose) resulted in a weight loss of less than 0.5 mg in all materials. The specimens were finally washed with water, dried with acetone, and reweighed. In Table A-1 of Appendix A, the corrosion weight loss is presented in $\mu g/cm^2/hr$ and converted into corrosion rate in mpy using the linear extrapolation:

$$mpy = \frac{534}{0.155} \times \frac{\text{Weight Loss (mg)}}{\text{Surface Area (cm}^2\text{) x Time (hr) x Density (g/cm}^3\text{)}}$$

Type M2 and 52100 steel in NaCl solution with concentration range between 10 and 5000 ppm showed heavy uniform corrosion, while 304 SS in 5000 ppm NaCl showed complete passivation on the free surface with a crevice type corrosion

TABLE 1. NOMINAL COMPOSITION OF TEST MATERIALS

Material	Composition, wt%							
	C	Mn	Si	Cr	Ni	Mo	Fe	Others
Armco Iron	-	-	-	-	-	-	100	-
1020 Steel	0.18-0.23	0.3-0.6	-	-	-	-	Bal.	P & S 0.04 max
52100 Steel	0.98-1.10	0.25-0.45	0.15-0.35	1.3-1.6	-	-	Bal.	P & S 0.025 max
M2 Tool Steel	0.85-1.00	-	-	4.0	-	5.0	Bal.	6.0W, 2.0V
304 Stainless Steel	0.08	2.0	1.0	18-20	8-10.5	-	Bal.	0.045P, 0.030S max

along the nylon string used for suspension of the specimen. Reduction of NaCl concentration from 5000 to 10 ppm reduced the weight loss of 52100 steel by a factor of about 4 (compare test A2 with A35-A37). Although M2 and 52100 steels in distilled water showed protective film formation, the presence of 1 ppm of NaCl in distilled water did not allow the formation of protective film on M2 steel (test A7).

The effect of solution pH on the corrosion character was studied on M2 and 1020 steels in 10 ppm NaCl solution by using NaOH, H_3BO_3, and $Na_2B_4O_7$. Control of pH from 5.5 to 10 did not change the corrosion character of M2 and 1020 steel (tests A6-A13), although it affected the weight loss to a certain degree. Addition of sodium borate (pH 8.7) significantly reduced the weight loss, but did not permit protective film formation on either M2 or 1020 steel. Sodium hydroxide and boric acid did not show any favorable effect on corrosion resistance of M2 steel; instead, they seemed to increase the weight loss slightly.

Passivation behavior of Armco iron and of M2 and 52100 steels in NaCl solutions was studied with sodium dichromate and sodium molybdate. The amount of $Na_2Cr_2O_7$ required for passivation increased as the concentration of NaCl was increased. To determine the concentration range of $Na_2Cr_2O_7$ needed to passivate M2 steel and Armco iron in NaCl solutions, several tests were performed in NaCl solutions with concentration range 10 to 1000 ppm (tests A14-A31). In 1000 ppm NaCl solution, complete passivation was not observed on M2 steel and Armco iron with 250 and 1000 ppm of $Na_2Cr_2O_7$, respectively. Although most free surface of both materials was passivated, there were several corrosion spots on the free surface and heavy crevice-type corrosion all along the nylon string. In 100 ppm NaCl solution with 500 ppm $Na_2Cr_2O_7$, Armco iron showed virtually complete passivation with a few corrosion spots. Complete passivation of Armco iron was observed in 10 ppm NaCl solution with $Na_2Cr_2O_7$ concentration of more than 100 ppm (tests A19, A20, and A29-A31). In general, the pH of test solutions increased with time under both corroding and noncorroding conditions. The pH of electrolyte for corroding electrode showed relatively higher value than the pH of electrolyte for passivated electrode. It is due to formation of hydrated iron oxide in the solution.

The effect of environment on the corrosion behavior of Armco iron and 52100 steel was evaluated in 10 ppm NaCl solution with and without corrosion

inhibitors (tests A32-A55). As mentioned earlier, the aerated environment refers to the electrolyte open to ambient air, whereas the deaerated environment refers to the electrolyte purged with argon gas. Armco iron and 52100 steel were completely passivated in 10 ppm NaCl solution with 500 ppm $Na_2Cr_2O_7$ and 500 ppm Na_2MoO_4 under both aerated and deaerated environments. In 10 ppm NaCl solution without corrosion inhibitor, deaeration reduced the weight loss of Armco iron and 52100 steel by factors of about 4 and 3, respectively. In deaerated condition, both materials had the black adherent iron oxide on the surface which was also covered by hydrated iron oxide. It is generally observed that the corrosion rates determined from the weight loss data are higher than those obtained from Tafel extrapolation of the polarization curves (compare test results listed in Table A-1 of Appendix A with later tables).

4.2 OPEN-CIRCUIT POTENTIAL BEHAVIOR

The open-circuit potential behavior of various materials with time varied depending upon corrosivity of the electrolyte. Table 2 indicates typical trends of open-circuit potential behavior of various materials with time in different electrolytes. In general, open-circuit potential of iron and steels became more electronegative when corroded, and more electropositive when passivated. However, open-circuit potential of 304 SS became more electronegative when passivated in 3.5% NaCl solution.

Figure 4 shows the open-circuit potential behavior of M2 and 52100 steels as function of time in 0.5% NaCl solution and distilled water. Both M2 and 52100 steels were severely corroded in 0.5% NaCl solution, but passivated in distilled water. The different behaviors in the electrolytes depended on whether or not a protective film was generated under a given set of test conditions. Removal of nonprotective corrosion product (possibly $Fe(OH)_2$), which formed on these steel surfaces in corroding environments, generally altered their open-circuit potentials to the noble direction. For example, the open-circuit potential of 52100 steel in 0.5% NaCl solution changed from -660 to -580 mV (step C in Fig. 4) due to removal of the corrosion product. This phenomenon would be related to the lower mobility of oxygen through the film of hydrated iron oxide, $Fe(OH)_2$. Upon removal of $Fe(OH)_2$ film, transport of oxygen to metal surface increased and, consequently, the open-circuit potential increased.

TABLE 2. TYPICAL OPEN-CIRCUIT POTENTIAL BEHAVIOR OF VARIOUS MATERIALS WITH TIME IN DIFFERENT ELECTROLYTES

Electrolyte	M2 Steel, 52100 Steel	Armco Iron, 1018 Steel	304 SS	Remarks
Distilled water	↑ Passivated	--	--	
NaCl solution	↓ Corroded	↓ Corroded	↓ Passivated	NaCl range 0-3.5%
NaOH solution	↑ Passivated	--	--	4 ppm NaOH
NaCl + additives[a]	↑ Passivated ↓ Corroded	↑ Passivated ↓ Corroded	--	Corrosivity depends on the concentration of both NaCl and additives.

↑ = $E_{o.c.}$ shifted in the noble direction.

↓ = $E_{o.c.}$ shifted in the active direction.

[a] $Na_2Cr_2O_7$, Na_2MoO_4, $Na_2B_4O_7$, NaOH, H_3BO_3.

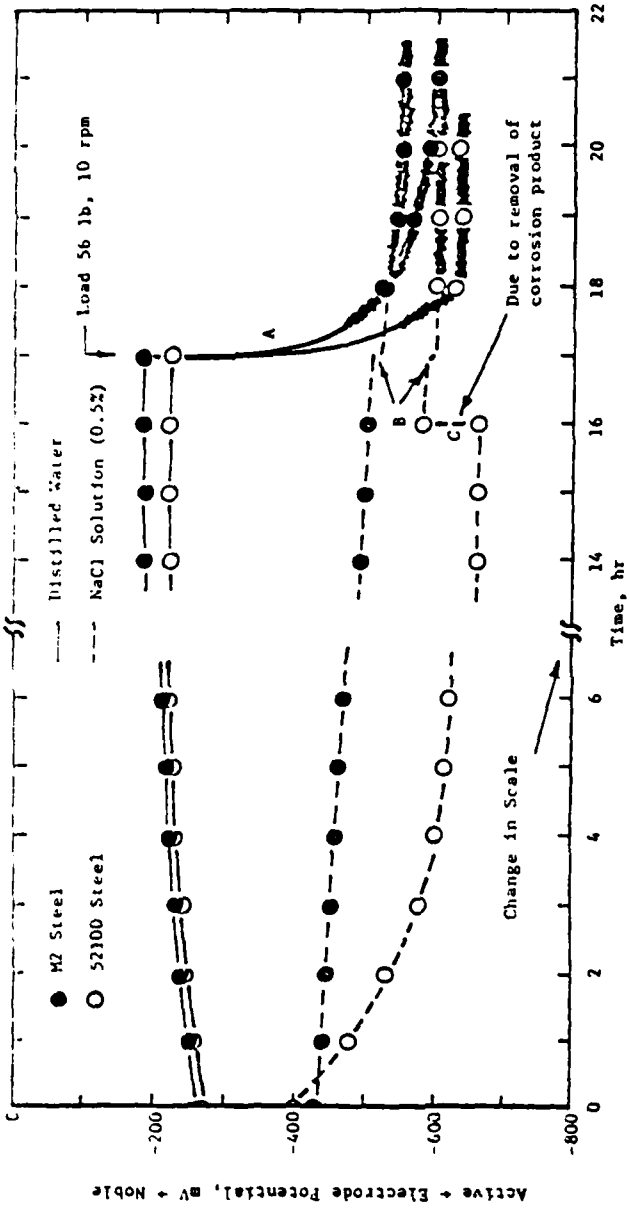

Figure 4. Effect of time on open-circuit potential without load in different alloys.

The Type 304 SS was passivated by the formation of a protective film on the surface in NaCl solutions with concentration up to 3.5%. The open-circuit potential gradually became electronegative until it reached a steady-state potential.

The effect of wear on open-circuit potential was observed on various materials in both protective and non-protective film forming conditions. Table 3 summarizes the effect of load at constant speed on the open-circuit potential of materials in the protective film forming condition: (1) M2 steel in distilled water, (2) 52100 steel in distilled water, (3) 304 SS in 0.5% NaCl solution, and (4) M2 steel in 4 ppm NaOH solution. The open-circuit potentials increased significantly in the active direction upon increase in load level, with lighter loads being more effective. However, it should be noted that the open-circuit potential did not change from the value obtained under no-wear condition when load was increased without rotational motion. In all cases, initial loading of 3.7 lb resulted in a large shift of the open-circuit potential in the active direction. The subsequent increment of load decreased the potential, but not significantly. It is believed that the initial large change in the open-circuit potential was due to disruption of a protective film, whereas the small change thereafter is due to additional structural deformation of the surface.

Similar large potential drop by initial disruption of passive film was observed on the effect of rotational speed at constant load on the open-circuit potential of materials in the protective film forming solutions. Table 4 shows the effect of speed at 3.7 lb (1.67 kg) load on the open-circuit potential of 304 SS in 3.5% NaCl solution. The amount of potential change decreased as the speed increased.

Wear of material surface did not significantly affect the open-circuit potentials in electrolyte where non-protective film formation was observed. Tables 5 and 6 show the effect of load at a constant speed of 3 rpm ($\pi/10$ rad/s) and the effect of speed at constant load of 56 lb (25.4 kg), respectively, on the open-circuit potential of M2 steel in 3.5% NaCl solution. Type M2 steel does not form a protective film in 3.5% NaCl solution. Virtually no discernible effects of load and speed on the open-circuit potential were observed.

TABLE 3. EFFECT OF LOAD ON OPEN-CIRCUIT POTENTIAL OF M2, 52100 AND 304 SS UNDER PROTECTIVE FILM FORMING CONDITIONS

Load		Open-Circuit Potential ($E_{o.c.}$), mV			
lb	(kg)	M2 Steel[a] in Distilled Water	52100 Steel[a] in Distilled Water	304 SS[a] in 0.5% NaCl Solution	M2 Steel[b] in 4 ppm NaOH Solution
0		-170	-180	-75	-180
3.7	(1.67)	-345	-395	-330	-350
16	(7.25)	-413	-490	-370	-357
41	(18.6)	-435	-540	-390	-360
56	(25.4)	-460	-625	-430	-362

[a]Speed = 10 rpm (π/3 rad/s).

[b]Speed = 1 rpm·(π/30 rad/s).

TABLE 4. EFFECT OF SPEED ON THE OPEN-CIRCUIT POTENTIAL OF 304 SS IN 3.5% NaCl SOLUTION

Speed, rpm	Load		$E_{o.c.}$, mV
	lb	(kg)	
0	0	(0)	-100
1	3.7	(1.67)	-290
2	3.7	(1.67)	-305
4	3.7	(1.67)	-325
11	3.7	(1.67)	-365

TABLE 5. EFFECT OF LOAD ON THE OPEN-CIRCUIT POTENTIAL OF M2 STEEL IN NON-PROTECTIVE FILM FORMING SOLUTION (3.5% NaCl) AT CONSTANT SPEED[a]

Load, lb (kg)	$E_{o.c.}$, mV
0	-657
3.7 (1.67)	-650
16 (7.25)	-640 to -650
41 (18.6)	-635 to -650
56 (25.4)	-630 to -650

[a] 3 rpm (π/10 rad/s)

TABLE 6. EFFECT OF SPEED ON THE OPEN-CIRCUIT POTENTIAL OF M2 STEEL IN NON-PROTECTIVE FILM FORMING SOLUTION (3.5% NaCl) AT CONSTANT LOAD

Load, lb (kg)	Speed, rpm (rad/s)	$E_{o.c.}$, mV
0	0	-563
56 (25.4)	0	-563
56 (25.4)	1 (π/30)	-563
56 (25.4)	3 (π/10)	-567
56 (25.4)	10 (π/3)	-572

Similar results were obtained for M2 steel, 52100 steel, and Armco iron in NaCl solutions with concentration range of 10 to 35,000 ppm (3.5%) without corrosion inhibitors. As the wear increased, the fluctuation amplitude of the open-circuit potential, caused by surface roughness, resulted in the observed small variations in the open-circuit potential due to change in load and speed.

4.3 POLARIZATION BEHAVIOR UNDER DYNAMIC CORROSION-WEAR CONDITIONS

4.3.1 Potentiostatic Polarization Behavior

Potentiostatic polarization measurements were performed to study the effect of wear on corrosion processes. Test materials and various test conditions are summarized in Table A-2 of Appendix A. The potentiostatic polarization technique was followed using the ASTM Standard G5-72. The working electrode (lower disk electrode) was allowed to reach a steady-state open-circuit potential. The open-circuit potential in a corrosion-wear system was not absolutely stable, so when a small potential change, 3 to 5 mV/hr, was attained, it was considered stable for experimentation. It took approximately 2 to 6 hr for the open-circuit potential to stabilize, depending on the test conditions, either with or without interfacial motion in contact under load.

Upon reaching a steady-state open-circuit potential, the specimen was polarized by impressing a potential either anodically or cathodically. Polarization measurements were performed at a stepping rate of 2 mV/s. This stepping rate permitted a reasonable time for the transition cell current to stabilize at each increment of the electrode potential. Specimen potential was measured with respect to a saturated calomel (SCE) reference electrode, while the rate of the surface reaction of the specimen electrode was estimated by measuring the cell current. Current readout and the potential controls were provided by a Wenking potentiostat (Model No. 70 TSI) with an attached Wenking stepping motor scanning potentiometer (Model No. 72).

Polarization behavior of various systems changed in many different ways; however, polarization behaviors showing similar trends could be grouped together as follows (depending on the corrosivity of material under various conditions):

a) Polarization behavior of materials in corroding, or non-protective film forming solution.

b) Polarization behavior of materials with naturally occurring passive film.

c) Polarization behavior of materials which form a passive film in the test solution.

(a) Materials in Corroding Solutions

Figure 5 shows typical polarization curves of a corroding material in non-protective film forming electrolyte under both wear and no-wear conditions. These types of polarization curves were obtained from M2 steel, 52100 steel, and Armco iron in NaCl solution with concentration range of 0.1 to 3.5%. The polarization curves shown in Fig. 5 were observed on M2 steel in 0.5% NaCl solution (test 38). Polarization curves of both conditions show typically two cathodic branches and one anodic branch. The first cathodic branch represents the reduction reaction of dissolved oxygen; the second branch, the hydrogen evolution; and the anodic branch, the dissolution of iron. Wear of the material surface did not significantly affect the polarization behavior. Displacement of the open-circuit potential observed in Fig. 5 does not necessarily represent the typical potential value of a material at a given load and motion since the open-circuit potential of a corroding system is generally transient in nature.

Reduction of NaCl concentration to 10 ppm range did not allow Armco iron, M2, and 52100 steel to passivate, although it corroded them moderately. As the concentration of NaCl was reduced, the slope of the anodic polarization curve increased; i.e., the dissolution rate of iron was reduced in the anodic overpotential range. However, the basic characteristics of polarization behavior remained the same until the NaCl concentration was substantially reduced to the 10 ppm range, whereupon the resistance polarization played a significant role due to the poor conductivity of the electrolyte.

Figure 6 shows polarization curves of Armco iron in 10 ppm NaCl solution under both wear and no-wear conditions (test 65). In this solution, the iron was heavily corroded. The polarization curves consist of a single anodic and a single cathodic branch under both wear and no-wear conditions. It is shown that the corrosion current density under wear increases by about one order of magnitude from that of no-wear condition. However, at higher NaCl concentrations, wear caused no significant change in the corrosion current density of iron and steels.

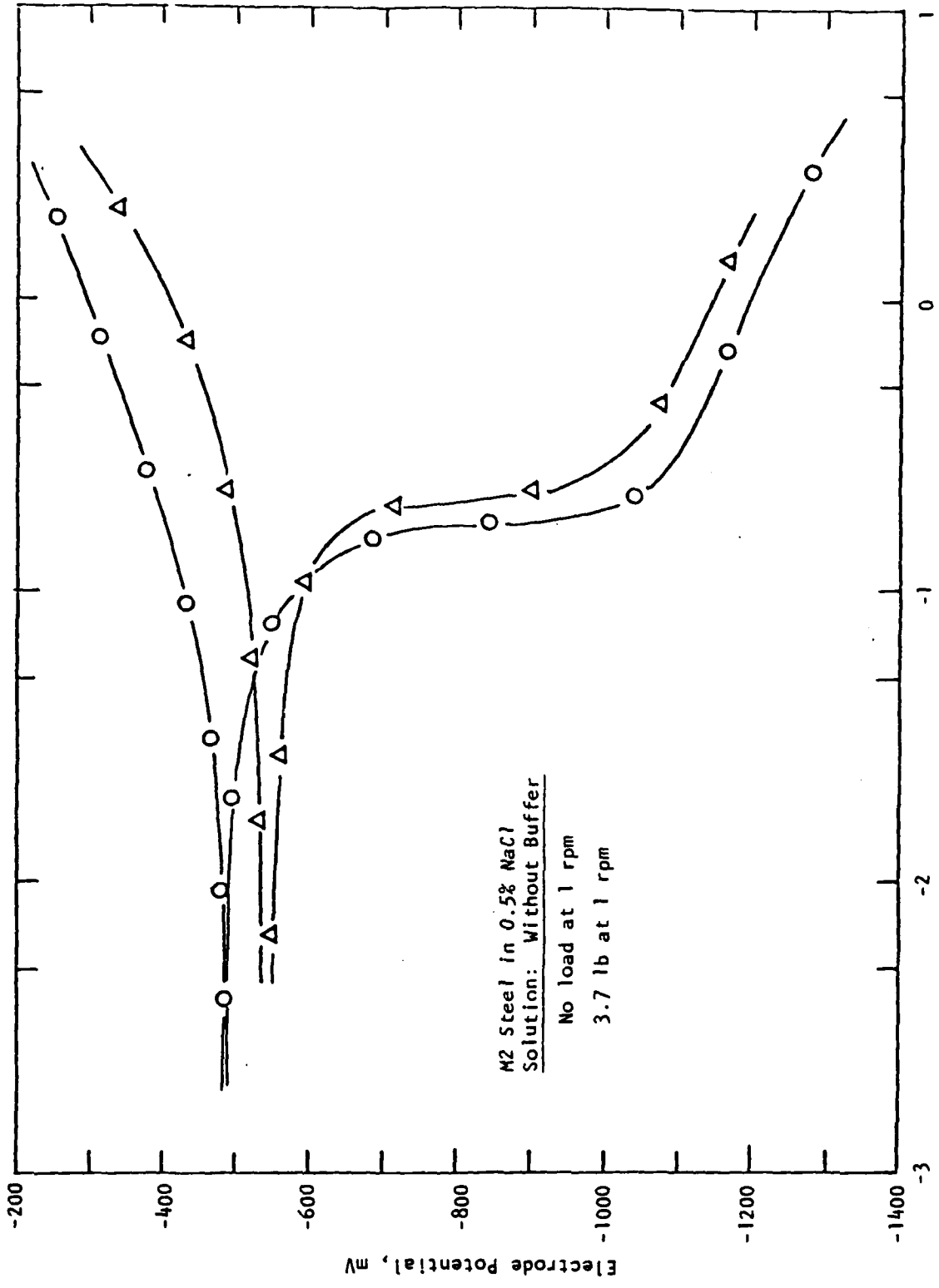

Figure 5. Polarization behavior of M2 steel in 0.5% NaCl solution with and without wear (test 38).

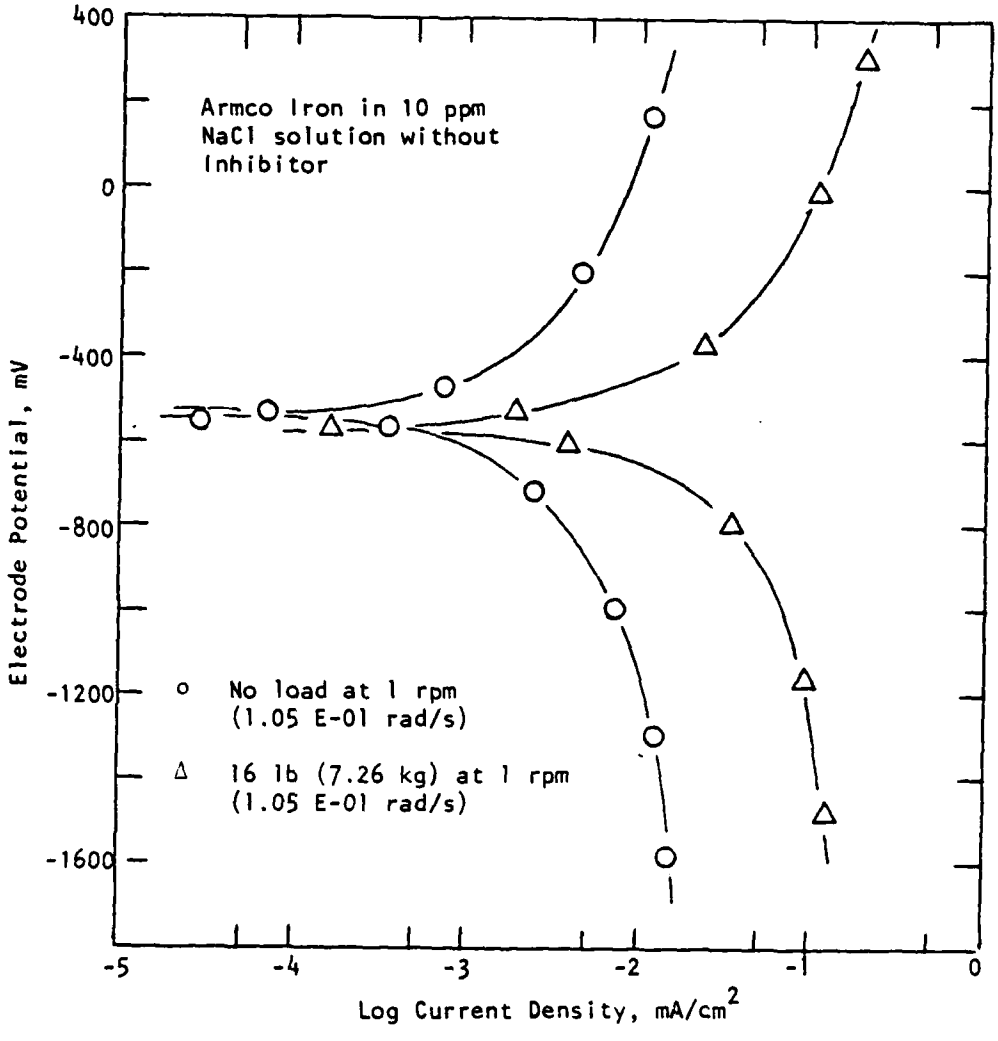

Figure 6. Polarization behavior of Armco iron in 10 ppm NaCl solution without corrosion inhibitor (test 65).

Polarization behavior of corroding steels in NaCl solutions was not affected significantly by pH adjustment of the electrolyte. Polarization characteristics of M2 and 52100 steels in 0.1 and 0.5% NaCl solutions of pH 10 adjusted with NaOH were not basically changed from those of respective NaCl solutions before pH adjustment. However, it was observed that the slope of the concentration polarization limit in the first cathodic branch changed slightly. The concentration polarization occurred a little faster with pH 10.

(b) Material with Naturally Occurring Passive Film

Figure 7 shows typical polarization behavior of a material with naturally occurring passive film. Type 304 SS in NaCl solutions is in this category. Figure 7 was obtained from 304 SS in 0.5% NaCl solution under both wear and no-wear conditions (test 39). Under no-wear condition, the anodic polarization curve shows a clear region of passivity up to about 200 mV. Upon reaching a transpassive region, the cell current increased very rapidly with a small increment of potential. Such sudden increase in the cell current is usually observed when pitting and/or crevice corrosion is initiated. A localized crevice-type corrosion was indeed confirmed by the examination of the sample surface.

Under wear condition, the open-circuit potential shifted in the active direction by about 300 mV. The disruption of protective film is clearly indicated in the anodic polarization curve, which represents the metal dissolution process of the active surface generated by wear. The scattered blips along the polarization curve might be due to the nonuniform surface condition created by wear. The corrosion current density increased by about two orders of magnitude between no-wear and wear conditions.

(c) Materials Forming Protective Film in Electrolyte

In this program, formation of a passive film on iron and steels was observed in distilled water, as well as with water having a low concentration of NaOH solution free of Cl^- ion. Polarization behavior of M2 steel in distilled water under wear and no-wear conditons is shown in Fig. 8 (tests 33 and 36); curve Nos. 1 and 4 represent the polarization behavior of a polished specimen under no load and no motion; curve Nos. 2 and 5, the polarization behavior of a preworn surface (run-in condition under 56 lb at 10 rpm) under no load and no motion; curve Nos. 3 and 6, the polarization behavior of a

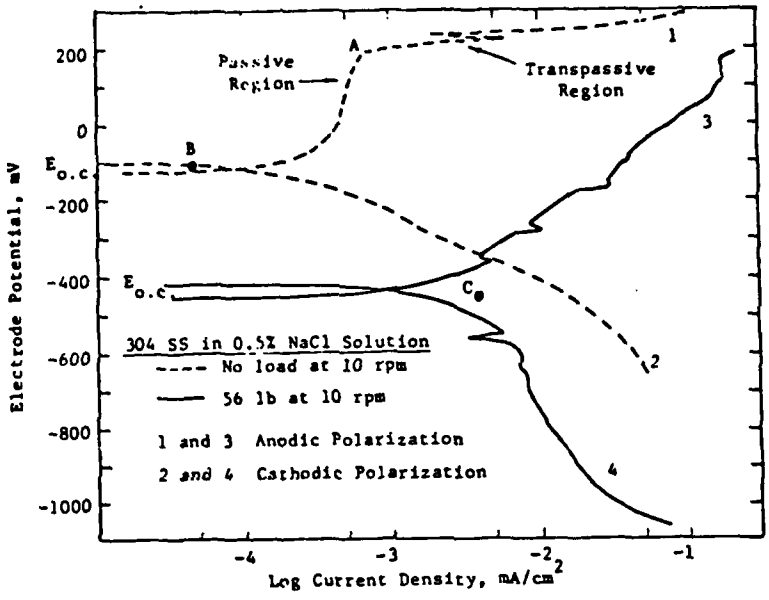

Figure 7. Polarization behavior of 304 SS in 0.5% NaCl solution with and without wear (test 39).

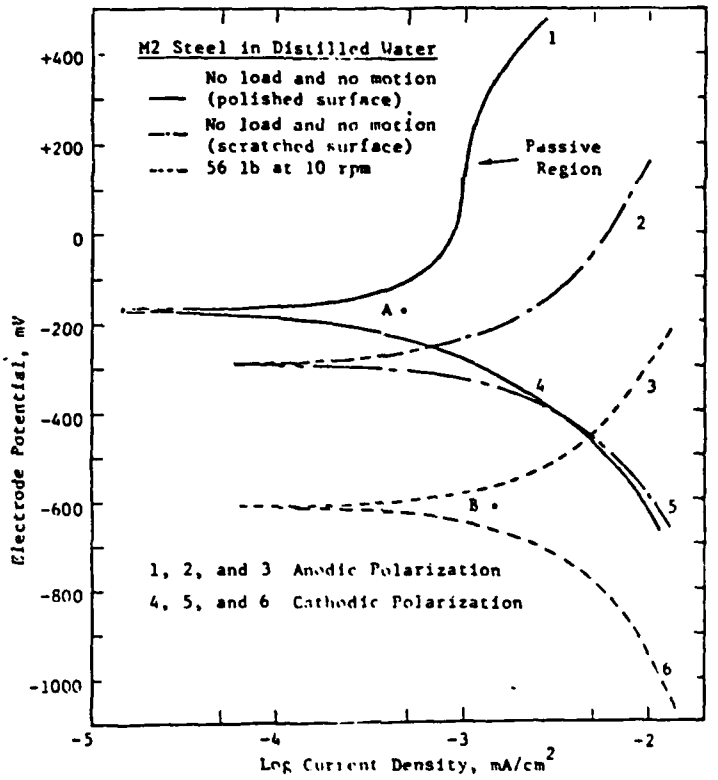

Figure 8. Polarization behavior of M2 steel in distilled water under various wear conditions (tests 33 and 36).

continually rubbing surface of M2 steel under 56 lb at 10 rpm. In the no-wear condition, the anodic curve of polished specimen clearly shows that a protective film is formed on the surface of M2 steel electrode in distilled water. A light brown oxide scale formation was, in fact, observed. The effect of surface condition on polarization behavior was reflected on the preworn surface (curve No. 2) on which no load or motion was applied during the course of polarization. No clear evidence of passivity was apparent on the anodic curve (No. 2) of this electrode. Displacement of the open-circuit potential between the two conditions stated above seemed to be associated with the formation of the protective film on two different types of surfaces. This result was consistent with the observed open-circuit potential in distilled water which gradually increased in the noble direction with time, i.e., the thickness of protective film increased (Fig. 4).

With continuous sliding under load, the open-circuit potential increased in the active direction from -180 to -610 mV (compare curves 1 and 3). Observations indicated that the response of the open-circuit potential change due to wear appears to be faster for 304 SS in NaCl solutions than for M2 or 52100 steels in distilled water, although all of them responded within only a few seconds. The anodic polarization curve in the continuous wear condition showed anodic oxidation of metal dissolution curve (No. 3), and cathodic reduction of the dissolved oxygen curve (No. 6). Significant increase in cell current was apparent, and the corrosion current density ($I_{corr.}$) increased from 4.7×10^{-4} mA/cm^2 (point A) in the non-wear condition to 1.5×10^{-3} mA/cm^2 in the continuous wear condition (point B).

Passivation of iron and steels which corrode in NaCl can be effectively achieved by using corrosion inhibitors such as chromate, dichromate, nitrate, and molybdate. The amount of corrosion inhibitors required for passivation, however, depends primarily on the concentration of NaCl in the solution. Typical polarization behavior observed for iron and steels passivated in NaCl solutions with inhibitors is shown in Figs. 9 and 10. Figure 9 is of Armco iron in 100 ppm NaCl solution with 500 ppm $Na_2Cr_2O_7$ and 500 ppm Na_2MoO_4 (test 69); and Fig. 10 is of 52100 steel in the same electrolyte (test 76). In this solution, Armco iron was passivated completely except for a few corrosion spots, while 52100 steel was completely passivated.

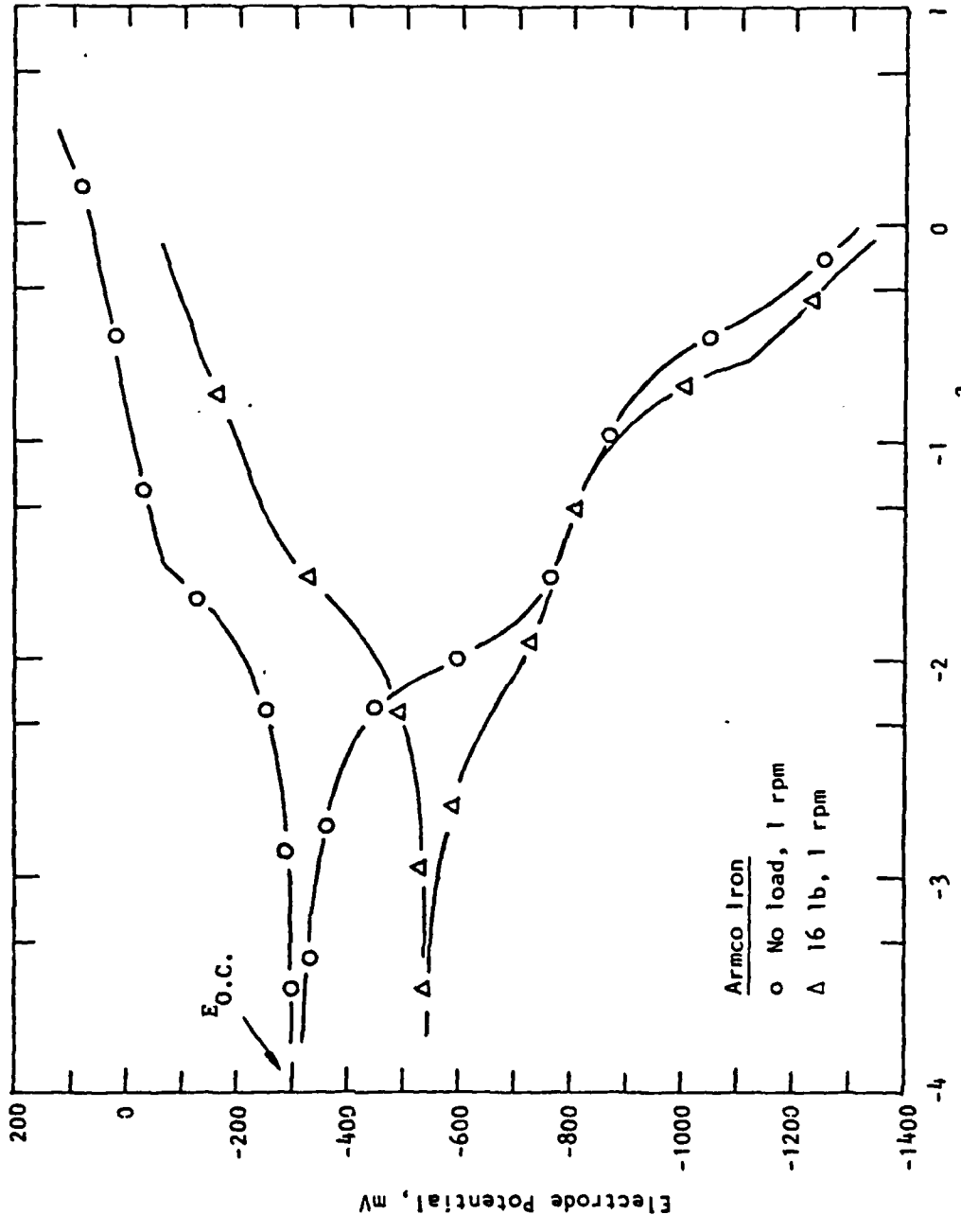

Figure 9. Polarization behavior of Armco iron in 100 ppm NaCl solution with 500 ppm $Na_2Cr_2O_7$ and 500 ppm Na_2MoO_4 (test 69).

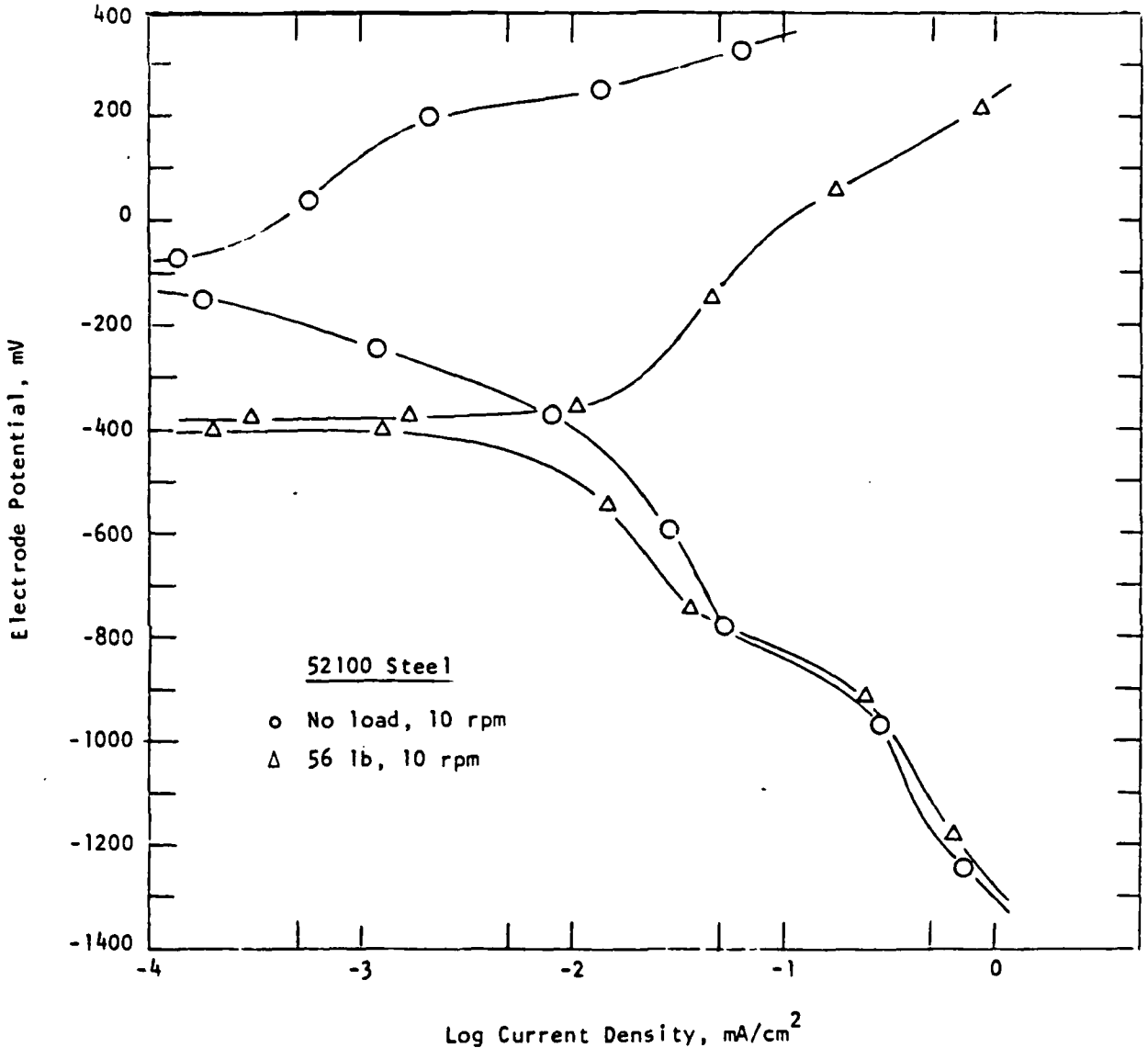

Figure 10. Polarization behavior of 52100 steel in 100 ppm NaCl solution with 500 ppm $Na_2Cr_2O_7$ and 500 ppm Na_2MoO_4 (test 76).

Under no-wear condition, the polarization behavior of both Armco iron and 52100 steel shows typically three cathodic branches and two anodic branches due to passivation. It appears that the three cathodic branches correspond to reduction of dichromate, reduction of dissolved oxygen, and hydrogen evolution with increasing cathodic potential. The first and second anodic reactions are dissolution of a passive film (Cr_2O_3 or $Cr(OH)_3$) layer deposited on the surface and dissolution of iron, respectively. Under wear condition, the open-circuit potential of both materials shifted in the active direction by about 250 mV due to disruption of passive film. Although the polarization characteristics remained basically the same in both wear and no-wear conditions, wear significantly reduced the potential range for the first cathodic branch, the reduction of dichromate. During the anodic polarization under wear, both Armco iron and 52100 steel were severely corroded. The corrosion current densities of both materials under wear increased about one half order of magnitude from those obtained under no-wear condition (Table A-2 of Appendix A).

Passivation of iron and steels depends on the relative concentration between NaCl and corrosion inhibitors. Armco iron in 1000 ppm NaCl solution with 500 ppm $Na_2Cr_2O_7$ and 500 ppm Na_2MoO_4 corroded severely, while Armco iron in 10 ppm NaCl solution with 100 ppm $Na_2Cr_2O_7$ and 100 ppm Na_2MoO_4 passivated completely. Figures 11 and 12 display the polarization behavior of the former (corroding Armco iron electrode) and the latter (passivated Armco iron electrode), respectively. Under corroding condition; the cathodic curve shows essentially three branches and the anodic curve shows only one branch of iron dissolution. With a fixed concentration of corrosion inhibitors, the effect of NaCl concentration on the polarization behavior was more significant on the first cathodic and the first anodic branches. The potential ranges of the first cathodic and anodic branches decreased as the concentration of NaCl increased. Examination of the polarization behaviors shown in Figs. 9 to 12 indicates that the corrosion current density is controlled anodically since the essential features of the cathodic reactions are not changed regardless of corrosive or passive condition established by addition of corrosion inhibitors and/or by wear, while anodic reactions do change.

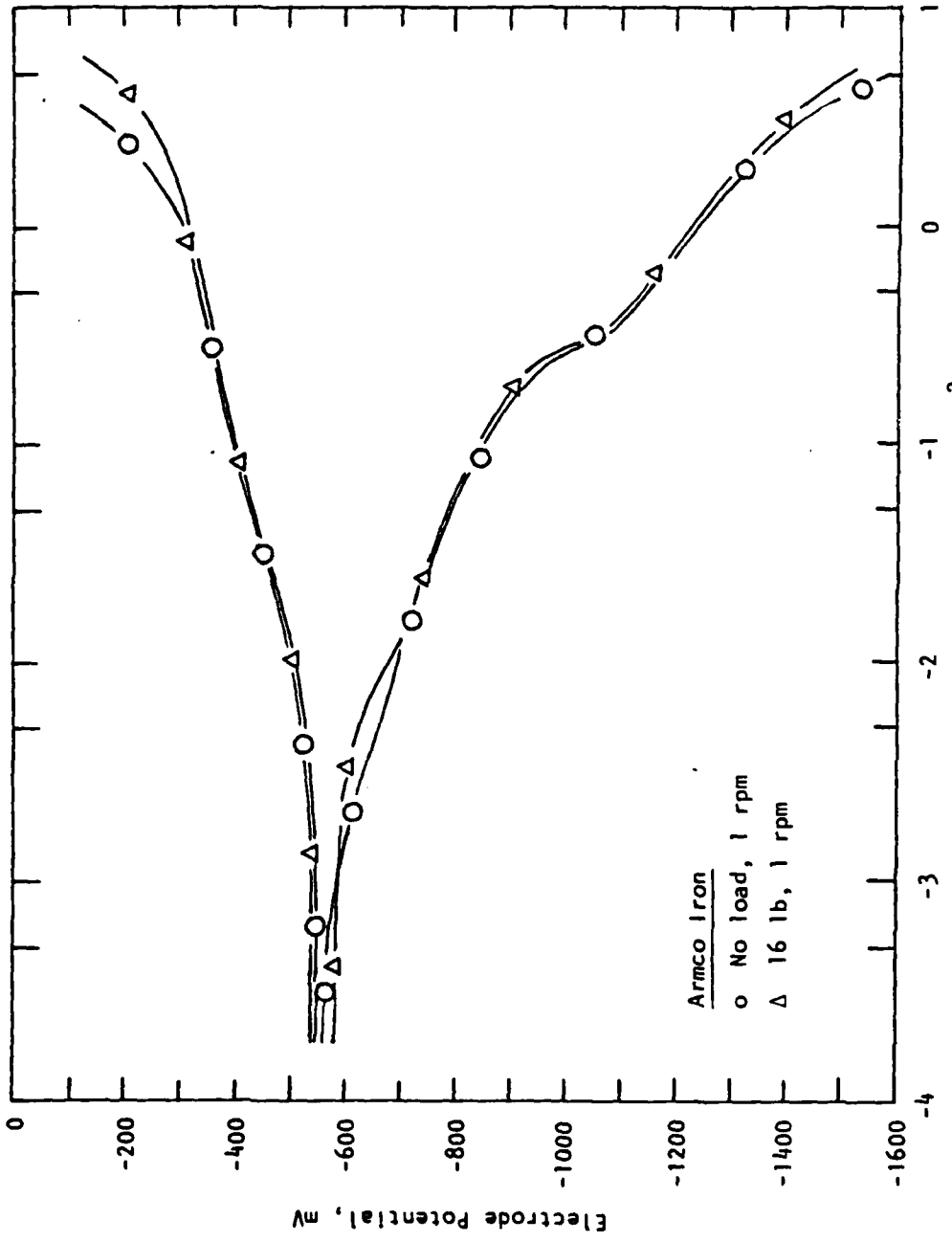

Figure 11. Polarization behavior of Armco iron in 1000 ppm NaCl solution with 500 ppm $Na_2Cr_2O_7$ and 500 ppm Na_2MoO_4 (test 68).

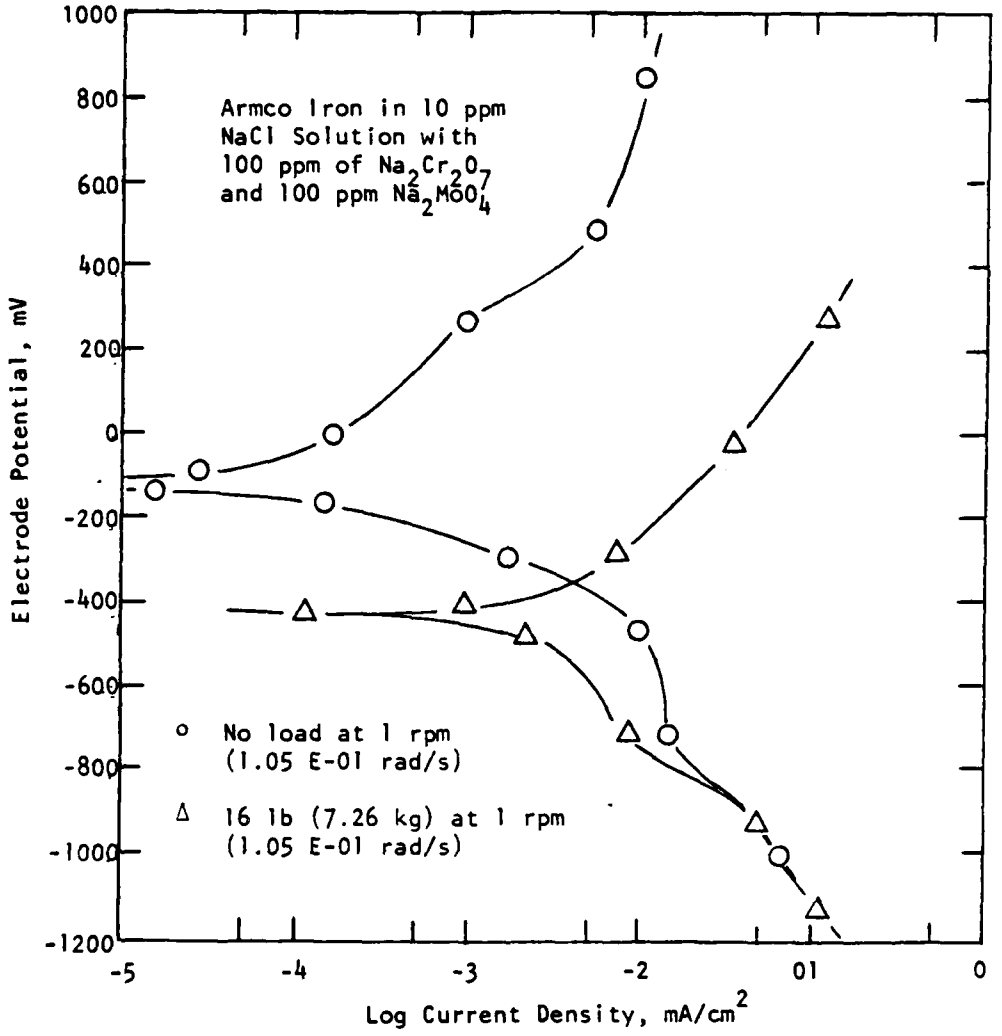

Figure 12. Polarization behavior of Armco iron in 10 ppm NaCl solution with 100 ppm $Na_2Cr_2O_7$ and 100 ppm Na_2MoO_4 (test 66).

(d) Role of Na_2MoO_4

When both $Na_2Cr_2O_7$ and Na_2MoO_4 were used, the cathodic potential range for reduction of molybdate appeared neither separately nor clearly. However, the effect of Na_2MoO_4, in addition to $Na_2Cr_2O_7$, is clearly reflected in the value of the open-circuit potential. The open-circuit potential of Armco iron, as shown in Table 7, shifted in the noble direction with addition of Na_2MoO_4. An Armco iron specimen was polarized in 100 ppm NaCl solution with 500 ppm Na_2MoO_4 alone (test 78), and results are shown in Fig. 13. The general form of polarization curve under no-wear condition shows two cathodic branches and one anodic branch. It appears that the cathodic curve shows reduction reaction of dissolved oxygen and hydrogen evolution, but not reduction of molybdate. In this electrolyte, concentration polarization of oxygen reduction was more pronounced than in 100 ppm NaCl solution with 500 ppm $Na_2Cr_2O_7$ and 500 ppm Na_2MoO_4 (Fig. 9). During anodic polarization in this electrolyte, the current increment was much less compared to those in 100 ppm NaCl with 500 ppm $Na_2Cr_2O_7$ and 500 ppm Na_2MoO_4. Armco iron in 100 ppm NaCl solution with 500 ppm Na_2MoO_4 was mostly passivated with a few localized corrosion spots in the freely immersed condition, but the polarization curve representing dissolution of the passive layer was not clearly demonstrated. Under wear condition, the effect of wear on the cell current is clearly observed on both anodic and cathodic curves; in particular, the anodic cell current under wear was almost two orders of magnitude higher than that observed under no-wear condition.

4.3.2 Electrode Polarization Mechanisms in Corrosion-Wear Systems

It has been observed that the effect of wear on the corrosion process is significant in materials on which a passive film forms naturally, or in an electrolyte. Under wear condition, disruption of passive film was primarily responsible for the increase in the corrosion rate. Therefore, it may be postulated that the electrode polarization process is controlled anodically under wear. The anodically controlled electrode polarization process can be illustrated as shown in Fig. 14. The experimentally obtainable current is the net cell current, which is the sum of the current components of anodic and cathodic, processes, i.e.,

$$i_{net} = \left| \Sigma i_a + \Sigma i_c \right|$$

TABLE 7. EFFECT OF Na_2MoO_4 ON THE OPEN-CIRCUIT POTENTIAL OF ARMCO IRON IN NaCl SOLUTIONS WITH CORROSION INHIBITORS

Distilled Water (Electrolyte)		$E_{o.c.}$, mV
NaCl, ppm	Additives, ppm	
10	500 $Na_2Cr_2O_7$	-150
	500 $Na_2Cr_2O_7$ and 500 Na_2MoO_4	0
100	500 $Na_2Cr_2O_7$	-400
	500 $Na_2Cr_2O_7$ and 500 Na_2MoO_4	-300

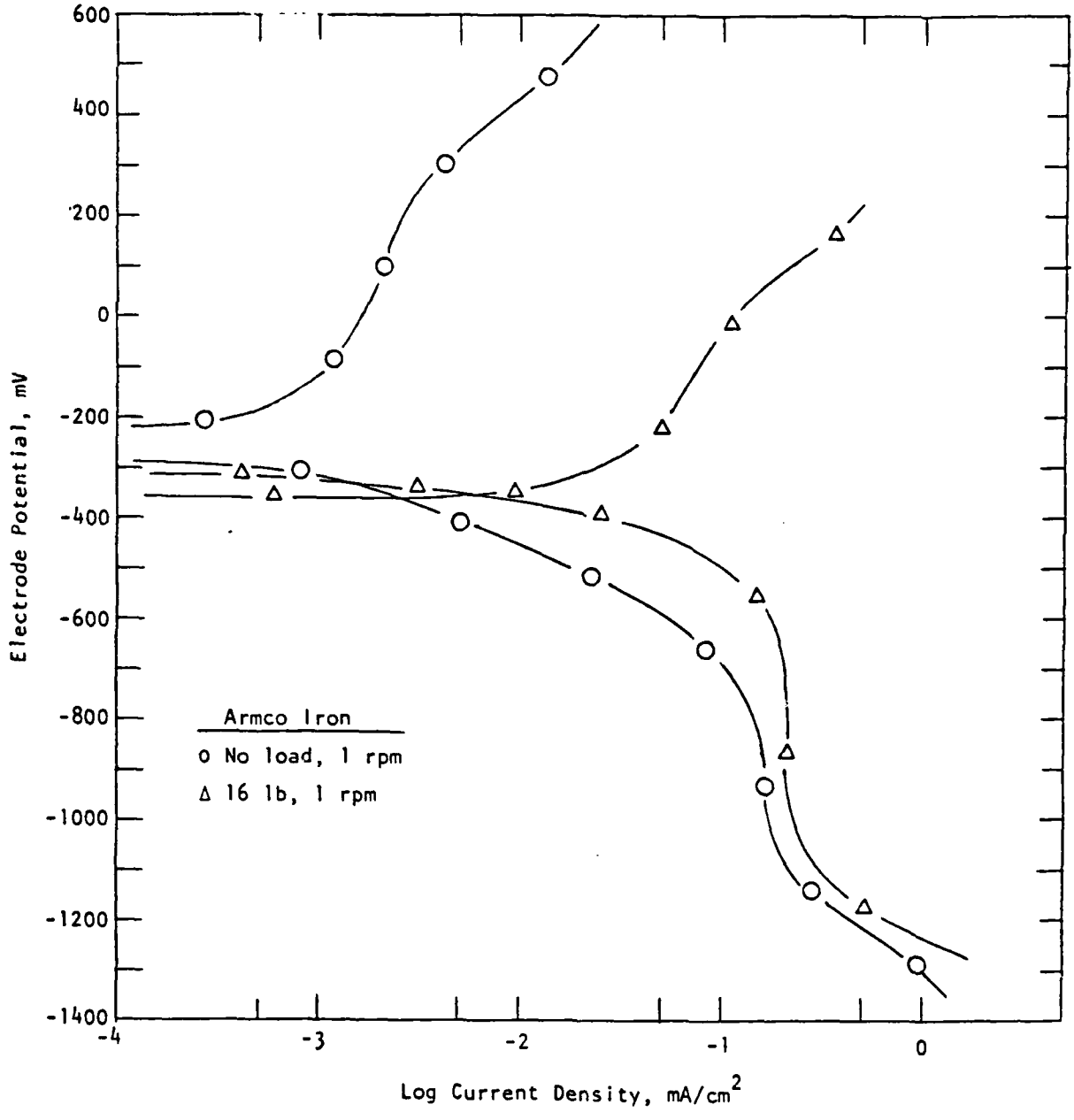

Figure 13. Polarization behavior of Armco iron in 100 ppm NaCl solution with 500 ppm Na_2MoO_4 (test 78).

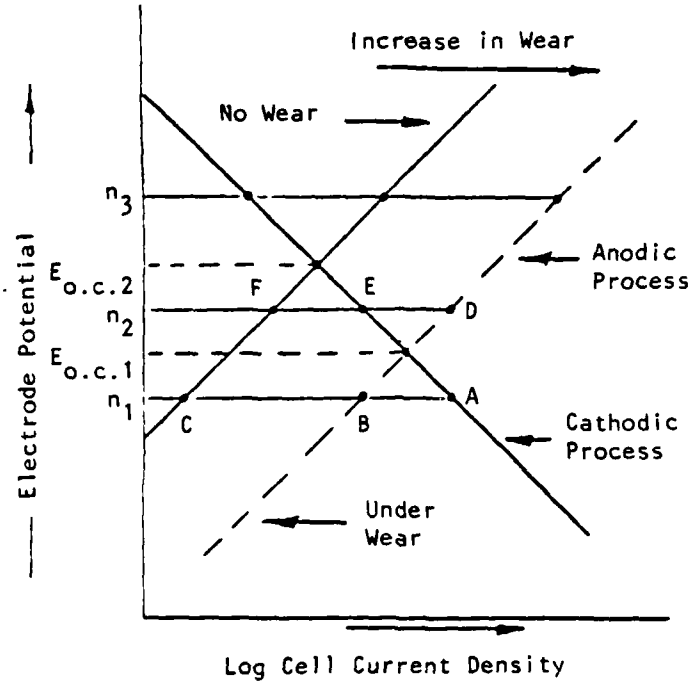

Figure 14. Schematic illustration of net cell current behavior under wear and no-wear conditions. Anodic control is assumed.

where i_a is the anodic current component having a positve value and i_c is the cathodic current component having a negative value. If the anodic process is only affected by wear, the anodic current component will shift to the right-hand side under wear condition. At a certain cathodic overpotential, say η_1 (Fig. 14), the net cell current under wear (w) conditions, $i_{net}(W)$, will be $(i_A - i_B)$; the net cell current in no-wear (nw) conditions, $i_{net}(nw)$, (or when wear process stopped) will be $(i_A - i_C)$. Therefore, increase in the net cell current during cathodic polarization will be observed when the wear process is stopped. However, the difference between $i_{net}(w)$ and $i_{net}(nw)$ will be small since the cell current values are plotted in logarithmic scale. Application of the same argument will explain the decrease in the net cell current in the high anodic overpotential region.

In the low anodic overpotential region (i.e., between $E_{o.c.1}$ and $E_{o.c.2}$), the overall net cell current will also be determined by two competing cell components, since the surface condition of the electrode is changing from the active to the passive state when the wear process stops. In Fig. 14, at a certain anodic overpotential, say η_2, the cathodic cell current component due to formation of a protective film (non-wear condition) will be $(i_E - i_F)$, and the anodic cell current component due to wear will be $(i_D - i_E)$. Therefore, polarity of the overall net cell current will depend on the magnitude of the difference between the two. If $(i_E - i_F) > (i_D - i_E)$, a cathodic polarity will result; an anodic polarity will require the condition $(i_E - i_F) < (i_D - i_E)$.

Experimentally, this phenomenon was observed by measuring the cell current at a given overpotential and at a fixed load with and without motion, i.e., with and without wear. The sample electrode was in the active state when the rotational motion was applied under load, whereas the sample electrode was allowed to be in the passive state when the rotation was stopped. A test result is shown in Fig. 15 as an example. The polarization curves in Fig. 15 represent M2 steel in 4 ppm NaOH solution (pH 10) under wear and no-wear conditions (test 53). Type M2 steel in this solution was passivated completely. During anodic polarization under wear, the cell current density was intermittently measured with the removal of wear condition (i.e,, the rotation was stopped but the load was not removed). The solid circle in Fig. 15 indicates the reduction of the cell current density due to regeneration of passive film with removal of wear at a given anodic overpotential. When motion was stopped, the cell current

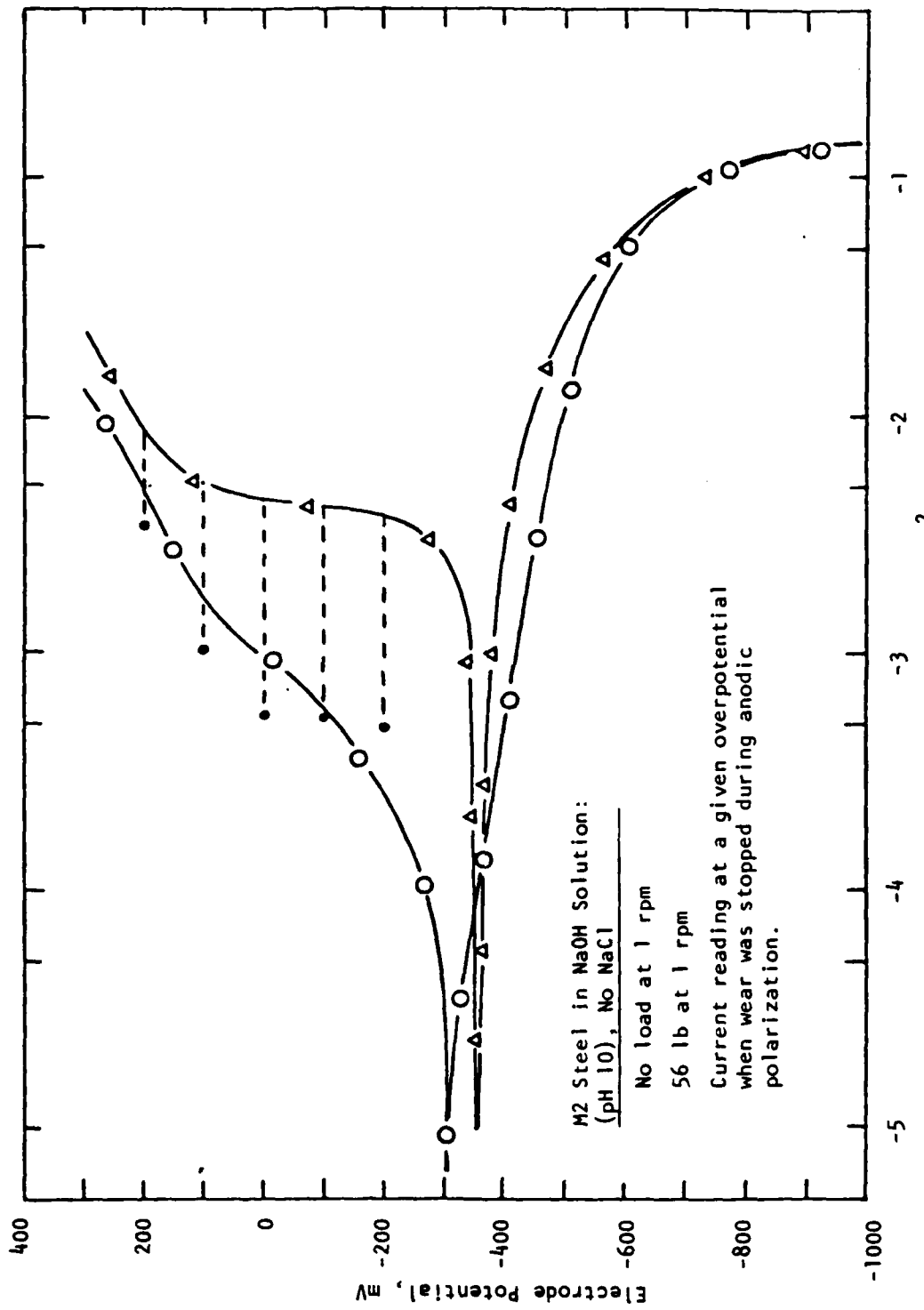

Figure 15. Polarization behavior of M2 steel in 4 ppm NaOH solution (pH 10) with and without wear (test 53). Cell current behavior at controlled overpotential is illustrated.

immediately dropped down to a level which would be obtainable without wear. This can be seen by comparing the open and solid circles. During cathodic polarization under wear, however, the removal of wear condition did not change the cell current at all. This observation confirms that the cathodic reaction process is not affected by wear. Particularly, with M2 steel in this solution, a clear linear Tafel region was observed under both wear and no-wear conditions. The corrosion rate increased significantly with wear, almost two orders of magnitude, from 1.7×10^{-5} mA/cm^2 (<0.01 mpy) for the no-wear condition to 1.3×10^{-3} mA/cm^2 (0.6 mpy) for a wear condition of 56 lb (25.4 kg) at 1 rpm (π/30 rad/s).

A similar result, showing the anodically controlled electrode polarization process under wear, was observed on the polarization of 304 SS in 0.5% and 3.5% NaCl solutions with removal of wear during both anodic and cathodic polarization under wear. It is suggested that this mechanism is operative in the polarization process under wear of Armco iron, M2 steel, and 52100 steel passivated in NaCl solutions with corrosion inhibitors.

A schematic diagram shown in Fig. 16 illustrates the kinetic mechanisms occurring in corrosion-wear systems. The solid lines represent each component of anodic and cathodic reactions. The dotted lines represent the total polarization curves under wear and no-wear conditions, respectively. These total polarization curves clearly demonstrate a change in the open-circuit potential in the active direction by wear ($E_{o.c.1}$ to $E_{o.c.2}$). Change in the open-circuit potential by wear generally resulted from an additive effect of two independent mechanisms: the disruption of the protective film, and the subsequent structural deformation of the metal surface. Increase in metal dissolution rate due to wear shifts the anodic component to the right-side, and consequently, increase in the corrosion rate is observed.

4.4 POTENTIODYNAMIC POLARIZATION TEST

The surface condition of a sample electrode is usually affected by polarization, although the relative significance depends on the corrosivity of test solutions. Armco iron is passivated in 10 ppm NaCl solution with 500 ppm $Na_2Cr_2O_7$ in immersion condition (open-circuit). However, it is severely corroded during anodic polarization. Since partial passivation was observed on

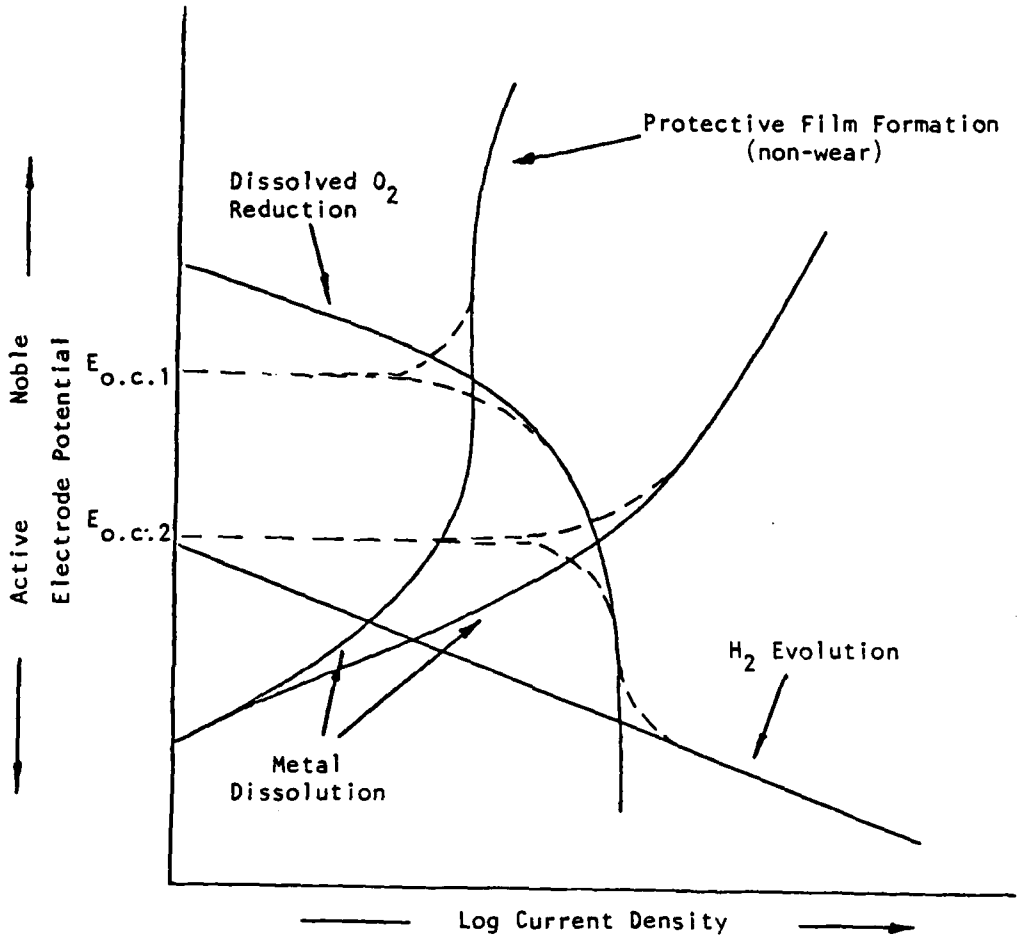

Figure 16. Suggested kinetic mechanisms of polarization process occurring in corrosion-wear systems.

Armco iron in 100 ppm NaCl solution with 500 ppm $Na_2Cr_2O_7$ as well as with 500 ppm $Na_2Cr_2O_7$ and 500 ppm Na_2MoO_4, the effect of anodic polarization on the stability of passive film was tested by potentiodynamic polarization measurement instead of potentiostatic technique.

Potentiodynamic testing was performed at the rate of 60 steps/min with each step of 2 mV, i.e., 120 mV/min. Potentiostatic polarization testing was performed at the rate of 3 steps/min with each step of 2 mV, i.e., 6 mV/min. Figure 17 shows the potentiodynamic polarization behavior of Armco iron in 100 ppm NaCl solution with 500 ppm $Na_2Cr_2O_7$ and 500 ppm Na_2MoO_4. Each polarization curve is marked with numerals starting with 1. In open-circuit condition, this electrode (Armco iron) was partially passivated with $E_{o.c.}$ of about -300 mV. The first cathodic loop (1 and 2) increased the open-circuit potential by approximately 100 mV. This is believed to be due to the effect of cathodic protection during cathodic potentiodynamic polarization.

During the first anodic loop (3 and 4) a small break appearing in curve 3 suggests that dissolution of the initial passive film is terminated at a lower anodic potential succeeded by the dissolution of iron at higher anodic potentials. When the scan was reversed at +200 mV, the cell current increased significantly instead of decreasing immediately, and severe corrosion resulted. With completion of the first anodic loop (3 and 4) the open-circuit potential shifted in the active direction to -520 mV. This value (-520 mV) of the open-circuit potential was usually observed under wear condition. It is apparent that the passive film is completely destroyed by the anodic loop.

The second cathodic loop (5 and 6) shifted the open-circuit potential in the active direction in contrast to the effect of the first cathodic loop. No presence of passive film was observed during the second anodic loop (7 and 8). When the scan was reversed, at +150 mV, a very large current increase was again observed. However, the open-circuit potential on completion of the second anodic loop (7 and 8) returned to the same value of $E_{o.c.}$ as at the start.

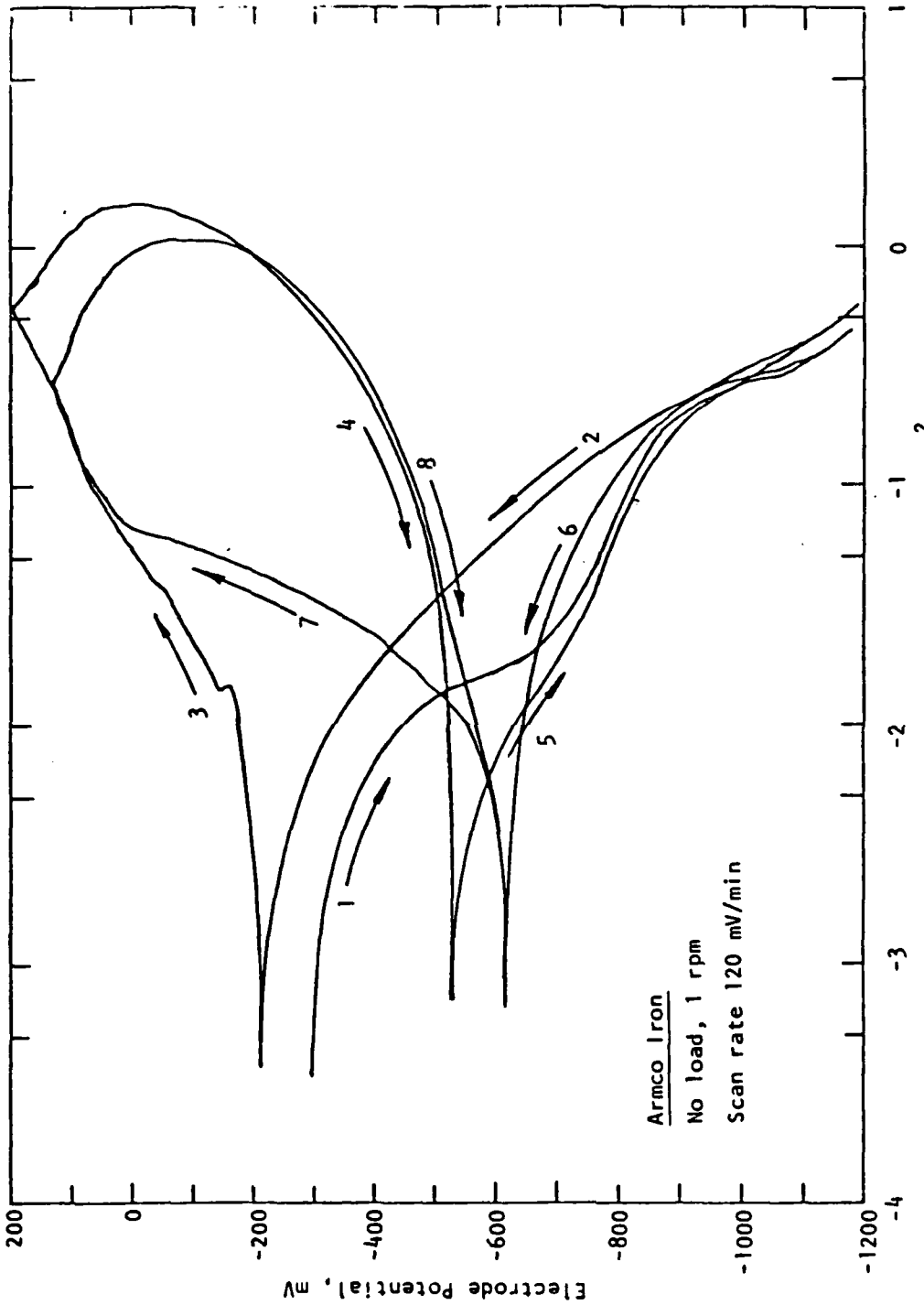

Figure 17. Potentiodynamic polarization behavior of Armco iron in 100 ppm NaCl solution with 500 ppm $Na_2Cr_2O_7$ and 500 ppm Na_2MoO_4 (test 71).

Potentiodynamic polarization is widely used to determine the range of pitting potential of a material with naturally occurring passive film (e.g., stainless steel in chloride solution). A schematic illustration of potentiodynamic polarization behavior of a material with naturally occurring passive film in pitting condition is shown in Fig. 18. In this case the cell current during the anodic loop decreases immediately as the scan is reversed. The characteristic difference in potentiodynamic behavior between a material with a naturally occurring passive film and a material with a passive film forming in the electrolyte is clearly evident in the anodic current at reverse scan. The reason why the anodic current at reverse scan increased as observed in Fig. 17 is not clearly understood yet. Further study with the potentiodynamic polarization technique is required to understand the stability of the passive film forming in the electrolyte.

4.5 STATISTICAL TEST DESIGN AND ANALYSIS

In order to determine the effectiveness of test variables (such as material, load, speed, etc.) on observed corrosion-wear properties (e.g., $E_{o.c.}$, $I_{corr.}$, weight change, etc.), a statistically designed test method based on the Plackett-Burman (P-B) design was utilized. In this design, a set of 6 independently controlled variables at 2 levels each was used. The levels selected for these variables were based on prior work and are given in the index of Table A-3 of Appendix A.

The P-B design calls for a set of 12 runs. Variables X1 to X6 of Table A-3 show the set of independently controlled parameters to be used in each experiment, whereas the remaining columns (X7 to X11) are used to estimate the experimental error during the analysis of the data. The statistical analyses were done separately for: (1) open-circuit potential behavior, (2) corrosion current density, and (3) weight changes in disk and pin electrodes.

4.5.1 Open-Circuit Potential Behavior

In this test program, the open-circuit potential reading was taken as the potential of the sample electrode immersed in electrolyte for the scheduled preexposure time before polarization. The open-circuit potentials under no-wear and wear conditions are given in Table 8 . Since the sample electrode potential was not stabilized long enough to reach a steady-state, the potential

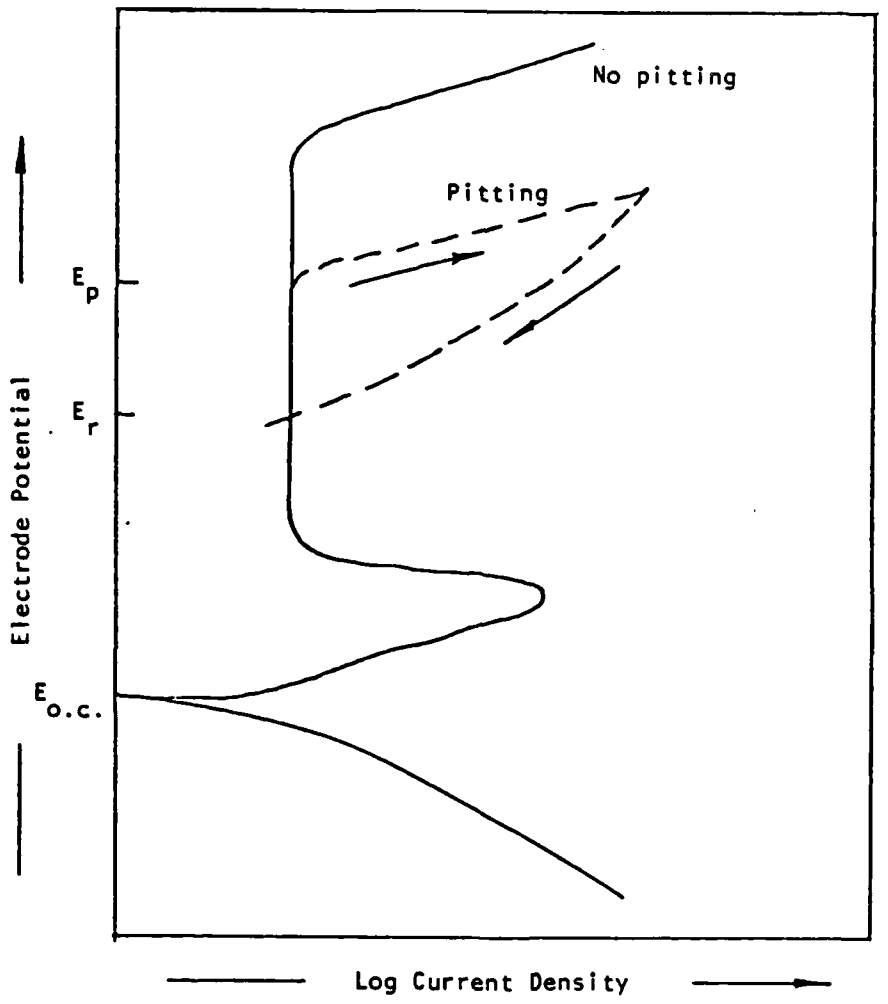

Figure 18. Schematic illustration of potentiodynamic polarization behavior of a material with naturally occurring passive film in pitting condition.

TABLE 8. OPEN CIRCUIT POTENTIAL MEASUREMENTS OF THE TWELVE-RUN MATRIX

Test No.	No-Wear Condition		Wear Condition[a]	
	Before Cathodic Polarization	After Cathodic Polarization	Before Cathodic Polarization	After Cathodic Polarization
80	-280	-240	-450	-440
81	-60	-60	-220	-220
82	+35	-50	-160	-160
83	-350	-730	-850	-850
84	+120	-380	-310	-295
85	+210	-30	-640	-630
86	-300	-340	-560	-560
87	+240	-245	-570	-580
88	-380	-720	-760	-720
89	+260	-60	-280	-530
90	-195	-260	-530	-530
91	-320	-675	-520	-680

[a]For statistical analysis, $\bar{Y}$ was taken as the average of $E_{o.c.}$ before and after cathodic polarization under wear condition.

readings taken before and after polarization showed some scatter, in some cases over a quite wide range.

(a) Under No-Wear Condition

The open-circuit potential values of both Armco iron and 52100 steel showed similar effects of corrosion inhibitors and cell environment, although no definite trend was observed due to lack of prior stabilization of potential. The formation of passive film by the presence of corrosion inhibitors would increase the open-circuit potential, while the deaeration of the cell environment would decrease the open-circuit potential due to removal of dissolved oxygen. The apparent order of electronegativity of the open-circuit potential fordifferent electrolyte conditions is as follows:

Material	Before Cathodic Polarization	After Cathodic Polarization
Armco iron	DP > AP > AA > DA	AP > DP > AA > DA
52100	DP > AP > AA > DA	AP > AA > DP > DA

where the abbreviations denote as below:

DP: Deaerated passive condition
AP: Aerated passive condition
AA: Aerated active condition
DA: Deaerated active condition

In all cases, the open-circuit potential showed the lowest value in deaerated active electrolyte among the respective groups. This observation would be a simple manifestation of the expected effects of electrolyte activity and environment on the open-circuit potential. Before cathodic polarization, both materials showed that the open-circuit potential in deaerated passive condition was higher than that in aerated passive condition. This result is contrary to the expected effect of environment, and is not clearly understood. However, the expected effect of environment on the open-circuit potential is reasonably well observed after cathodic polarization, by which time a considerable amount of dissolved oxygen removal is assumed. In this case, the open-circuit potential of both materials in deaerated passive electrolyte becomes more electronegative.

(b) Under Wear Condition

The open-circuit potential readings taken before and after cathodic polarization showed almost the same value except in tests 89 and 91. Although the open-circuit potentials were affected by six different variables, it is clearly seen that the open-circuit potentials of 52100 steel in deaerated active electrolyte (tests 83 and 91), as well as those of Armco iron in deaerated active electrolyte (test 88), had the most electronegative values within their respective material groups.

Table 9 summarizes the results of statistical analysis of the open-circuit potential behavior. Using the unassigned factor effects (X7 to X11), the minimum significant factor effect at a 90% confidence level was calculated to be 130. Any variable with an absolute factor effect value greater than this minimum has significance on the electronegativity of the open-circuit potential. This analysis indicated that the nature of electrolyte (X2), cell environment (X5), and material (X1) were the variables that showed statistically significant effect (at 90% confidence level) on the electronegativity of the open-circuit potential. At a lower level of confidence, only the load level was not significant. At the higher 95% confidence level, the activity of the electrolyte is significant in controlling the open-circuit potential.

Comparing the numerical values of "effect" of each variable, it may be noted that the effect of electrolyte on the open-circuit potential is predominant over all other factors. From a physical standpoint, it is also true that the potential of an electrode is mainly dependent on the ion activity (or corrosivity) of the electrolyte. This analysis also suggests that the open-circuit potential under wear condition is not very sensitive to the degree of wear (load and speed).

4.5.2 Potentiostatic Polarization Tests

Polarization studies of Armco iron and 52100 steel were performed under various test conditions based on the statistical design shown in Table A-3 of Appendix A. Typical polarization curves for each environmental group are presented in Figs. 19 through 22, and additional polarization curves are given in Appendix B. The corrosion current densities determined from the anodic polarization curves are given in Table 10 for both no-wear and wear conditions.

TABLE 9. RESULTS OF STATISTICAL ANALYSIS OF THE OPEN-CIRCUIT POTENTIAL ($\bar{Y}$)

Test No.	Trial	Mean	X1	X2	X3	X4	X5	X6	X7	X8	X9	X10	X11	$\bar{Y}$, (mV)
84	1	+	+	+	-	+	+	+	-	-	-	+	-	-302
83	2	+	+	-	+	+	+	-	-	-	+	-	+	-850
85	3	+	-	+	+	+	-	-	-	+	-	+	+	-635
82	4	+	+	+	+	-	-	-	+	-	+	+	-	-160
81	5	+	+	+	-	-	-	+	-	+	+	-	+	-220
91	6	+	+	-	-	-	+	-	+	+	-	+	+	-600
86	7	+	-	-	-	+	-	+	+	-	+	+	+	-560
88	8	+	-	-	+	-	+	+	-	+	+	+	-	-740
87	9	+	-	+	-	+	+	-	+	+	+	-	-	-575
80	10	+	+	-	+	+	-	+	+	+	-	-	-	-445
89	11	+	-	+	+	-	+	+	+	-	-	-	+	-405
90	12	+	-	-	-	-	-	-	-	-	-	-	-	-530
	Sum +	-6022	-2577	-2297	-3235	-3367	-3472	-2672	-2745	-3215	-3105	-2997	-3270	
	Sum -	0	-3445	-3725	-2787	-2655	-2550	-3350	-3277	-2807	-2917	-3025	-2752	
	Overall Sum	-6022	-6022	-6022	-6022	-6022	-6022	-6022	-6022	-6022	-6022	-6022	-6022	
	Diff.	-6022	868	1428	-448	-712	-922	678	532	-408	-188	28	-518	
	Effect	-501.8	144.7	238	-74.7	-118.7	-153.7	113	88.6	-68.0	-31.3	4.6	-86.3	

S_{FE} = 64.68

[MIN]: 1.476 x 64.68 = 95.4 [80% confidence level]

2.015 x 64.68 = 130.0 [90% confidence level]

2.571 x 64.68 = 166.3 [95% confidence level]

	(+)	(-)
X1	52100	Armco Fe
X2	Passive	Active
X3	56 lb	16 lb
X4	10 rpm	1 rpm
X5	No air	Air
X6	4 hr	1 hr

$\bar{Y}$ Average open-circuit potential.

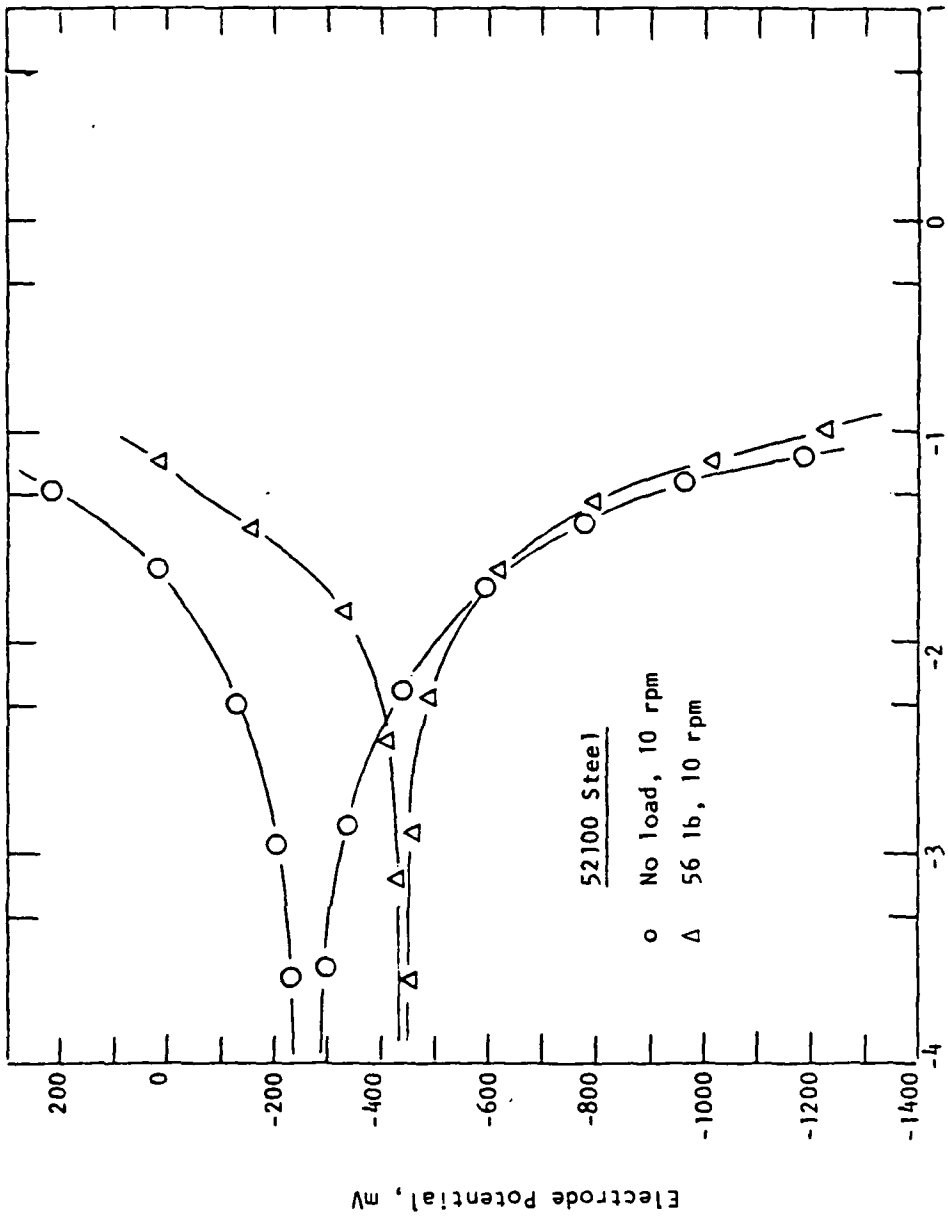

Figure 19. Polarization behavior of 52100 steel in 10 ppm NaCl solution in ambient air (test 80).

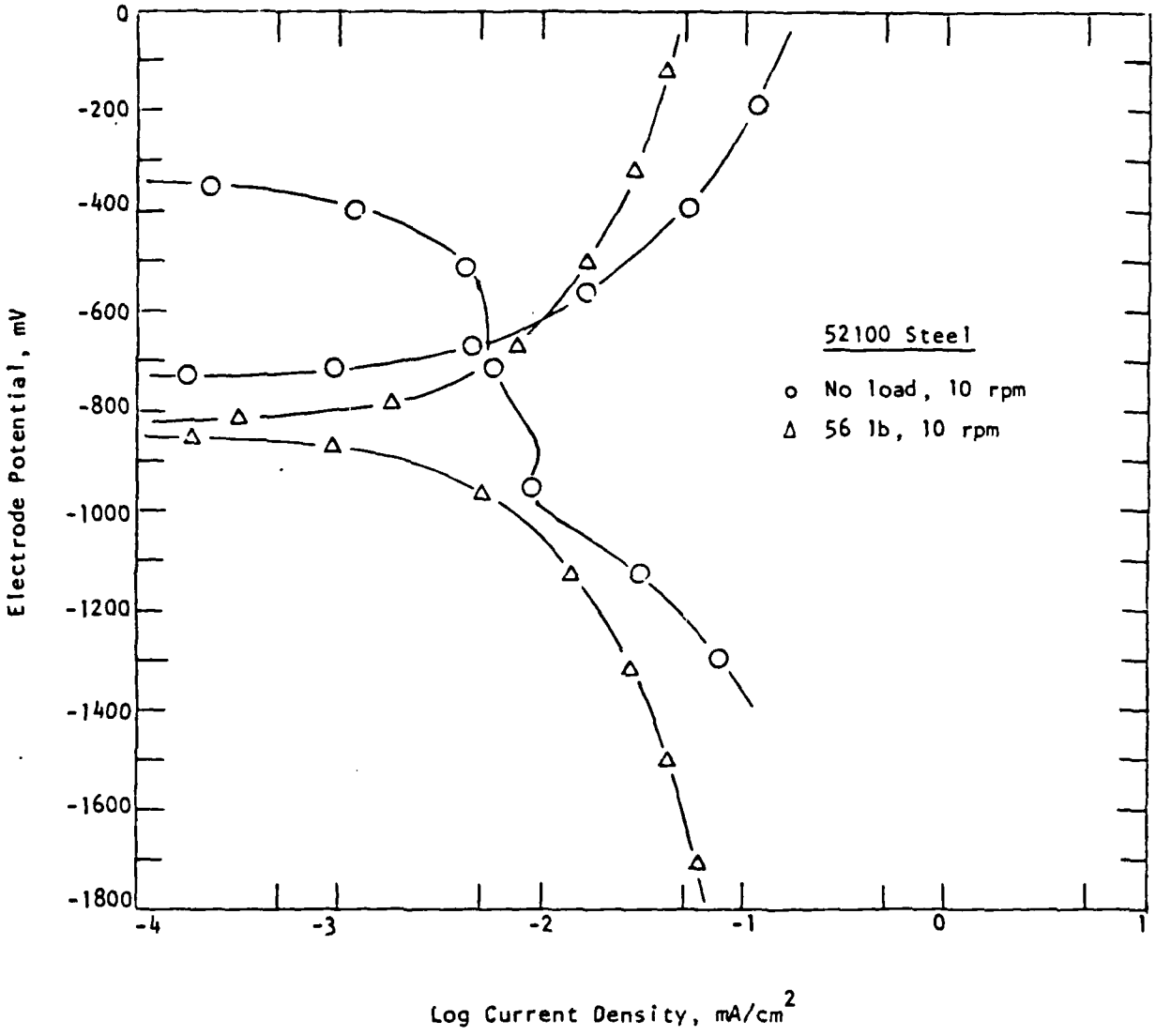

Figure 20. Polarization behavior of 52100 steel in 10 ppm NaCl solution in deaerated condition (test 83).

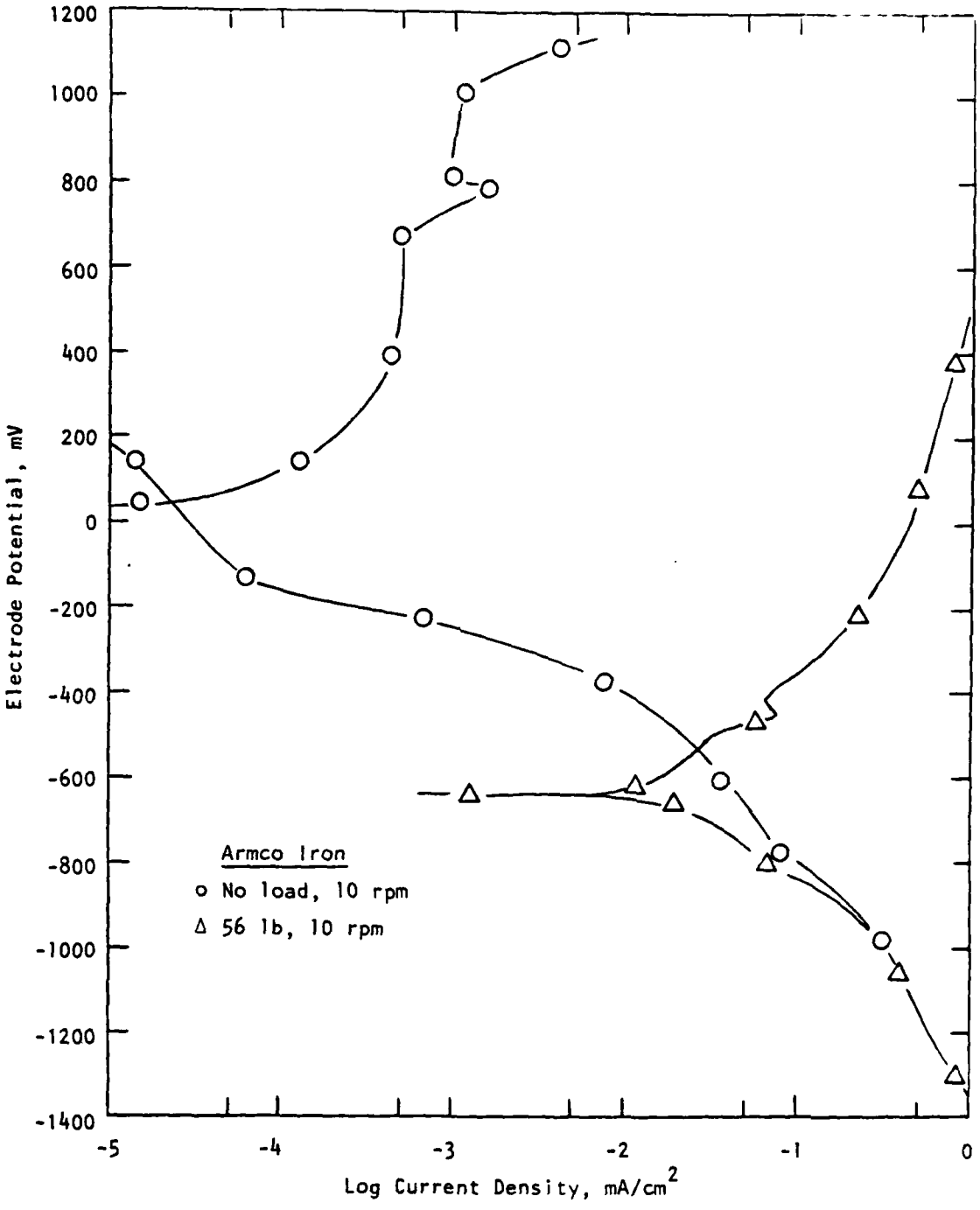

Figure 21. Polarization behavior of Armco iron in 10 ppm NaCl solution with 500 ppm $Na_2Cr_2O_7$ and 500 ppm Na_2MoO_4 in ambient air (test 85).

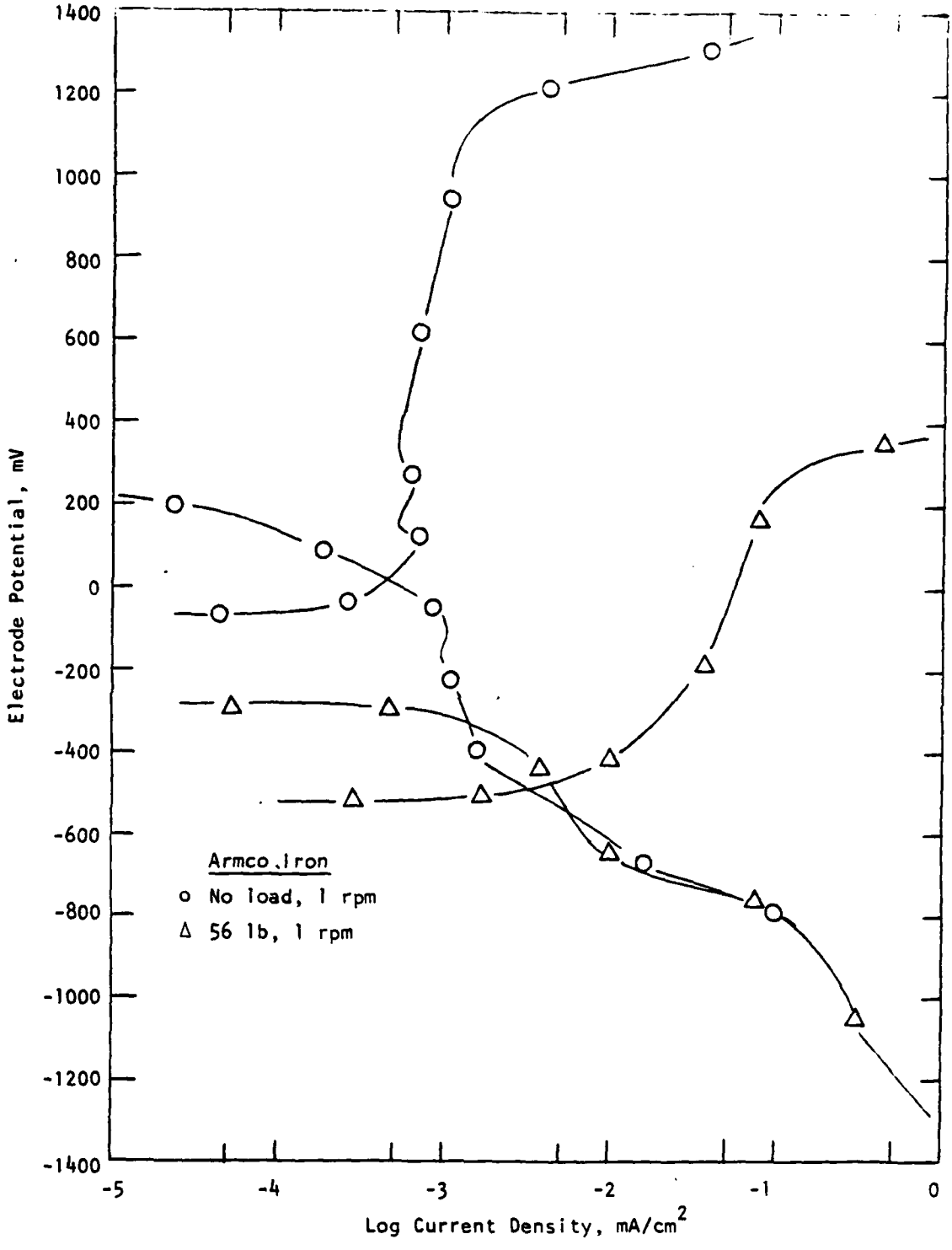

Figure 22. Polarization behavior of Armco iron in 10 ppm NaCl solution with 500 ppm $Na_2Cr_2O_7$ and 500 ppm Na_2MoO_4 in deaerated condition (test 89).

TABLE 10. CORROSION CURRENT DENSITY DETERMINED FROM POLARIZATION CURVES[a]

Test No.	Material	$I_{corr.}$, mA/cm^2 (mpy)	
		No-Wear Condition	Wear Condition
80	52100 steel	2.5×10^{-3} (1.14)	4.5×10^{-3} (2.06)
81	52100 steel	7.0×10^{-4} (0.32)	3.8×10^{-3} (1.74)
82	52100 steel	7.0×10^{-4} (0.32)	4.0×10^{-3} (1.83)
83	52100 steel	2.7×10^{-3} (1.23)	1.0×10^{-3} (0.46)
84	52100 steel	6.0×10^{-4} (0.27)	1.5×10^{-3} (0.68)
85	Armco iron	4.0×10^{-4} (0.18)	1.4×10^{-2} (6.41)
86	Armco iron	2.5×10^{-3} (1.14)	6.0×10^{-3} (2.75)
87	Armco iron	7.0×10^{-4} (0.32)	6.4×10^{-3} (2.93)
88	Armco iron	1.5×10^{-3} (0.68)	4.0×10^{-4} (0.18)
89	Armco iron	6.0×10^{-4} (0.27)	2.0×10^{-3} (0.91)
90	Armco iron	1.3×10^{-3} (0.59)	7.0×10^{-3} (3.21)
91	52100 steel	2.7×10^{-3} (1.24)	3.0×10^{-3} (1.37)

[a]Determined from extrapolating the anodic curve.

There are four factors under no-wear condition (no load and speed) and six factors under wear condition that affect the corrosion current density and the polarization behavior. The corrosion current density ($I_{corr.}$) data under no-wear condition were analyzed in a phenomenological manner. Later, the $I_{corr.}$ values under wear condition were analyzed both phenomenologically and statistically.

(a) Phenomenological Analysis of $I_{corr.}$ Data Under No-Wear Conditions

The detailed test conditions of polarization measurement under no-wear and the corrosion current densities determined from the polarization curves are presented in Table 11. By comparing the test conditions of one experiment with another, a set of two experiments for which the conditions of three variables are the same with only one differing can be found, Then, the effect of the single variable on corrosion current density can be isolated and analyzed. This analysis is given in Table 12.

Effect of Electrolyte. The analysis showed that the active electrolyte was 2 to 4 times more aggressive than the passive, under no-wear condition, on both materials and in different environments.

Effect of Environment. The analysis showed that aerated environment under 4 hr exposure was more aggressive by about 50% over deaerated environment in both active and passive electrolytes. In 1 hr exposure, aerated environment appeared to be less aggressive than deaerated environment in passive electrolyte.

Effect of Material. Under 4 hr preexposure in both active and passive environment, the two materials corroded more or less in equal degrees. Under 1 hr preexposure in a passive/aerated environment, Armco iron appeared to be corroding a lesser amount when compared to 52100 steel.

Effect of Preexposure Time. Under active electrolyte in an aerated condition, Armco iron corroded twice as much with a preexposure of 4 hr compared to 1 hr preexposure. In a passive electrolyte, neither Armco iron nor 52100 steel showed any different effect with longer preexposure.

Replicated Data. Tests 83 and 91 were conducted under identical conditions and the $I_{corr.}$ values were also identical, indicating a good reproducibility of tests done over an extended period. This also indicated reliability of the experimental approach and equipment design.

TABLE 11. TEST CONDITIONS OF POLARIZATION MEASUREMENTS UNDER NO WEAR AND CORROSION CURRENT DENSITY DATA

Test No.	X1	X2	X5	X6	$I_{corr.}$, mA/cm^2 (mpy)
80	+	-	-	+	2.5×10^{-3} (1.14)
81	+	+	-	+	7.0×10^{-4} (0.32)
82	+	+	-	-	7.0×10^{-4} (0.32)
83	+	-	+	-	2.7×10^{-3} (1.23)
84	+	+	+	+	6.0×10^{-4} (0.27)
85	-	+	-	-	4.0×10^{-4} (0.18)
86	-	-	-	+	2.5×10^{-3} (1.14)
87	-	+	+	-	7.0×10^{-4} (0.32)
88	-	-	+	+	1.5×10^{-3} (0.68)
89	-	+	+	+	6.0×10^{-4} (0.27)
90	-	-	-	-	1.3×10^{-3} (0.59)
91	+	-	+	-	2.7×10^{-3} (1.24)

	Index of Variables	
	(+)	(-)
X1	52100 steel	Armco iron
X2	Passive	Active
X5	No air	Air
X6	4 hr	1 hr

TABLE 12. PHENOMENOLOGICAL ANALYSIS OF CORROSION CURRENT DENSITY UNDER NO-WEAR CONDITIONS

Factor Effect	Test	I_{corr} Ratio	Remarks
1. Effect of Electrolyte, Active/Passive	80 vs. 81	3.6	52100 steel/aerated/4 hr
	90 vs. 85	3.3	Armco iron/aerated/1 hr
	88 vs. 89	2.5	Armco iron/deaerated/4 hr
2. Effect of Oxygen, Aeration/Deaeration	86 vs. 88	1.7	Armco iron/active/4 hr
	81 vs. 84	1.2	52100 steel/passive/4 hr
	85 vs. 87	0.6	Armco iron/passive/1 hr
3. Effect of Material Armco iron/52100 steel	86 vs. 80	1.0	active/aerated/4 hr
	89 vs. 84	1.0	passive/deaerated/4 hr
	85 vs. 82	0.6	passive/aerated/1 hr
4. Effect of Preexposure Time, 4 hr/1 hr	86 vs. 90	1.9	Armco iron/active/aerated
	81 vs. 82	1.0	52100 steel/passive/aerated
	89 vs. 87	0.9	Armco iron/passive/deaerated
5. Replicable Testing	83 vs. 91	1.0	Identical conditions of 52100 steel/active/deaerated/ 1 hr

(b) Phenomenological Analysis of $I_{corr.}$ Data Under Wear Condition

In Aerated Active Electrolyte (Tests 80, 86, and 90). Both Armco iron and 52100 steel were moderately corroded. The polarization curve for either polarity showed only one branch under both wear and no-wear conditions. It would be due to the significant effect of resistant polarization occurring in poorly conductive electrolyte. Under wear condition, the open-circuit potential shifted in the active direction, and consequently, appreciable increase in the corrosion current density resulted.

In Deaerated Active Electrolyte (Tests 83, 88, and 91). Nonuniform corrosion occurred on both Armco iron and 52100 steel in this solution. Fairly adherent, black iron oxides were formed locally; however, most of them were washed off by gentle scrubbing. Only one branch appeared on all polarization curves other than the cathodic curve under no-wear condition which had two branches. It should be noted that the control of electrolyte environment before setting the disk electrode in the electrolyte was not possible because of the present arrangement of the experiment. Therefore, the disk electrode was already placed in the electrolyte at the beginning of deaeration. During the cathodic polarization under no-wear, it was clear that appreciable amounts of dissolved oxygen were still present in the electrolyte since the oxygen reduction curve appeared as the first cathodic branch; however, it disappeared as deaeration continued. The anodic polarization curves suggest that the iron dissolution rate under wear condition would be approximately the same, or not greater than, the iron dissolution rate under no-wear condition. Particularly, polarization curves of test 88 showed that the anodic dissolution rate under wear was much less than that under no-wear condition. A similar result was observed on test 83.

In Aerated Passive Electrolyte (Tests 81, 82, and 85). In this solution, both Armco iron and 52100 steel were passivated completely. However, polarization behaviors of these materials were quite different. Under no-wear condition, Armco iron showed three branches in the cathodic curve, each of which would represent the reduction reaction of dichromate, dissolved oxygen, and hydrogen evolution in the increasing order of cathodic potential, and two branches of anodic curve representing passive and transpassive states. Under wear condition, the open-circuit potential of Armco iron shifted about 800 mV

in the active direction; an almost three orders of magnitude increase in anodic cell current was observed. Armco iron under wear condition showed two branches of cathodic curve which eventually merged with the cathodic curve under no-wear condition at high cathodic overpotentials. It is clear that the corrosion current of the sample electrode is controlled anodically. Type 52100 steel showed two cathodic branches (oxygen reduction and hydrogen evolution), and one anodic branch under both wear and no-wear conditions. A heavy concentration of polarization occurred in the oxygen reduction process under wear. Anodic cell current under wear condition increased about one order of magnitude from that under no-wear condition.

In Deaerated Passive Electrolyte (Tests 84, 87, and 89). Polarization behaviors of Armco iron and 52100 steel in this solution were similar to those observed in the aerated passive solution except that the potential range for oxygen reduction decreased significantly due to deaeration. In general, the anodic cell current of Armco iron was more affected by wear than that of 52100 steel.

(c) Statistical Analysis of $I_{corr.}$ Data Under Wear Condition

The corrosion current densities given in Table 10 were determined from extrapolation of the anodic curve since the preexposure time, which was not long enough for the potential to be stabilized, resulted in some discrepancy between the values of the corrosion current density determined from the cathodic and the anodic curve. Table 13 lists the results from the twelve-run Plackett-Burman analysis of the corrosion rate. The corrosion rates given in Table 13 are in mpy units converted from the corrosion current densities given in Table 10.

The statistical analysis showed the minimum significant factor effect (from random effects) at a 90% confidence level to be 1.12. The analysis further indicated that cell environment, material, and preexposure time were the variables that showed statistically significant effects on the corrosion rate under wear condition. From a physical standpoint, the cell environment and material should be significant factors determining the corrosion characteristics. The preexposure time appears to have more significance on corrosion rate under wear condition than electrolyte, load, and speed. Electrolyte was found to be very important under no-wear condition.

TABLE 13. RESULTS OF STATISTICAL ANALYSIS OF THE CORROSION RATE

Test No.	Trial	Mean	X1	X2	X3	X4	X5	X6	X7	X8	X9	X10	X11	$\bar{Y}$, (mpy)
84	1	+	+	+	-	+	+	+	-	-	-	+	-	0.68
83	2	+	+	-	+	+	+	-	-	-	+	-	+	0.46
85	3	+	-	+	+	+	-	-	-	+	-	+	+	6.41
82	4	+	+	+	+	-	-	-	+	-	+	+	-	1.83
81	5	+	+	+	-	-	-	+	-	+	+	-	+	1.74
91	6	+	+	-	-	-	+	-	+	+	-	+	+	1.37
86	7	+	-	-	-	+	-	+	+	-	+	+	+	2.75
88	8	+	-	-	+	-	+	+	-	+	+	+	-	0.18
87	9	+	-	+	-	+	+	-	+	+	+	-	-	2.93
80	10	+	+	-	+	+	-	+	+	+	-	-	-	2.06
89	11	+	-	+	+	-	+	+	+	-	-	-	+	0.91
90	12	+	-	-	-	-	-	-	-	-	-	-	-	3.21
	Sum +	24.53	8.14	14.50	11.85	15.29	6.53	8.32	11.85	14.69	9.89	13.22	13.64	
	Sum -	0	16.39	10.03	12.68	9.24	18.00	16.21	12.68	9.84	14.64	11.31	10.89	
	Overall Sum	24.53	24.53	24.53	24.53	24.53	24.53	24.53	24.53	24.53	24.53	24.53	24.53	
	Diff.	24.53	-8.25	4.47	-0.83	6.05	-11.47	-7.89	-0.83	4.85	-4.75	1.91	2.75	
	Effect	2.04	-1.37	0.74	-0.14	1.01	-1.91	-1.31	-0.13	0.81	-0.79	0.32	0.46	

S_{FE} = 0.56

[MIN]: 1.476 x 0.56 = 0.82 [80% confidence level]

2.01 x 0.56 = 1.12 [90% confidence level]

2.571 x 0.56 = 1.44 [95% confidence level]

	(+)	(-)
X1	52100	Armco Fe
X2	Passive	Active
X3	56 lb	16 lb
X4	10 rpm	1 rpm
X5	No air	Air
X6	4 hr	1 hr
$\bar{Y}$	Corrosion rate	

At the higher confidence level of 95%, only environment appears to be the most significant. At a lower confidence level of 80%, only load appears to be insignificant and the electrolyte is marginally significant. More data are needed to substantiate these tentative observations.

4.5.3 Gravimetric Analysis

The weights of both disk and pin electrodes were measured before and after the corrosion-wear test. Table 14 summarizes the weight change data of tests 80-91. The unit of weight loss is given in $mg/cm^2/hr$ for the disk electrode and mg/hr for the pin electrode. The geometric factor for pin electrode is ignored since all the pin electrodes have the same geometry of hemispherical end, and the actual wear surface is very small. The negative sign represents weight loss, and the positive sign represents weight gain. In the present corrosion-wear system, the weight change occurs due to the synergism of wear and corrosion. However, it was observed that weight change due to corrosion was negligibly small compared to the weight change due to wear. Therefore, an effort to separate individual contribution to the weight change was not attempted in the present analysis.

Tables 15 and 16 summarize the results of the statistical analysis on the weight change of disk and pin electrodes, respectively. For the weight change of disk electrodes, the minimum significant factor effect is 1.310 at 90% confidence level and 0.962 at 80% confidence level. At 90% confidence level, material is the only variable that has statistically significant effect on the weight change of disk electrodes. At lower confidence level of 80%, the three most significant variables that affect the weight change of disk electrodes were material, speed, and environment. The limited data with a large unassigned factor effect indicate that with a larger data base further reduction in this factor might be possible and a more significant determination of the controlled variables effects could be obtained.

For the weight change of pin electrodes, the minimum significant factor effect is 0.729 at a 90% confidence level. The absolute factor effect values of load and speed were greater than the value of the minimum significant factor effect. Therefore, these two variables had statistically significant effects

TABLE 14. WEIGHT CHANGE DATA OF DISK AND PIN ELECTRODES

Test No.	Material	Disk Electrode			Pin Electrode	
		Weight Change, mg	Area, cm^2	Weight Change Rate, $mg/cm^2/hr$	Weight Change, mg	Weight Change Rate, mg/hr
80	52100 Steel	-0.8	3.59	-0.036	-14.1	-2.35
81	52100 Steel	+0.5	1.48	+0.040	-0.2	-0.02
82	52100 Steel	+3.3	2.39	+0.146	-2.0	-0.21
83	52100 Steel	-0.2	3.97	-0.007	-15.4	-2.57
84	52100 Steel	-0.5	2.31	-0.030	-1.8	-0.24
85	Armco Iron	-41.5	3.10	-2.232	-3.7	-0.61
86	Armco Iron	-62.1	1.79	-5.124	-2.4	-0.35
87	Armco Iron	-21.3	2.39	-1.365	-1.1	-0.17
88	Armco Iron	-4.2	2.50	-0.259	-0.4	-0.06
89	Armco Iron	-3.2	3.74	-0.130	-5.2	-0.80
90	Armco Iron	-21.5	2.58	-1.071	-1.3	-0.17
91	52100 Steel	-3.2	1.47	-0.326	-0.7	-0.10

TABLE 15. RESULTS OF STATISTICAL ANALYSIS OF WEIGHT CHANGE OF DISK ELECTRODES

Test No.	Trial	Mean	X1	X2	X3	X4	X5	X6	X7	X8	X9	X10	X11	$\bar{Y}_3$ mg/cm^3/hr
84	1	+	+	+	-	+	+	+	-	-	-	+	-	-0.030
83	2	+	+	-	+	+	+	-	-	-	+	-	+	-0.007
85	3	+	-	+	+	+	-	-	-	+	-	+	+	-2.232
82	4	+	+	+	+	-	-	-	+	-	+	+	-	+0.146
81	5	+	+	+	-	-	-	+	-	+	+	-	+	+0.040
91	6	+	+	-	-	-	+	-	+	+	-	+	+	-0.326
86	7	+	-	-	-	+	-	+	+	-	+	+	+	-5.124
88	8	+	-	-	+	-	+	+	-	+	+	+	-	-0.259
87	9	+	-	+	-	+	+	-	+	+	+	-	-	-1.365
80	10	+	+	-	+	+	-	+	+	+	-	-	-	-0.036
89	11	+	-	+	+	-	+	+	+	-	-	-	+	-0.130
90	12	+	-	-	-	-	-	-	-	-	-	-	-	-1.071
	Sum +	-10.39	-0.21	-3.57	-2.51	-8.79	-2.11	-5.53	-6.83	-4.17	-6.56	-7.82	-7.77	
	Sum -	0	-10.18	-6.82	-7.87	-1.60	-8.27	-4.85	-3.55	-6.21	-3.82	-2.56	-2.61	
	Overall Sum	-10.39	-10.39	-10.39	-10.39	-10.39	-10.39	-10.39	-10.39	-10.39	-10.39	-10.39	-10.39	
	Diff.	-10.39	9.96	3.25	5.35	-7.19	6.16	-0.68	-3.27	2.03	-2.74	-5.25	-5.16	
	Effect	-0.86	1.66	0.54	0.89	-1.19	1.02	-0.11	-0.54	0.33	-0.45	-0.87	-0.86	

S_{FE} = 0.652

[MIN]: 1.476 x 0.652 = 0.962 [80% confidence level]

2.01 x 0.652 = 1.310 [90% confidence level]

2.571 x 0.652 = 1.67 [95% confidence level]

	(+)	(-)
X1	52100	Armco Fe
X2	Passive	Active
X3	56 lb	16 lb
X4	10 rpm	1 rpm
X5	No air	Air
X6	4 hr	1 hr

$\bar{Y}$ Weight change of disk electrode.

TABLE 16. RESULTS OF STATISTICAL ANALYSIS OF WEIGHT CHANGE OF PIN ELECTRODES

Test No.	Trial	Mean	X1	X2	X3	X4	X5	X6	X7	X8	X9	X10	X11	$\bar{Y}$, (mg/hr)
84	1	+	+	+	-	+	+	+	-	-	-	+	-	0.24
83	2	+	+	-	+	+	+	-	-	-	+	-	+	2.57
85	3	+	-	+	+	+	-	-	-	+	-	+	+	0.61
82	4	+	+	+	+	-	-	-	+	-	+	+	-	0.21
81	5	+	+	+	-	-	-	+	-	+	+	-	+	0.02
91	6	+	+	-	-	-	+	-	+	+	-	+	+	0.10
86	7	+	-	-	-	+	-	+	+	-	+	+	+	0.35
88	8	+	-	-	+	-	+	+	-	+	+	+	-	0.06
87	9	+	-	+	-	+	+	-	+	+	+	-	-	0.17
80	10	+	+	-	+	+	-	+	+	+	-	-	-	2.35
89	11	+	-	+	+	-	+	+	+	-	-	-	+	0.80
90	12	+	-	-	-	-	-	-	-	-	-	-	-	0.17
	Sum +	7.65	5.49	2.05	6.6	6.29	3.94	3.82	3.98	3.31	3.38	1.57	4.45	
	Sum -	0	2.16	5.6	1.05	1.36	3.71	3.83	3.67	4.34	4.27	6.08	3.20	
	Overall Sum	7.65	7.65	7.65	7.65	7.65	7.65	7.65	7.65	7.65	7.65	7.65	7.65	
	Diff.	7.65	3.33	-3.55	5.55	4.93	0.23	-0.01	0.31	-1.03	-0.89	-4.51	1.25	
	Effect	0.64	0.55	0.59	0.92	0.82	0.04	-0.001	0.05	-0.17	-0.14	0.75	0.20	

S_{FE} = 0.363

[MIN]: 1.476 x 0.363 = 0.53 [80% confidence level]

2.01 x 0.363 = 0.729 [90% confidence level]

2.571 x 0.363 = 0.93 [95% confidence level]

	(+)	(-)
X1	52100	Armco Fe
X2	Passive	Active
X3	56 lb	16 lb
X4	10 rpm	1 rpm
X5	No air	Air
X6	4 hr	1 hr

$\bar{Y}$ Weight change of pin electrode.

on the weight change of pin electrodes. At the lower confidence level of 80%, additional variables that become significant are electrolyte and material.

The above analysis shows that the wear-corrosion of pin and disk electrodes was influenced in different ways under the test conditions. These differences are related to the geometry of the electrodes and the nature of their motion. The pin surface is under constant wear condition while the disk surface is continuously being exposed to electrolyte after wearing. Thus, the sensitivity of pin wear to load and speed can be understood.

4.6 METALLURGICAL EXAMINATION OF CORROSION-WEAR SURFACES

Analytical scanning electron microscopy, which combines the examination of surface morphology with energy-dispersive (EDX) and/or wavelength-dispersive (WDX) X-ray elemental analysis, was used for qualitative characterization of surfaces of selected corrosion-wear test specimens of 52100 steel and Armco iron.

SEM examination was performed at IITRI's analytical SEM facility that includes a JEOL JSM-50A SEM fitted with a JEOL 4-crystal WDX spectrometer and a computerized ORTEC QUAN II EDX spectrometer. In each case, the metallurgical evaluation consisted of low-magnification (20X-50X) SEM examination of the surface of the pins and the disk from a given test to select typical as well as non-typical affected areas for further detailed examination of surface morphologies. EDX spectra were obtained from these areas of interest to identify the various elements present in the corrosion-wear debris, and then elemental maps showing relative abundance of various elements in the area of interest were generated with the help of the EDX spectrometer. The EDX system is capable of detecting elements from atomic number 11 (sodium) and above.

Elemental X-ray maps, along with SEM photomicrographs of a certain area of the surface, provide useful information pertaining to the nature of wear and/or corrosion, wear-corrosion product(s), and wear debris, in relation to the test conditions used.

The following paragraphs summarize the results of metallurgical examination of various specimens studied in this project. Generally, the following discussion refers to the test numbers corresponding to a particular specimen.

Details of test conditions such as materials, electrolyte used, wear condition employed (load, speed, time), preexposure time, and electrolyte environment (aerated or deaerated) are tabulated elsewhere in this report. Both disk and pin electrodes of Armco iron from tests 68, 69, 70, 72, 77, 78, 79, 87, and 88, and of 52100 steel from tests 74, 75, 76, 83, and 84, were selected for SEM examination of corrosion-wear surfaces. However, only a few representative analyses are presented in the following discussion.

4.6.1 Armco Iron Electrodes

Surface features of Armco iron pin electrodes from various tests were typical of the wear surface of a soft material arising from local cold welding. In general, rough surfaces with heavy wear in some areas exhibiting deep tracks resulting from large metal removal were observed. At higher magnifications, the wear tracks displayed deep gouged-out areas filled with granular wear-corrosion debris of varying coarseness. Depending upon the electrolyte and inhibitors employed, wear debris present on the pin electrodes showed retention of varying amounts of Cr and Mo.

Figure 23 presents typical SEM photomicrographs, EDX spectra, and X-ray elemental maps of Armco iron pin electrode wear surface (test 69). The pin wear surface showed essentially parallel wear tracks with some damaged areas at low magnifications (Fig. 23a). A general EDX spectra of the above pin surface showed presence of mainly Fe with small amounts of Cr and Mo (Fig. 23b). Figures 23c and d show high-magnification views of the pin wear surface. Inside the damaged areas, entrapped fine granular wear-corrosion debris is clearly visible. Mo and Cr X-ray maps of the area shown in Fig. 23c are presented in Figs. 23e and f, respectively. These X-ray maps confirm that both Mo and Cr are deposited on the wear surfaces. The higher density of bright spots in the Cr map indicated that Cr deposition may be relatively higher than Mo.

Figures 24a and b show low-magnification views of the pin electrode wear surfaces from tests 87 and 86, respectively. The wear area was smaller and somewhat elongated on test 88 pin (Fig. 24b). Both the pin electrodes displayed essentially parallel wear tracks. At higher magnifications, test 87 pin wear surface displayed smoother tracks and tracks containing many gouged-out areas. Both these areas were covered with a thick corrosion-wear debris that exhibited a granular morphology. In addition, corrosion products in smoother areas

SEM No. 6737 ~20X

(a)

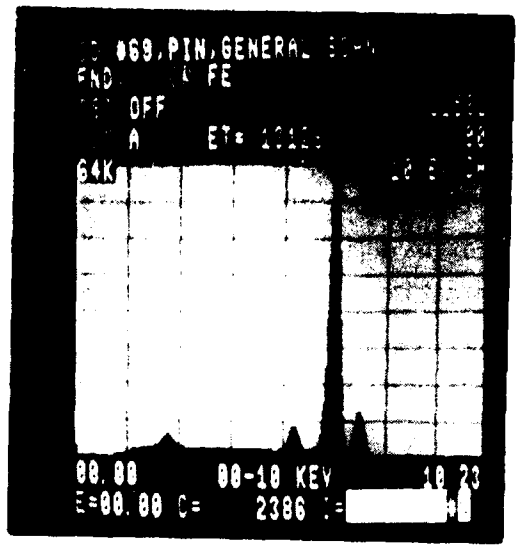

(b)

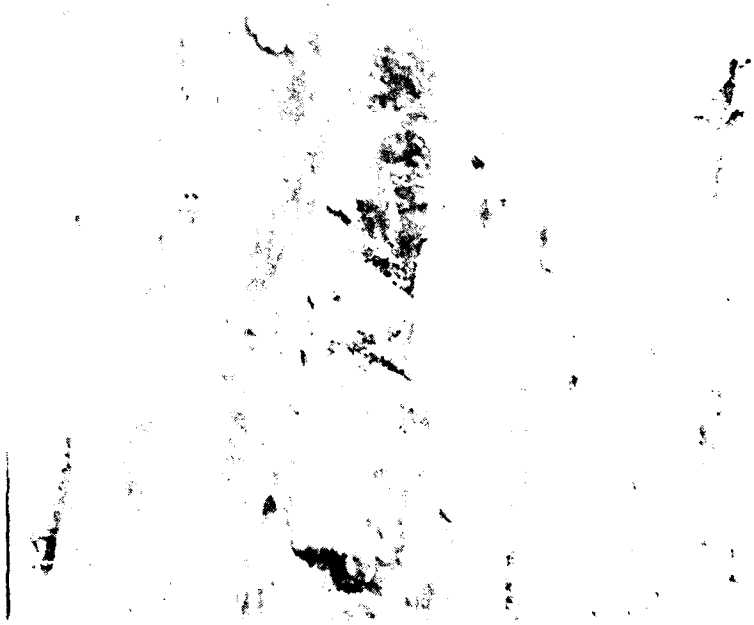

SEM No. 6738 75X

(c)

Figure 23. SEM micrographs, EDX spectra, and [illegible] of the corrosion-wear surface of the pin electrode from [illegible]; (a) low-magnification view of the pin wear surface; (b) EDX spectra [illegible]; (c) low-magnification view of the wear surface; (d) high-magnification view [illegible] wear-debris surface; (e) Mo X-ray map of (d); and (f) Cr X-[illegible] (d).

(d)

(f)

(e)

SEM No. 8085 30X

(a)

SEM No. 8089 30X

SEM No. 8086 250X

(c)

SEM No. 8090 250X

Figure 24. Typical low and high magnification SEM wear areas from Armco iron pin electrodes [illegible] wear area; (b) pin 88 wear area; (c) cor[illegible] (d) wear surface of pin 88 near the gouge[illegible]

(Fig. 24C) displayed significant cracking and peeling. As compared to test 87 pin, wear tracks on test 88 pin appeared very smooth except in a larger gouged-out area towards the lower right edge in Fig. 24b. Figure 24d shows a typical high-magnification view of the wear surface in the vicinity of the gouged-out area. Test 88 pin surface did not show any significant wear-corrosion debris. EDX spectra taken from typical areas of wear surfaces showed presnece of Fe, Cr, and Mo for test 87 surface and only Fe was detected on test 88 pin surface. No Na or Cl was detected in either case.

As observed above in the case of pin electrodes, the Armco iron disk electrodes showed corrosion-wear tracks with varying degree of smoothness. In general, disk electrode surfaces appeared less rough as compared to corresponding pin electrodes. At higher magnificaitons, damaged areas showed rough wear tracks with deep gouged-out areas in certain cases. Wear-corrosion debris was mostly granular in nature.

Typical SEM micrographs and EDX maps of Mo and Cr are presented in Fig. 25 (test 77). The wear pattern shown at low magnification (Fig. 25a) looked fairly uniform all over. Damaged areas showed deeper gouging of the surface at higher magnifications. Wear-corrosion debris was mostly granular and entrapped in gouged-out wear tracks (Fig. 25b). EDX analysis of wear debris showed presence of mainly Mo, Cr, and Fe with some Si. A small peak of Cl was also detected in EDX spectra from debris material after counting for longer periods. The source of the Si is not known. Figures 25c and d show Mo and Cr X-ray maps of the area in Fig. 25b. The Mo map in Fig. 25c does not show any significant difference in concentration of Mo in various areas shown in Fig. 25b. However, the Cr map (Fig. 25d) does show higher concentrations of Cr in the areas (Fig. 25b) where wear debris had accumulated.

4.6.2 52100 Steel Electrodes

Wear damage areas on pin and disk electrodes from tests 74, 75, 76, 83, and 84 were examined by analytical SEM techniques. Figure 26 shows typical low-magnification views of the wear surfaces of the pin electrodes (tests 74, 75, and 76). The wear surfaces of a pin experiencing a lighter load (16 lb) appeared relatively smoother (Fig. 26a) and displayed parallel wear tracks, and the wear area was located in the center of the pin. In test 75 pin (Fig. 26b) which experienced a heavy load (56 lb), the wear area was off-center, wear tracks were rougher and coarser, and they showed considerable wear debris

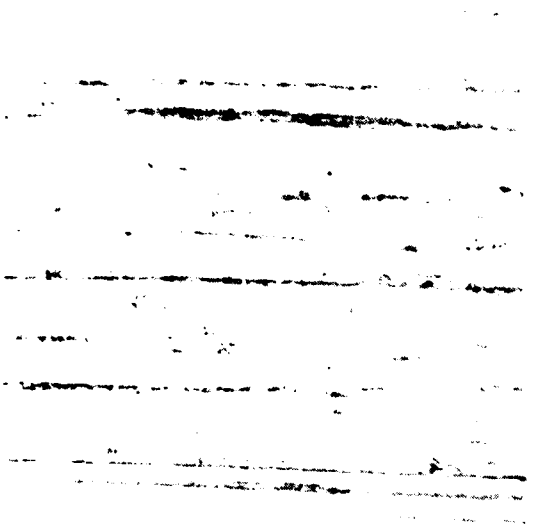

SEM No. 7159 25X

(a)

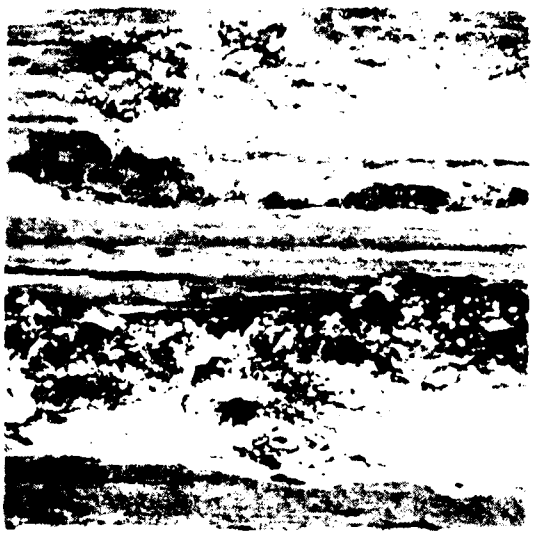

SEM No. [illegible] [illegible]X

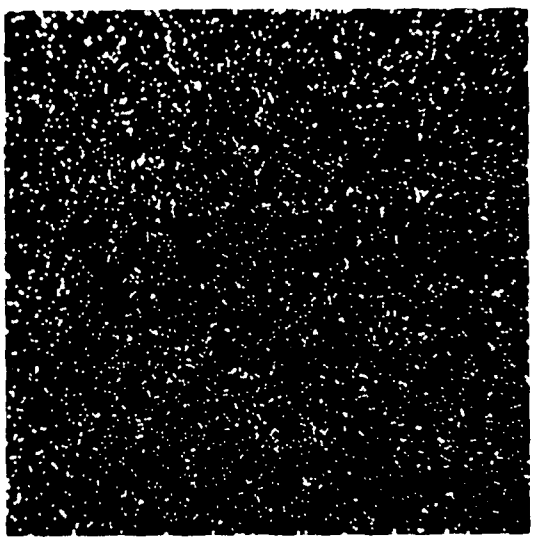

SEM No. 7161 150X

(c)

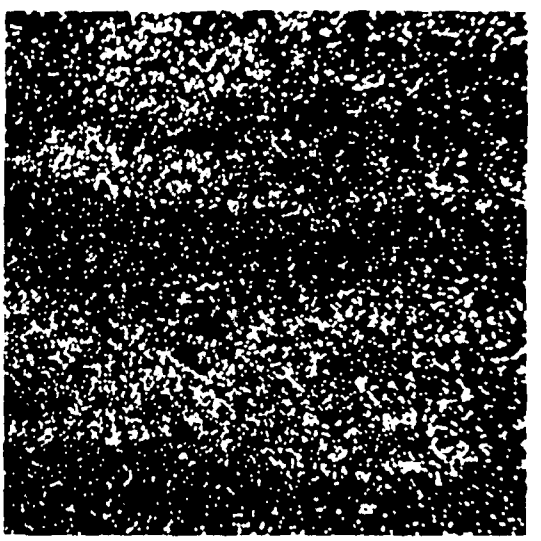

SEM No. 7162 [illegible]X

[illegible]. SEM micrographs and elomental X-ray maps [illegible] of Armco iron disk. (a) Low-magnification [illegible] wear debris and damage at higher magnification [illegible] X-ray map of (b).

SEM No. 7136 50X

(a)

SEM No. 7141 40X

(b)

SEM No. 7145 25X

(c)

Figure 24. SEM micrographs showing low-magnification views of the wear surfaces of 52100 steel pin electrodes from tests 74 to 76. (a) Test 74; (b) test 75; and (c) test 76.

accumulation. Also, outer edges of the wear circle were zagged. Test 76 pin wear surface (Fig. 26c) displayed parallel wear tracks which were between tests 74 and 75 pin surfaces in roughness, and displayed some accumulated debris although much les than from test 75 (Fig. 26b).

At higher magnifications, wear surfaces of all pin electrodes showed a granular wear debris, with areas showing thicker deposits of corrosion-wear debris appearing smooth and cracked. EDX analysis of corrosion-wear debris found on all the pin electrode wear surfaces showed presence of mainly Mo, Cr, and Fe with some Mn. No Na or Cl was detected in any of the three tests. Elemental X-ray maps generated from the wear debris of the above tests showed higher concentrations of both Mo and Cr in the areas where debris deposits were thicker. In general, concentration of Cr was somewhat higher than Mo. Figures 27a to c show a typical area of thick debris and corresponding Mo and Cr X-ray maps for the test 75 pin wear surface.

Wear tracks on disk electrodes from tests 74, 75, 76, 83, and 84 were examined in the present work. Wear tracks on the 52100 steel disk electrodes from tests 74 through 76 exhibited features that were quite dissimilar. In test 74 disk, the wear track appeared shiny as compared to the free surface that had a dull yellowish appearance. SEM examination showed the wear track to consist of mostly parallel lines around the circumference of the disk. Most wear damage was confined to the two strings of damage features which ran parallel to and just inside the outer edges of the wear track (Fig. 28a). Only at one location, larger damaged wear areas were found to occur across the wear track (Fig. 28a). Both smaller and bigger wear features shown in Fig. 28a showed a blocky wear damage containing some granular and fine wear debris in the center (Fig. 28b). Wear damage in the disk from test 76, in contrast to that of test 74, was spread across the width of the wear track in the form of long streaks (Fig. 28c). However, the appearance of the wear track at higher magnifications (Fig. 28d) was very similar to that for test 74 (Fig. 28b). Only one larger area showing significant wear damage was observed (Fig. 28c). EDX analysis from corrosion-wear debris on tests 74 and 76 disk electrodes showed higher concentrations of Mo and Cr in damaged areas. The wear track on test 76 disk was considerably wider than the tests 74 and 75 disk wear tracks.

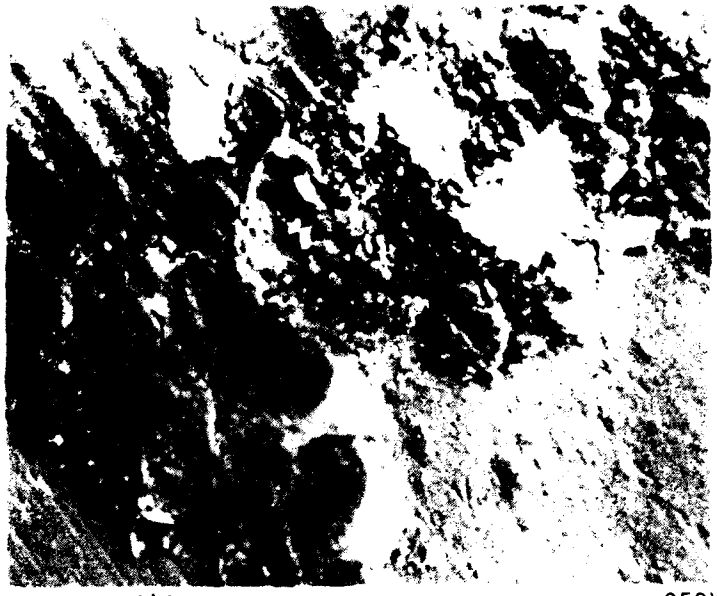

SEM No. 7141B 250X

(a)

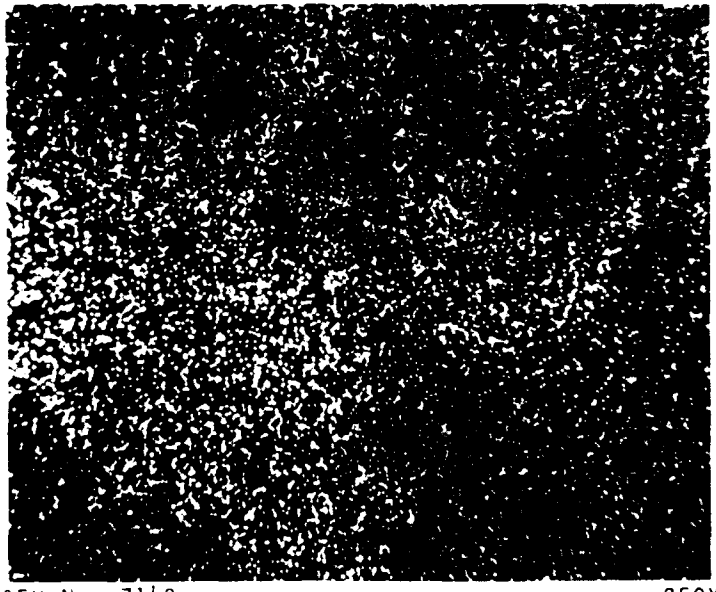

SEM No. 7142 250X

(b)

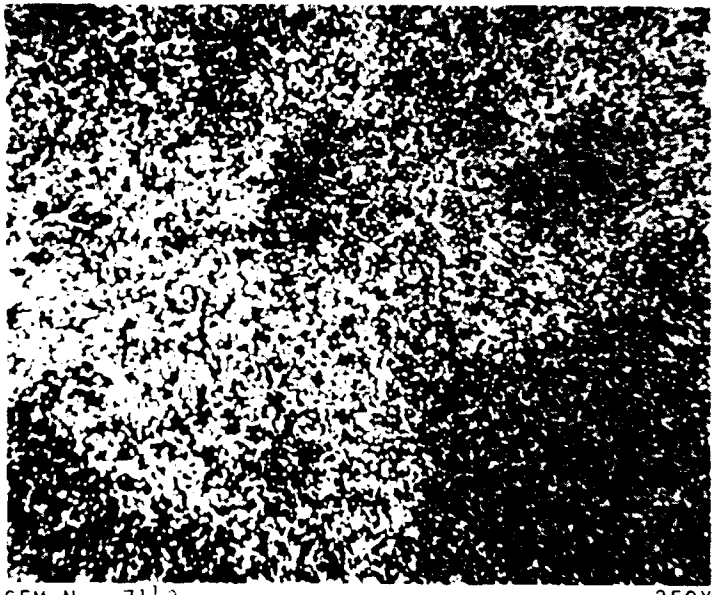

SEM No. 7143 250X

(c)

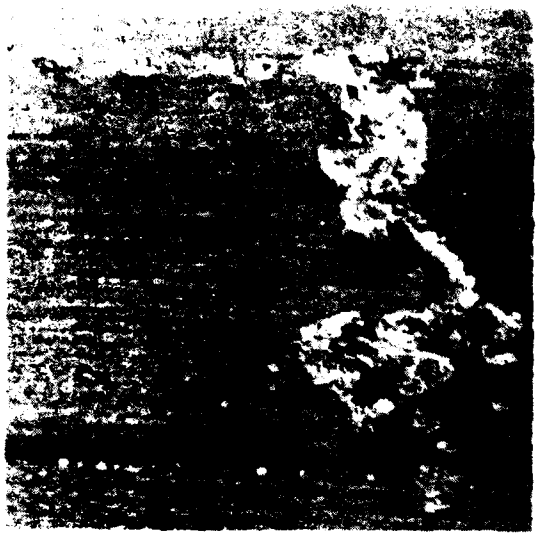

SEM No. 7151 30X

(a)

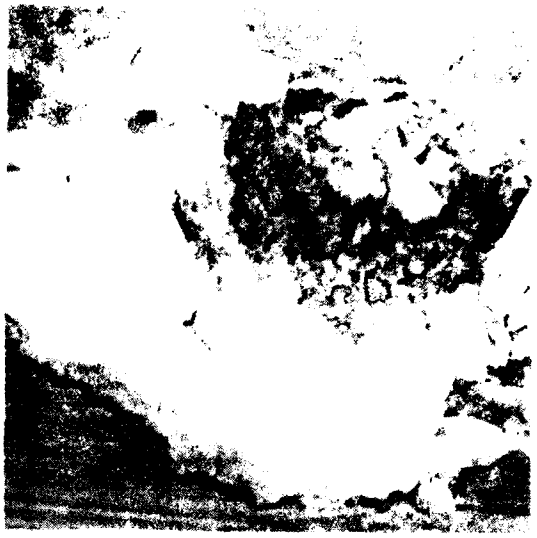

SEM No. 7152 350X

(b)

SEM No. 7157 30X

(c)

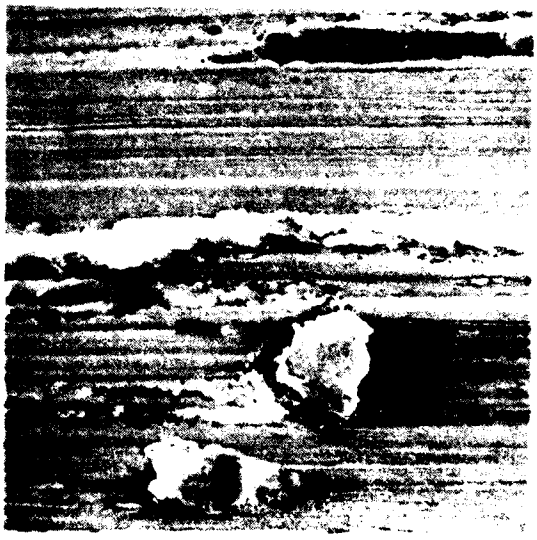

SEM No. 7158

(d)

Figure 24. SEM micrographs showing wear damage on the [illegible] from tests 74 and 76. (a) Test 74 wear track; (b) [illegible], both magnification; (c) test 76, wear track; and (d) [illegible] wear debris.

On test 75 disk electrode, most of the damage in the wear track was confined to one-half of the width (Fig. 29a) in the form of dark discontinuous bands arranged along parallel lines. Relative width of these wear damage bands increased successively from the outer edge of the wear track toward the center. High-magnification SEM examination showed that the wear features in test 75 disk were different from those observed in tests 74 and 76 disks. Dark bands consisted of a smooth-looking corrosion-wear product with some cracks running across the width of the band (Fig. 29b). The areas between the bands contained numerous smaller pits with irregular shapes. Elemental EDX X-ray maps showed a higher than average concentration of Mo and Cr in the damaged areas. Figures 29c and d show Mo and Cr X-ray maps of the area in Fig. 29b. Again, as was also observed for tests 74 to 76 pin wear surfaces, the accumulation of Cr in the wear debris appears to be larger than that of Mo as indicated by relative densities of the bright spots in Figs. 29c and d.

4.6.3 Metallurgical Analysis Summary

In general, for samples of Armco iron as well as 52100 steel, corrosion-wear tracks on the disks seem to have a rougher surface and more wear debris than the surrounding areas that are not in contact with the pins. It seems that the higher corrosive activity of the wear surface accelerates reaction that results in higher Cr and/or Mo concentrations in the damaged areas. Because of rotation, disk electrode areas are not in continuous rubbing contact whereas the pin is; consequently, the pin from a certain test shows more wear damage and Cr and/or Mo pickup than the corresponding disk.

Present results show that the size of the wear damage area, especially for the 52100 steel specimens, is determined by the combination of load and speed. In general, the wear pattern was less rough for 52100 steel than for Armco iron. Armco iron, being softer, showed much deeper wear tracks and coarser wear debris. For both materials, in tests where both $Na_2Cr_2O_7$ and Na_2MoO_4 were added, Cr concentration was always higher than Mo concentration in wear debris. No significant concentrations of Na or Cl were detected in any of the specimens examined. The lower detection limit of EDX for most elements is in the range of 0.1 to 1.0 wt%. Therefore, it is possible that Na and Cl buildup in wear-corrosion debris in the present experiments was probably below the detectability limit.

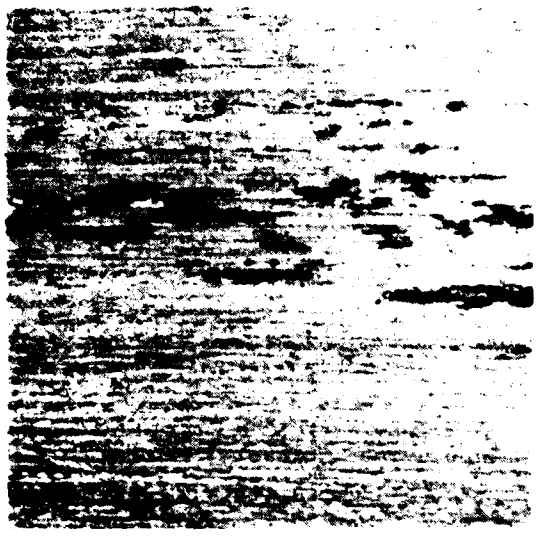

SEM No. 7153 25X

(a)

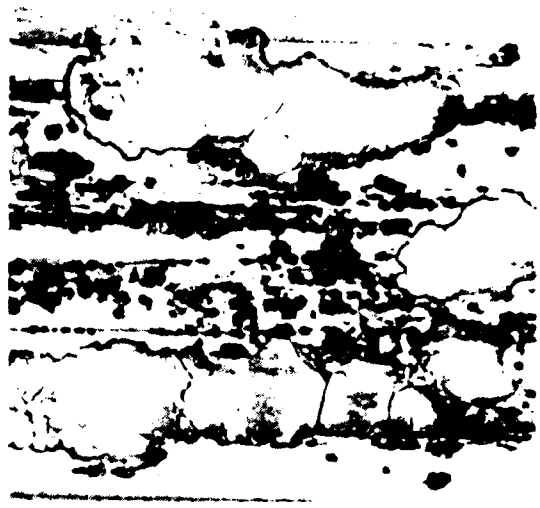

SEM No. 7154 250X

(b)

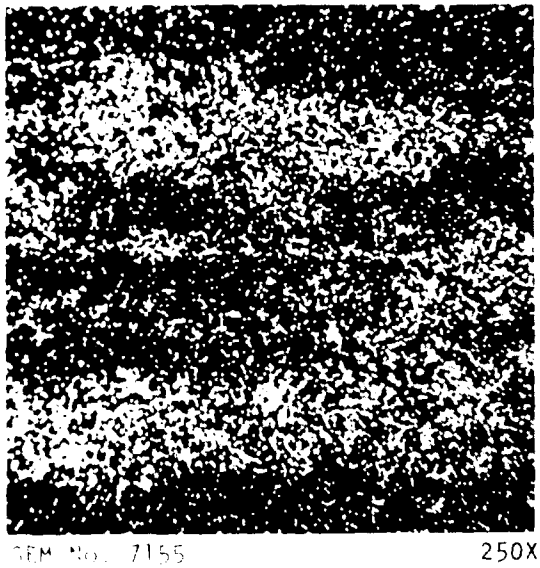

SEM No. 7155 250X

(c)

SEM No. 7156 250X

(d)

Figure 4. SEM micrographs of the wear track on the 52100 steel disk [illegible] and elemental EDX maps from damaged areas. (a) Wear track at [illegible]; (b) Detailed view of wear damage; (c) Mo X-ray [illegible] (d) Cr X-ray map of (b).

4.7 SURFACE ROUGHNESS MEASUREMENTS

The surface roughness of several disk electrodes was measured before and after the corrosion-wear test with a profilometer and a Proficorder. Table 17 lists the surface roughness data taken with the profilometer; all values given are the average values determined by root mean square. In general, the surface roughness of 52100 steel changed negligibly because of wear; and in some cases (test 76), the wear resulted in a "polishing effect" reducing the surface roughness. However, the anodic cell current was increased remarkably by wear compared to that of no-wear condition. It may be presumed that the contribution of surface roughness to the electrode polarization behavior may not be significant. Increase in the cell current may be due mainly to the disruption of the passive layer rather than due to the change in the surface roughness. Figure 30 presents the traces of the 52100 steel disk electrode free surface (no wear) and the wear track obtained by Proficorder in test 76. A few occasional valleys (corroded depressions) due to local corrosion spots appear in the wear track, and a large one is also shown.

The surface roughness of Armco iron was very sensitive to the wear condition. At a load level of 16 lb, increase in the rotational speed from 1 to 3 rpm changed the surface roughness from 110 to 170 μin. (tests 78 and 77). The traces of typical Proficorder measurements for Armco iron are presented in Fig. 31 for test 77.

The cell current change in anodic polarization did not show a corresponding effect of wear condition. In general, it seems that the cell current change by wear is more dependent on the disruption of passive layer than on the change in surface roughness. The surface roughness may affect the polarization behavior, but with negligible contribution.

TABLE 17. SURFACE ROUGHNESS MEASUREMENT OF ARMCO IRON AND 52100 STEEL DISK ELECTRODES UNDER VARIOUS WEAR CONDITIONS[a]

Test No.	Disk Material	Load, lb	Speed, rpm	Surface Roughness, μin.[b] Free Surface (No Wear)	Wear Track
74	52100 steel	16	3	18-20	22-24
75	52100 steel	56	3	23-28	23-28
76	52100 steel	56	10	30-35	22
77	Armco iron	16	3	8-9	170
78	Armco iron	16	1	7-8	110
79	Armco iron	5	3	10	60

[a]See Table A-2 of Appendix A for details.

[b]Bendix Profilometer Pilotor Model VEB.

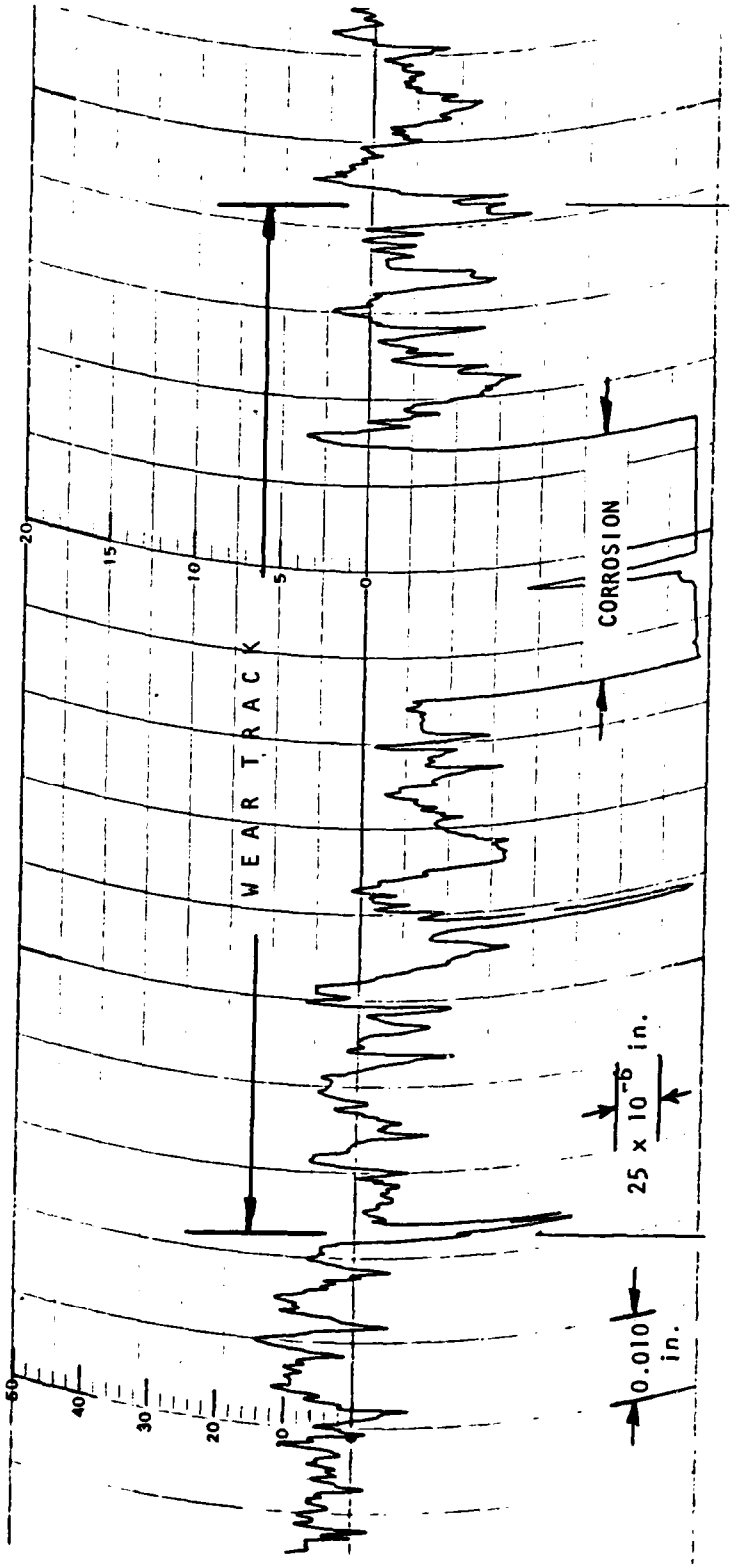

Figure 30. Surface profile of 52100 steel under wear condition of 56 lb at 10 rpm (test 76).

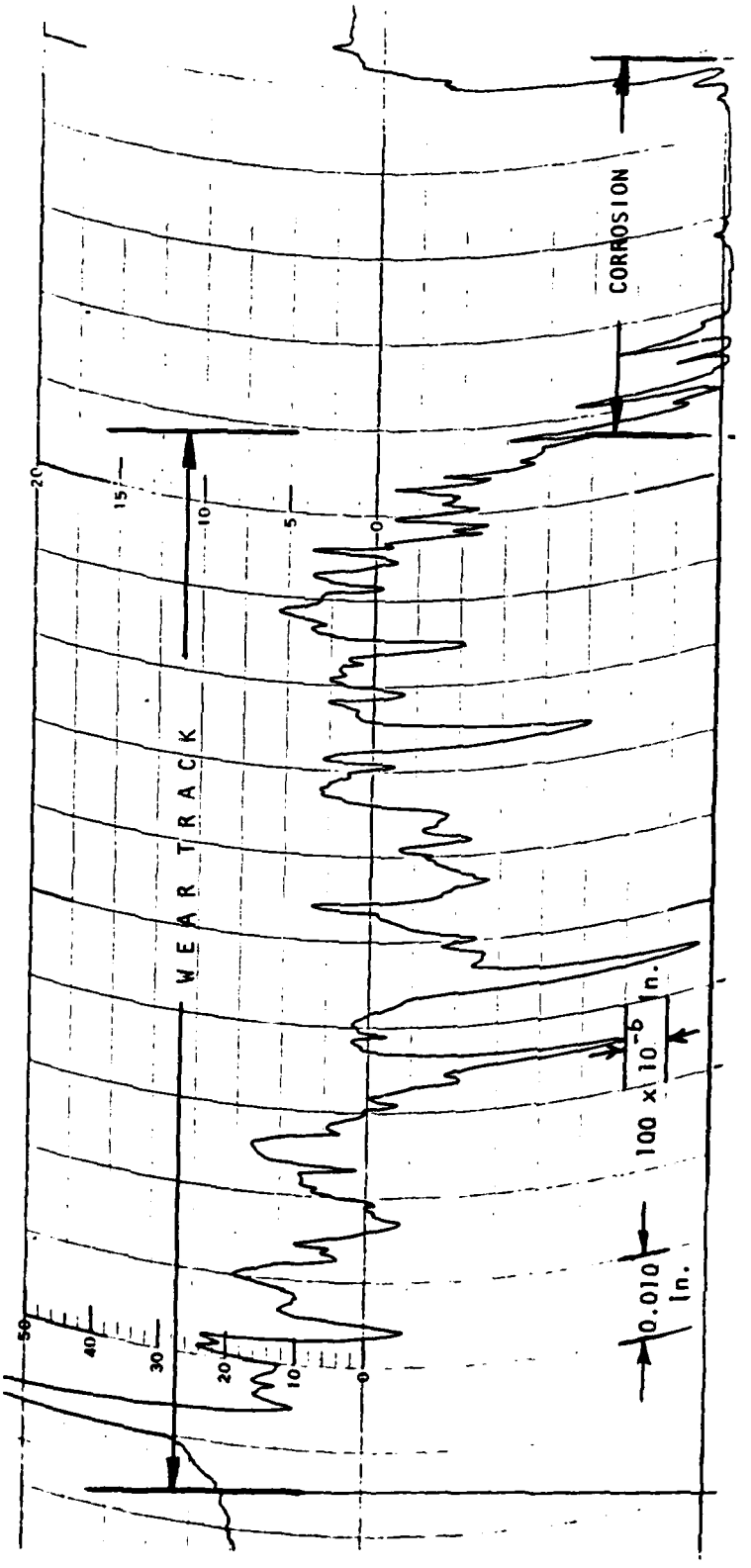

Figure 31. Surface profile of Armco iron under wear condition of 16 lb at 3 rpm (test 77).

5. CONCLUSIONS

The various studies performed in this program contributed significantly to the understanding of the corrosion-wear process occurring on load-bearing components in sea environment. The experimental results show that the IITRI "Dynamic Corrosion-Wear Cell" is a versatile tool capable of conducting a meaningful and reproducible study of simultaneous occurrence of corrosion and wear in any electrolytic system. It has been proved that both potentiostatic and potentiodynamic polarization techniques are pertinent methods to study the effect of wear on the corrosion process in corrosion-wear systems.

It is clearly understood that the effect of continuous wear condition on the electrode polarization behavior is very significant for materials with naturally occurring passive film or materials which form a passive film in the electrolyte, but almost negligible for the materials in a non-protective film forming electrolyte. Armco iron, M2 steel, and 52100 steel were effectively passivated in NaCl solutions (10-100 ppm) with proper amount of $Na_2Cr_2O_7$ and Na_2MoO_4, although they corroded even in 1 ppm NaCl solution without corrosion inhibitors. Control of pH of NaCl solution with NaOH, H_3BO_3, and $Na_2B_4O_7$ was not effective in the passivation of those materials.

Generation of active metal surface on passivated materials under wear shifted the open-circuit potential in the active direction. The initial disruption of passive film resulted in a large shift of the open-circuit potential. The additional structural deformation by the subsequent increment of load or speed shifted the potential further in the active direction, but not significantly. Similar effect of wear on the corrosion current was observed on the materials with passive film: a large increase by disruption of passive film and a small increase by structural deformation. The surface roughness measurement also revealed that increase in the cell current was mainly due to disruption of passive film rather than due to change in the surface roughness.

Wear controls the anodic polarization process significantly, but not the cathodic polarization process. It has been shown that corrosion-wear mechanisms can be studied by observing cell current behavior at controlled overpotential

5. CONCLUSIONS

The various studies performed in this program contributed significantly to the understanding of the corrosion-wear process occurring on load-bearing components in sea environment. The experimental results show that the IITRI "Dynamic Corrosion-Wear Cell" is a versatile tool capable of conducting a meaningful and reproducible study of simultaneous occurrence of corrosion and wear in any electrolytic system. It has been proved that both potentiostatic and potentiodynamic polarization techniques are pertinent methods to study the effect of wear on the corrosion process in corrosion-wear systems.

It is clearly understood that the effect of continuous wear condition on the electrode polarization behavior is very significant for materials with naturally occurring passive film or materials which form a passive film in the electrolyte, but almost negligible for the materials in a non-protective film forming electrolyte. Armco iron, M2 steel, and 52100 steel were effectively passivated in NaCl solutions (10-100 ppm) with proper amount of $Na_2Cr_2O_7$ and Na_2MoO_4, although they corroded even in 1 ppm NaCl solution without corrosion inhibitors. Control of pH of NaCl solution with NaOH, H_3BO_3, and $Na_2B_4O_7$ was not effective in the passivation of those materials.

Generation of active metal surface on passivated materials under wear shifted the open-circuit potential in the active direction. The initial disruption of passive film resulted in a large shift of the open-circuit potential. The additional structural deformation by the subsequent increment of load or speed shifted the potential further in the active direction, but not significantly. Similar effect of wear on the corrosion current was observed on the materials with passive film: a large increase by disruption of passive film and a small increase by structural deformation. The surface roughness measurement also revealed that increase in the cell current was mainly due to disruption of passive film rather than due to change in the surface roughness.

Wear controls the anodic polarization process significantly, but not the cathodic polarization process. It has been shown that corrosion-wear mechanisms can be studied by observing cell current behavior at controlled overpotential

with alternative application of wear and no-wear condition. A kinetic mechanism occurring in corrosion-wear systems was suggested.

A series of 12 tests based on a statistical design was performed to study quantitatively the effect of different variables on the corrosion-wear process. Several variables have statistically significant (90% confidence level) effect on electrochemical corrosion and wear, as shown below:

Parameter	Variables
Open-circuit potential	Electrolyte, environment, material
Corrosion rate	Environment, material, preexposure time
Weight change of disk electrode	Material (speed, environment)
Weight change of pin electrode	Load, speed (electrolyte)

( ) = Not significant at 90% confidence level.

Analytical scanning electron microscopy is very helpful in the understanding of corrosion-wear surface morphology. Typically, a soft material, such as Armco iron, undergoes extensive metal removal arising from local cold welding, and hard materials, such as M2 and 52100 steels, show relatively smooth wear surface with occasional granular wear debris. Elemental maps of the materials passivated in NaCl solutions with $Na_2Cr_2O_7$ and Na_2MoO_4 show that deposition of Cr and Mo is higher in the activated wear debris than at general wear scar areas.

6. FUTURE PLANS

The test results obtained from the present study (September 1979-September 1981) provided much useful information necessary for a basic understanding of corrosion-wear processes. Future study should advance our understanding to the control of corrosion-wear. Since it was shown that disruption of the passive film was mainly responsible for a large increase in the corrosion rate under wear condition, development of stable passive film may be an effective way to minimize the effect of wear on corrosion. It may be accomplished by proper selection of corrosion inhibitor and lubricant; the former will assist the formation of a more chemically stable passive film, and the latter will assist the mechanical stability of the passive film by reducing the friction and the resulting wear.

In this regard, it is suggested that the future program be pursued to further develop our understanding of conjoint corrosion-wear mechanisms in the presence of sea water and lubricant. There may be restrictions on applications of lubricants in corrosion-wear systems where electrochemical measurements are to be made. Introduction of oscillatory motion would be desirable to simulate more closely the actual service condition. The future study may be divided into two phases as follows:

Phase I: A Four-Task Study (9/81-12/82)

Tasks 1 and 2: Design modification of existing equipment and fabrication of modified apparatus to introduce oscillatory motion and torque measurement. Preliminary evaluation with several tests.

Tasks 3 and 4: Trial with new inhibitors, and evaluation of a set of 12 tests using Plackett-Burman design. The test parameters will involve different steels, types of motions, loads, inhibitors, NaCl concentration, and aeration.

The results will be analyzed using polarization measurements, immersion test, torque data, gravimetric analysis, and SEM evaluation, and the statistical analysis of the data will determine the significance of the major effects and the likely mechanisms governing the observations.

Phase II: Lubricant Evaluation Study (12/82-9/83)

Based on Phase I results and a literature study, selected levels of test parameters will be further evaluated in the presence of lubricants incorporated in the electrolyte. A statistical test design will be used to develop the significance of the major effects and to elucidate the mechanisms underlying the observations.

APPENDIX A

CONDITIONS FOR ELECTROCHEMICAL AND IMMERSION TESTS

TABLE A-1. IMMERSION TEST CONDITIONS AND WEIGHT CHANGE DATA

Test No.	Material	Sample Surface Area, cm^2	Distilled Water (Electrolyte) NaCl, ppm	Chemical Additives, ppm	pH Start	pH End	Exposure Time, hr	Weight Loss, mg	Corrosion Rate, $\mu g/cm^2/hr$ (mpy)	Remarks
A1	M2 steel	7.92	5000	None	5.9	-	145	171	149 (65)	a
A2	52100 steel	7.92	5000	None	5.9	-	145	284	248 (108)	a
A3	304 SS	7.92	5000	None	5.9	-	145	-	-	a, e
A4	M2 steel	7.92	1000	None	5.5	-	239	255	135 (59)	a
A5	52100 steel	7.92	1000	None	5.5	-	239	502	266 (116)	a
A6	M2 steel	7.92	10	None	5.8	6.8	120	12.7	13.3 (5.7)	a, not agitated
A7	M2 steel	7.92	1	None	5.8	6.6	120	-	-	a, d, not agitated
A8	M2 steel	7.92	10	NaOH (-)	10	7.5	120	15.5	16.3 (7.1)	a, not agitated
A9	M2 steel	7.92	10	H_3BO_3 (-)	5.5	6.3	120	16.1	16.9 (7.4)	a, not agitated
A10	M2 steel	7.92	10	$Na_2Cr_2O_7$ (48)	5.2	5.8	120	0.6	0.6 (0.3)	a
A11	M2 steel	7.92	10	$Na_2B_4O_7$ (48)	8.7	7.7	120	6.1	6.4 (2.8)	a
A12	1020 steel	8.33	10	$Na_2Cr_2O_7$ (48)	5.1	6.0	120	1.8	1.8 (0.8)	a, not agitated
A13	1020 steel	8.28	10	$Na_2B_4O_7$ (48)	9.0	7.7	120	11.3	11.3 (4.9)	a, not agitated
A14	M2 steel	7.92	1000	$Na_2Cr_2O_7$ (25)	5.4	6.0	120	0.5	-	a, e
A15	M2 steel	7.92	1000	$Na_2Cr_2O_7$ (50)	5.0	5.7	120	0.7	-	a, e
A16	M2 steel	7.92	1000	$Na_2Cr_2O_7$ (100)	4.9	5.4	120	0.5	-	a, e
A17	M2 steel	7.92	1000	$Na_2Cr_2O_7$ (250)	4.7	5.1	120	0.5	-	a, e
A18	Armco iron	7.92	10	None	7.13	7.42	120	88.9	93.5 (41)	a
A19	Armco iron	7.92	10	$Na_2Cr_2O_7$ (100)	5.35	5.72	120	-	-	a, c
A20	Armco iron	7.92	10	$Na_2Cr_2O_7$ (100) Na_2MoO_4 (100)	5.24	5.60	120	-	-	a, c
A21	Armco iron	7.92	1000	$Na_2Cr_2O_7$ (1000) Na_2MoO_4 (1000)	5.28	5.53	120	2.7	2.8 (1.2)	a

TABLE A-1 (cont.)

Test No.	Material	Sample Surface Area, cm^2	Distilled Water (Electrolyte) NaCl, ppm	Chemical Additives, ppm	pH Start	pH End	Exposure Time, hr	Weight Loss, mg	Corrosion Rate, $\mu g/cm^2/hr$ (mpy)	Remarks
A22	Armco iron	7.92	1000	$Na_2Cr_2O_7$ (500) Na_2MoO_4 (500)	5.27	5.67	120	3.2	3.4 (1.5)	a, not agitated
A23	Armco iron	8.27	1000	$Na_2Cr_2O_7$ (500)	4.39	5.06	240	9.8	4.9 (2.2)	a
A24	Armco iron	8.27	1000	$Na_2Cr_2O_7$ (500)	4.39	5.06	240	7.3	3.6 (1.6)	a
A25	Armco iron	8.27	1000	$Na_2Cr_2O_7$ (500)	4.39	5.06	240	7.3	3.6 (1.6)	a
A26	Armco iron	8.27	100	$Na_2Cr_2O_7$ (500)	4.37	4.51	240	-	-	a, d
A27	Armco iron	8.27	100	$Na_2Cr_2O_7$ (500)	4.37	4.51	240	-	-	a, d
A28	Armco iron	8.27	100	$Na_2Cr_2O_7$ (500)	4.37	4.51	240	-	-	a, d
A29	Armco iron	8.27	10	$Na_2Cr_2O_7$ (500)	4.35	4.36	240	-	-	a, c
A30	Armco iron	8.27	10	$Na_2Cr_2O_7$ (500)	4.35	4.36	240	-	-	a, c
A31	Armco iron	8.27	10	$Na_2Cr_2O_7$ (500)	4.35	4.36	240	-	-	a, c
A32	Armco iron	21.87	10	None		6.5	260	263.7	46.4 (20.3)	a
A33	Armco iron	21.87	10	None		6.5	260	262.7	46.2 (20.2)	a
A34	Armco iron	21.87	10	None		6.5	260	253.2	44.5 (19.5)	a
A35	52100 steel	8.23	10	None		6.5	260	121.5	56.7 (24.9)	a
A36	52100 steel	8.23	10	None		6.5	260	117.0	54.6 (23.9)	a
A37	52100 steel	8.23	10	None		6.5	260	120.3	56.2 (24.6)	a
A38	Armco iron	21.87	10	$Na_2Cr_2O_7$ (500) Na_2MoO_4 (500)		5.26	260	-	-	a, c
A39	Armco iron	21.87	10	$Na_2Cr_2O_7$ (500) Na_2MoO_4 (500)		5.26	260	-	-	a, c
A40	Armco iron	21.87	10	$Na_2Cr_2O_7$ (500) Na_2MoO_4 (500)		5.26	260	-	-	a, c
A41	52100 steel	8.23	10	$Na_2Cr_2O_7$ (500) Na_2MoO_4 (500)		5.26	260	-	-	a, c

TABLE A-1 (cont.)

Test No.	Material	Sample Surface Area, cm^2	Distilled Water (Electrolyte) NaCl, ppm	Distilled Water (Electrolyte) Chemical Additives, ppm	pH Start	pH End	Exposure Time, hr	Weight Loss, mg	Corrosion Rate, $\mu g/cm^2/hr$ (mpy)	Remarks
A42	52100 steel	8.23	10	$Na_2Cr_2O_7$ (500) Na_2MoO_4 (500)		5.26	260	-	-	a, c
A43	52100 steel	8.23	10	$Na_2Cr_2O_7$ (500) Na_2MoO_4 (500)		5.26	260	-	-	a, c
A44	Armco iron	21.87	10	None		7.49	260	71.5	12.5 (5.51)	b
A45	Armco iron	21.87	10	None		7.49	260	89.4	15.7 (6.89)	b
A46	Armco iron	21.87	10	None		7.49	260	79.4	13.9 (6.12)	b
A47	52100 steel	8.23	10	None		7.49	260	36.3	16.9 (7.43)	b
A48	52100 steel	8.23	10	None		7.49	260	34.5	16.1 (7.06)	b
A49	52100 steel	8.23	10	None		7.49	260	41.2	19.2 (8.43)	b
A50	Armco iron	21.87	10	$Na_2Cr_2O_7$ (500) Na_2MoO_4 (500)		5.13	260	-	-	b, c
A51	Armco iron	21.87	10	$Na_2Cr_2O_7$ (500) Na_2MoO_4 (500)		5.13	260	-	-	b, c
A52	Armco iron	21.87	10	$Na_2Cr_2O_7$ (500) Na_2MoO_4 (500)		5.13	260	-	-	b, c
A53	52100 steel	8.23	10	$Na_2Cr_2O_7$ (500) Na_2MoO_4 (500)		5.13	260	-	-	b, c
A54	52100 steel	8.23	10	$Na_2Cr_2O_7$ (500) Na_2MoO_4 (500)		5.13	260	-	-	b, c
A55	52100 steel	8.23	10	$Na_2Cr_2O_7$ (500) Na_2MoO_4 (500)		5.13	260	-	-	b, c

[a]Aerated environment. [b]Deaerated environment. [c]Complete passivation.

[d]Virtually complete passivation with a few corrosion spots. No determinable weight change.

[e]Virtually complete passivation with crevice-type corrosion along the nylon string. No determinable weight change.

TABLE A-2. ELECTROCHEMICAL CORROSION-WEAR TEST CONDITIONS AND CORROSION CURRENT DENSITIES UNDER WEAR AND NO-WEAR CONDITIONS

Test No.	Electrode Material	Electrolyte[a] NaCl, ppm	Electrolyte[a] Chemical Additives (ppm)	Load, lb[b]	Speed, rpm[c]	Time, hr	Corrosion Current Density, mA/cm^2 (mpy) No-Wear Condition	Corrosion Current Density, mA/cm^2 (mpy) Wear Condition
19	304 SS	35,000	None	-	-	-	2×10^{-4} (0.09)	--
20	304 SS	35,000	None	3.7	1	-	--	2×10^{-3} (0.9)
24	52100 steel	35,000	None	-	-	-	8.6×10^{-2} (39.4)	--
25	M2 steel	35,000	None	-	-	-	1.0×10^{-1} (45.8)	--
26	52100 steel	35,000	None	-	-	-	9.7×10^{-2} (42.1)	--
27	M2 steel	35,000	None	3.7	3	-	--	7.6×10^{-2} (34.8)
28	52100 steel	35,000	None	56	3	-	--	7.5×10^{-2} (34.3)
30	M2 steel	35,000	None	56	10	-	--	1.5×10^{-1} (48.1)
31	M2 steel	5000	None	56	10	-	--	7.7×10^{-2} (35.3)
33	M2 steel	None	None	56	10	-	1.0×10^{-3} (0.45)	1.5×10^{-3} (0.68)
34	52100 steel	5000	None	56	10	-	7×10^{-2} (32.0)	4.5×10^{-2} (20.6)
36	M2 steel	None	None	-	0	-	4.7×10^{-4} (0.21)	--
38	M2 steel	5000	None	3.7	1	18	1.1×10^{-1} (50.4)	1.7×10^{-1} (77.9)
39	304 SS	5000	None	56	10	-	4.5×10^{-5} (0.02)	3.0×10^{-3} (1.37)
40	52100 steel	5000	None	3.7	1	20	1.0×10^{-1} (50)	1.2×10^{-1} (55)
41	52100 steel	None	None	56	10	-	7.8×10^{-4} (0.35)	1.2×10^{-2} (5.49)
47	M2 steel	5000	NaOH	56	10	23	9.0×10^{-2} (41)	9.2×10^{-2} (42)
49	52100 steel	5000	NaOH	56	10	-	9.8×10^{-2} (45)	1.6×10^{-1} (73)
50	M2 steel	1000	None	56	1	40	7.0×10^{-2} (32)	6.4×10^{-2} (39)
52	M2 steel	1000	NaOH	56	1	4	9.8×10^{-2} (45)	1.0×10^{-1} (46)
53	M2 steel	None	NaOH (4)	56	1	4.5	1.7×10^{-5} (<0.01)	1.3×10^{-3} (0.6)
56	M2 steel	10	$Na_2Cr_2O_7$ (2.8)	-	-	-	5.8×10^{-4} (0.26)	--

AD-A113 813 IIT RESEARCH INST CHICAGO IL F/6 13/9
WEAR AND CORROSION OF COMPONENTS UNDER STRESS AND SUBJECTED TO --ETC(U)
FEB 82 K Y KIM, S BHATTACHARYYA N62269-79-C-0702
UNCLASSIFIED IITRI-M06060-8 NADC-79137-60 NL

2 OF 2
AD A
113 813

END
DATE FILMED
05-82
DTIC

TABLE A-2 (cont.)

Test No.	Electrode Material	Electrolyte[a] NaCl, ppm	Chemical Additives (ppm)	Load, lb[b]	Speed, rpm[c]	Time, hr	Corrosion Current Density, mA/cm^2 (mpy) No-Wear Condition	Wear Condition
58	M2 steel	10	$Na_2Cr_2O_7$ (5.7)	56	1	10.	5.0×10^{-4} (0.23)	9.0×10^{-3} (4.1)
59	M2 steel	1000	$Na_2Cr_2O_7$ (5.7)	56	1	8	4.2×10^{-2} (19)	8.2×10^{-2} (36)
61	M2 steel	1000	$Na_2Cr_2O_7$ (100)	56	1	8	2.0×10^{-3} (0.9)	2.6×10^{-3} (1.2)
63	M2 steel	1000	$Na_2Cr_2O_7$ (100)	56	1	3.75	4.5×10^{-4} (0.20)	2.0×10^{-3} (0.91)
64	M2 steel	1000	$Na_2Cr_2O_7$ (100)	16	1	9.5	5.0×10^{-4} (0.23)	2.5×10^{-3} (1.14)
65	Armco iron	10	None	16	1	4	2×10^{-3} (0.91)	2×10^{-2} (9.16)
66	Armco iron	10	$Na_2Cr_2O_7$ (100) Na_2MoO_4 (100)	16	1	4	1×10^{-4} (0.04)	2.5×10^{-3} (1.14)
67	Armco iron	1000	$Na_2Cr_2O_7$ (100) Na_2MoO_4 (100)	16	1	-	2.0×10^{-3} (0.91)	1.1×10^{-2} (5.04)
68	Armco iron	1000	$Na_2Cr_2O_7$ (500) Na_2MoO_4 (500)	16	1	8	7.8×10^{-4} (0.36)	1.4×10^{-3} (0.64)
69	Armco iron	100	$Na_2Cr_2O_7$ (500)	16	1	27	1×10^{-3} (0.45)	1.4×10^{-3} (0.64)
70	Armco iron	100	$Na_2Cr_2O_7$ (500) Na_2MoO_4 (500)	16	1	4	--	1.5×10^{-3} (0.68)
71[d]	Armco iron	100	$Na_2Cr_2O_7$ (500) Na_2MoO_4 (500)	-	-	-	--	--
72	Armco iron	10	$Na_2Cr_2O_7$ (500) Na_2MoO_4 (500)	16	1	24.5	2.5×10^{-4} (0.11)	8×10^{-4} (0.36)
73	Armco iron	10	$Na_2Cr_2O_7$ (500) Na_2MoO_4 (500)	16	1	31.5	3×10^{-4} (0.13)	3×10^{-3} (1.37)
74	52100 steel	100	$Na_2Cr_2O_7$ (500) Na_2MoO_4 (500)	16	3	6	8.0×10^{-4} (0.36)	1.6×10^{-3} (0.73)
75	52100 steel	100	$Na_2Cr_2O_7$ (500) Na_2MoO_4 (500)	56	3	5.25	2.6×10^{-4} (0.12)	3.0×10^{-3} (1.37)

TABLE A-2 (cont.)

Test No.	Electrode Material	Electrolyte[a] NaCl, ppm	Electrolyte[a] Chemical Additives (ppm)	Load, lb[b]	Speed, rpm[c]	Time, hr	Corrosion Current Density, mA/cm^2 (mpy) No-Wear Condition	Corrosion Current Density, mA/cm^2 (mpy) Wear Condition
76	52100 steel	100	$Na_2Cr_2O_7$ (500) Na_2MoO_4 (500)	56	10	5.25	2.2×10^{-4} (0.10)	6.0×10^{-3} (2.75)
77	Armco iron	100	$Na_2Cr_2O_7$ (500) Na_2MoO_4 (500)	16	3	8.5	1.0×10^{-3} (0.46)	1.6×10^{-3} (0.73)
78	Armco iron	100	Na_2MoO_4 (500)	16	1	3.25	8.0×10^{-4} (0.36)	5.0×10^{-3} (2.29)
79	Armco iron	100	$Na_2Cr_2O_7$ (500) Na_2MoO_4 (500)	5	3	9.5	6.0×10^{-4} (0.27)	1.8×10^{-3} (0.82)
80	52100 steel	10	None	56	10	6	7.0×10^{-4} (0.32)	4.5×10^{-3} (2.06)
81	52100 steel	10	$Na_2Cr_2O_7$ (500) Na_2MoO_4 (500)	16	1	7.75	7.0×10^{-4} (0.32)	3.8×10^{-3} (1.74)
82	52100 steel	10	$Na_2Cr_2O_7$ (500) Na_2MoO_4 (500)	56	1	9.5	7.0×10^{-4} (0.32)	4.0×10^{-3} (1.83)
83	52100 steel	10	None	56	10	6	2.7×10^{-3} (1.23)	1.0×10^{-3} (0.46)
84	52100 steel	10	$Na_2Cr_2O_7$ (500) Na_2MoO_4 (500)	16	10	7.5	6.0×10^{-4} (0.27)	1.5×10^{-3} (0.68)
85	Armco iron	10	$Na_2Cr_2O_7$ (500) Na_2MoO_4 (500)	56	10	6	4.0×10^{-5} (0.02)	1.4×10^{-2} (6.41)
86	Armco iron	10	None	16	10	6.75	2.5×10^{-3} (1.14)	6.0×10^{-3} (2.75)
87	Armco iron	10	$Na_2Cr_2O_7$ (500) Na_2MoO_4 (500)	16	10	6.5	7.0×10^{-4} (0.32)	6.4×10^{-3} (2.93)
88	Armco iron	10	None	56	1	6.5	1.5×10^{-3} (0.68)	4.0×10^{-4} (0.18)
89	Armco iron	10	$Na_2Cr_2O_7$ (500) Na_2MoO_4 (500)	56	1	6.5	6.0×10^{-4} (0.27)	2.0×10^{-3} (0.91)
90	Armco iron	10	None	16	1	7.75	1.3×10^{-3} (0.59)	7.0×10^{-3} (3.21)
91	52100 steel	10	None	16	1	6.67	2.7×10^{-3} (1.24)	3×10^{-3} (1.37)

[a]Distilled water

[b]1 lb = 0.454 kg

[c]1 rpm = $\pi/30$ rad/s

[d]Potentiodynamic test

TABLE A-3. STATISTICAL DESIGN OF TESTS FOR ELECTROCHEMICAL EVALUATION UNDER CORROSION-WEAR CONDITIONS

Trial	Mean	X1	X2	X3	X4	X5	X6	X7	X8	X9	X10	X11	$\bar{Y}$
1	+	+	+	-	+	+	+	-	-	-	+	-	
2	+	+	-	+	+	+	-	-	-	+	-	+	
3	+	-	+	+	+	-	-	-	+	-	+	+	
4	+	+	+	+	-	-	-	+	-	+	+	-	
5	+	+	+	-	-	-	+	-	+	+	-	+	
6	+	+	-	-	-	+	-	+	+	-	+	+	
7	+	-	-	-	+	-	+	+	-	+	+	+	
8	+	-	-	+	-	+	+	-	+	+	+	-	
9	+	-	+	-	+	+	-	+	+	+	-	-	
10	+	+	-	+	+	-	+	+	+	-	-	-	
11	+	-	+	+	-	+	+	+	-	-	-	+	
12	+	-	-	-	-	-	-	-	-	-	-	-	

Index of Variables

	(+)	(-)
X1	52100	Armco Fe
X2	Passive	Active
X3	56 lb	16 lb
X4	10 rpm	1 rpm
X5	No air	Air
X6	4 hr	1 hr

$\bar{Y}$ { Open circuit potential
I_{corr}
Weight change - disk electrode
- pin electrode

APPENDIX B

POLARIZATION CURVES OBTAINED FROM 12-RUN PLACKETT-BURMAN STATISTICAL TESTS (Tests 81, 82, 84, 86-88, 90, and 91)

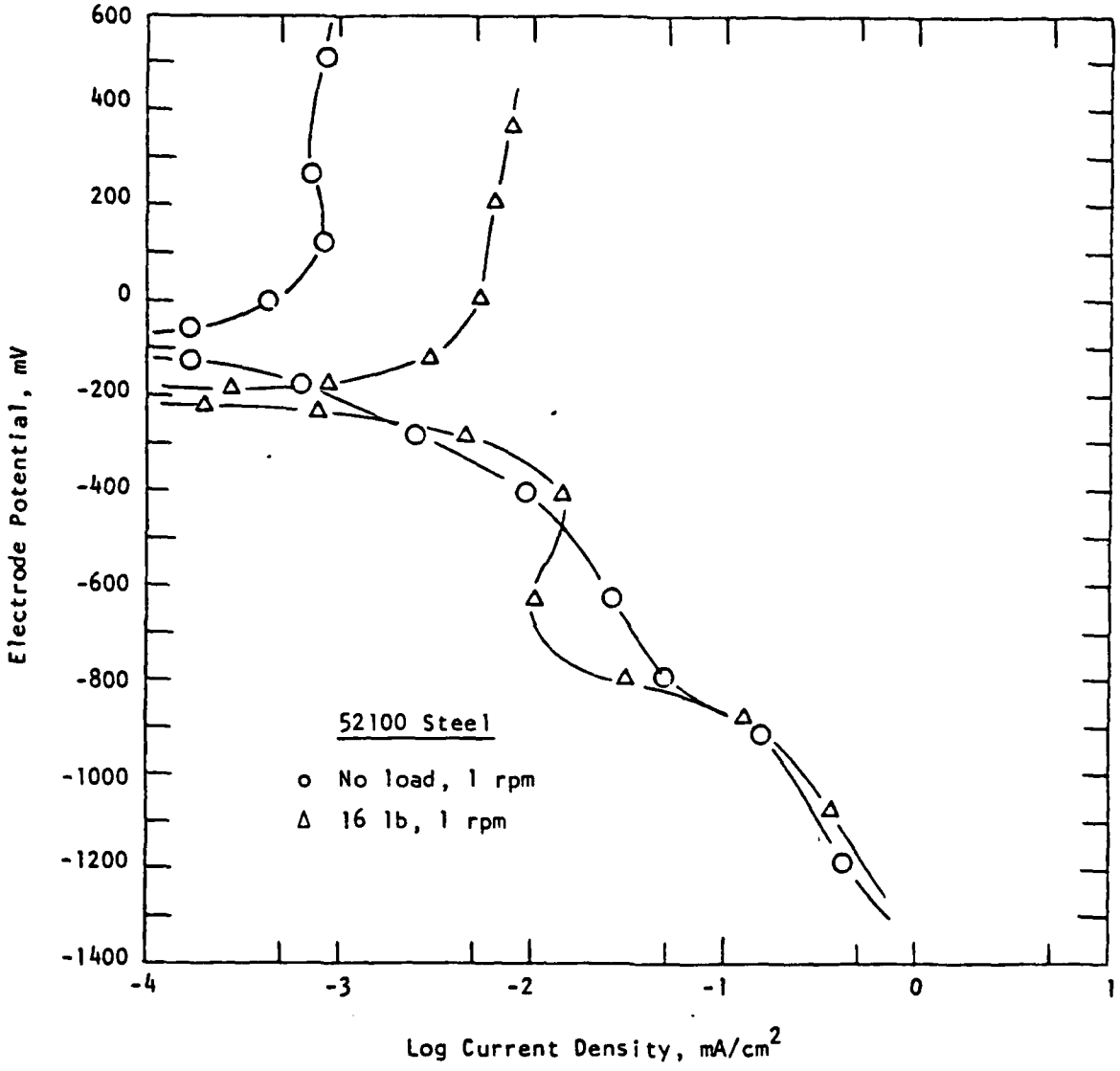

Figure 3-1. Polarization behavior of 52100 steel in 10 ppm NaCl solution with 500 ppm $Na_2Cr_2O_7$ and 500 ppm Na_2MoO_4 in ambient air (test 81).

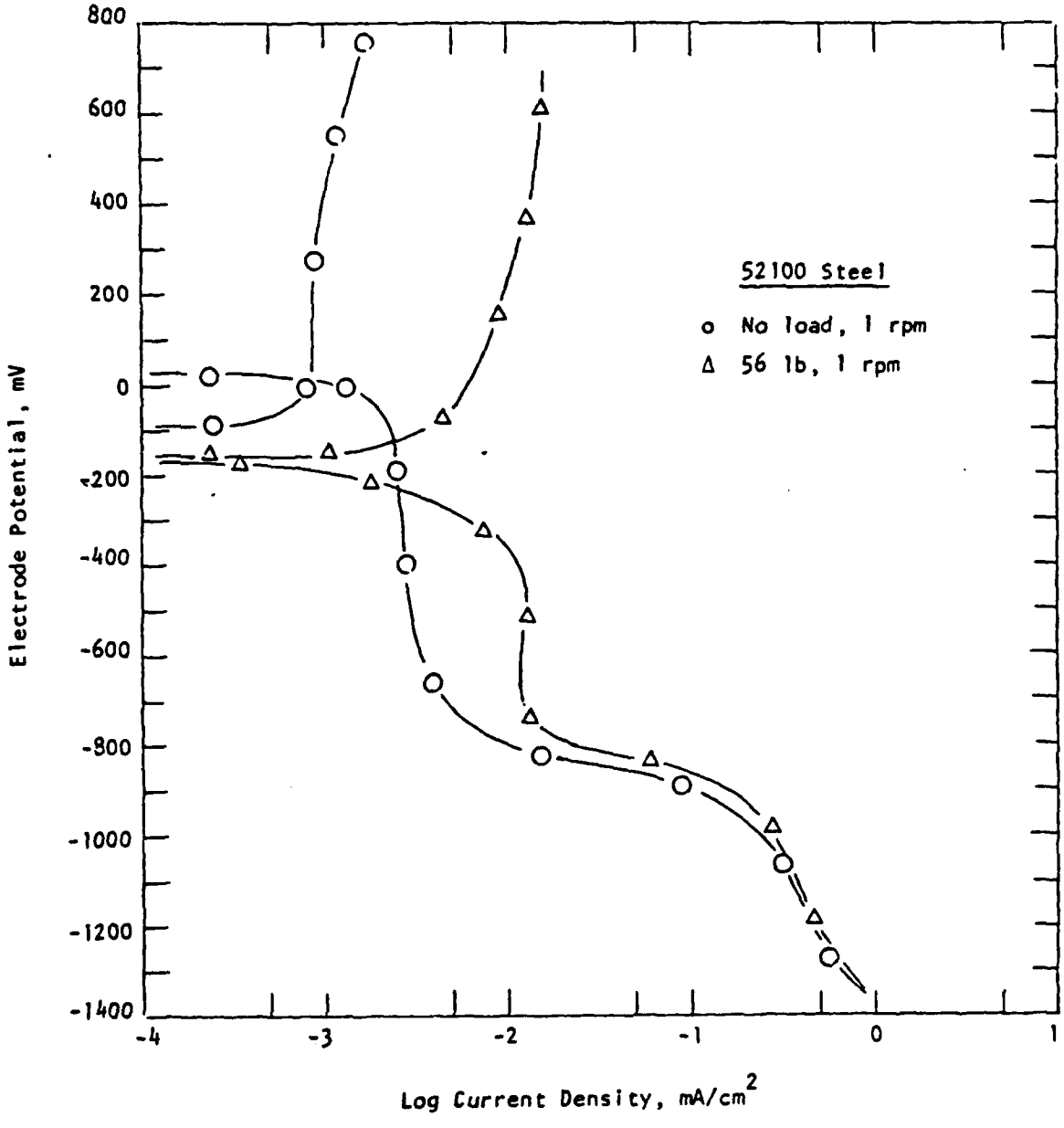

Figure B-2. Polarization behavior of 52100 steel in 10 ppm NaCl solution with 500 ppm $Na_2Cr_2O_7$ and 500 ppm Na_2MoO_4 in ambient air (test 82).

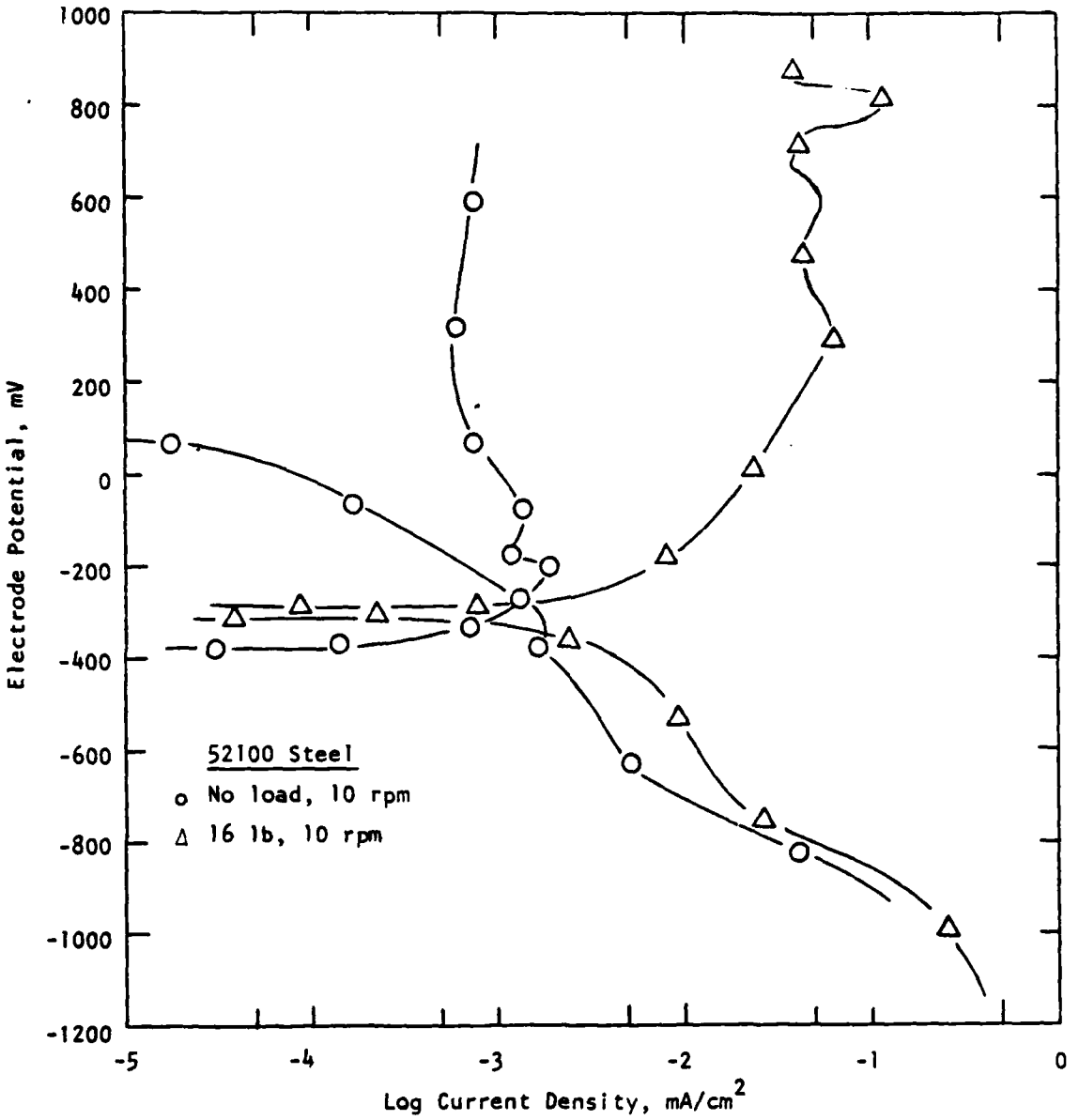

Figure B-3. Polarization behavior of 52100 steel in 10 ppm NaCl solution with 500 ppm $Na_2Cr_2O_7$ and 500 ppm Na_2MoO_4 in deaerated condition (test 84).

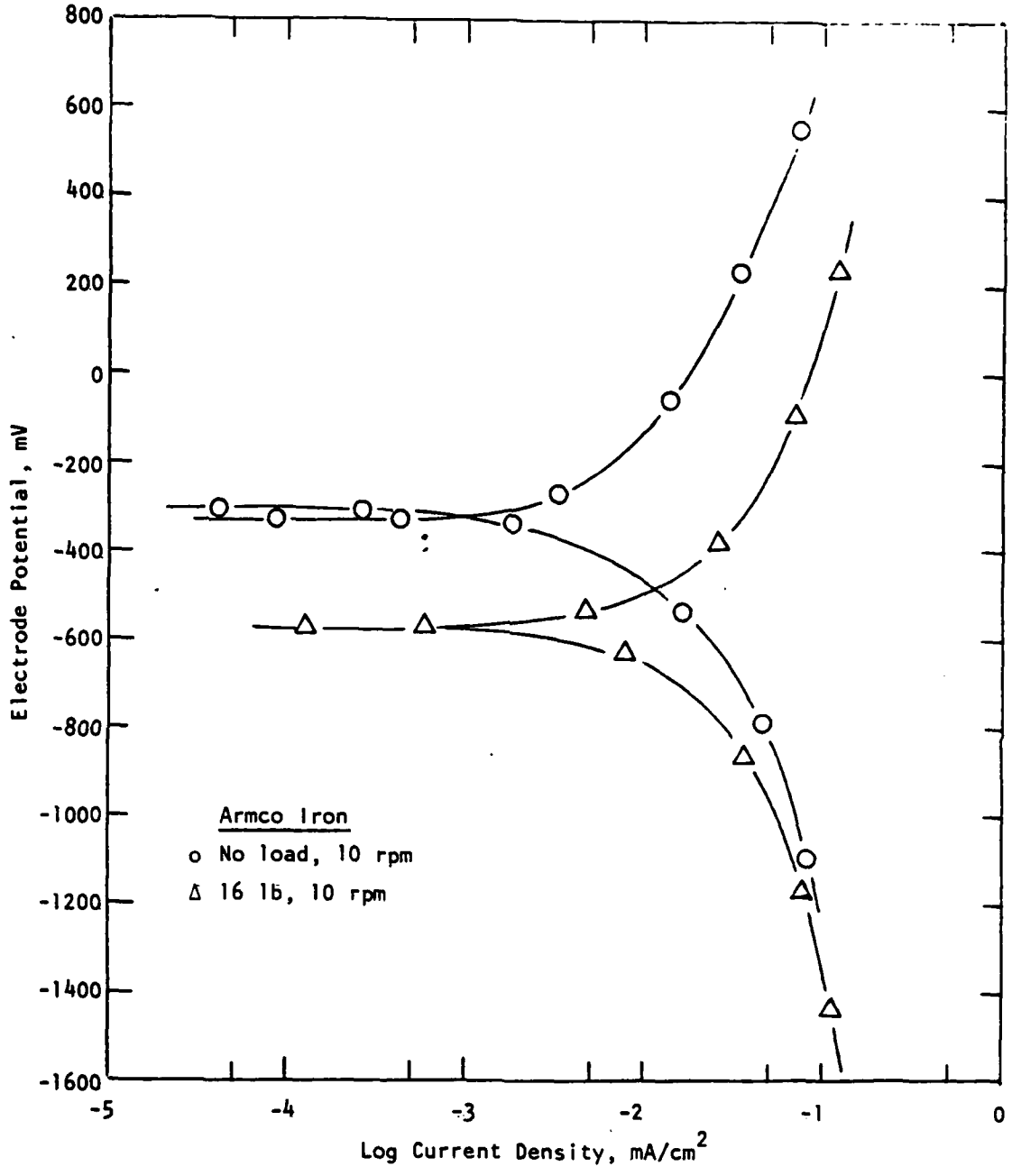

Figure B-4. Polarization behavior of Armco iron in 10 ppm NaCl solution in ambient air (test 86).

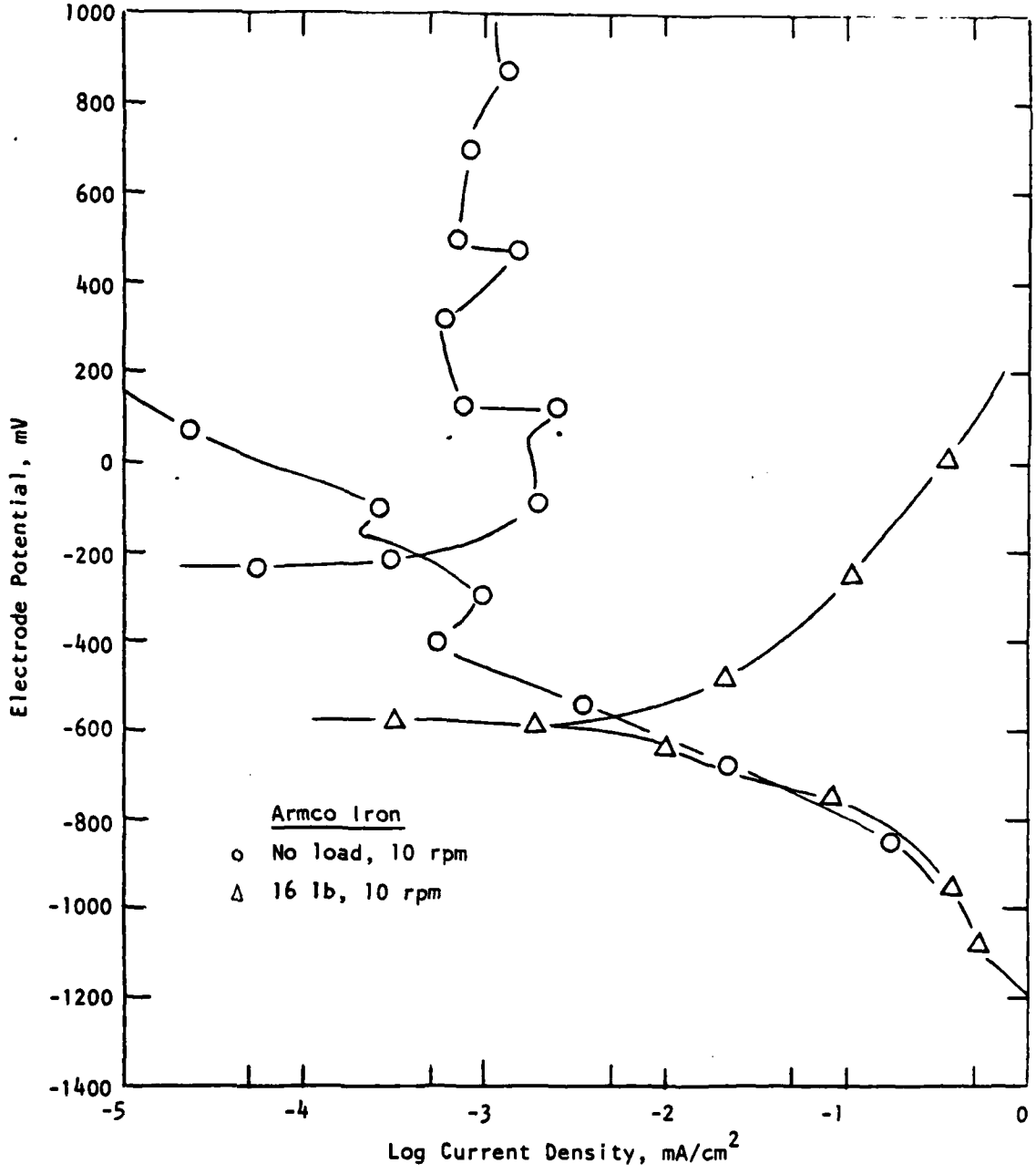

Figure B-5. Polarization behavior of Armco iron in 10 ppm NaCl solution with 500 ppm $Na_2Cr_2O_7$ and 500 ppm Na_2MoO_4 in deaerated condition (test 87).

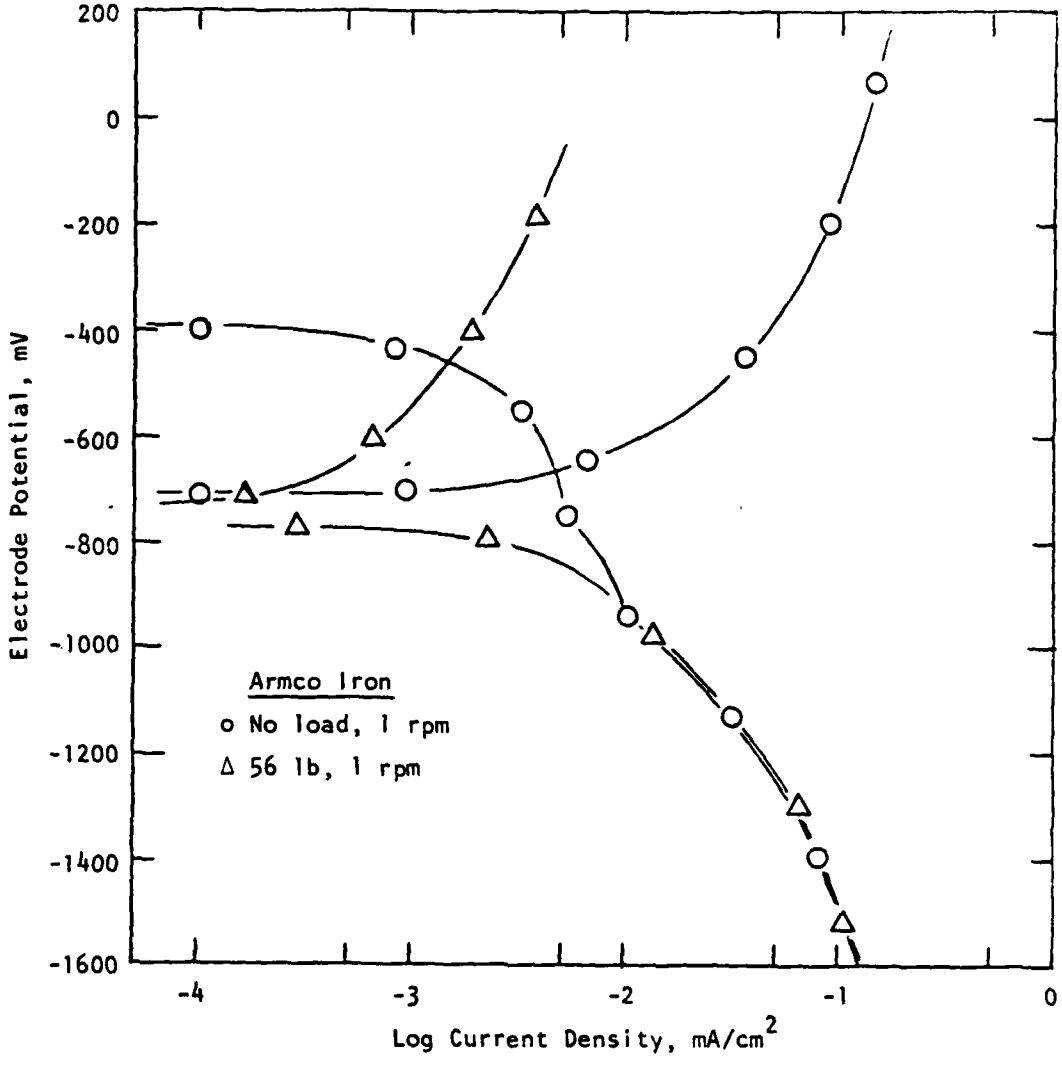

Figure B-6. Polarization behavior of Armco iron in 10 ppm NaCl solution in deaerated condition (test 88).

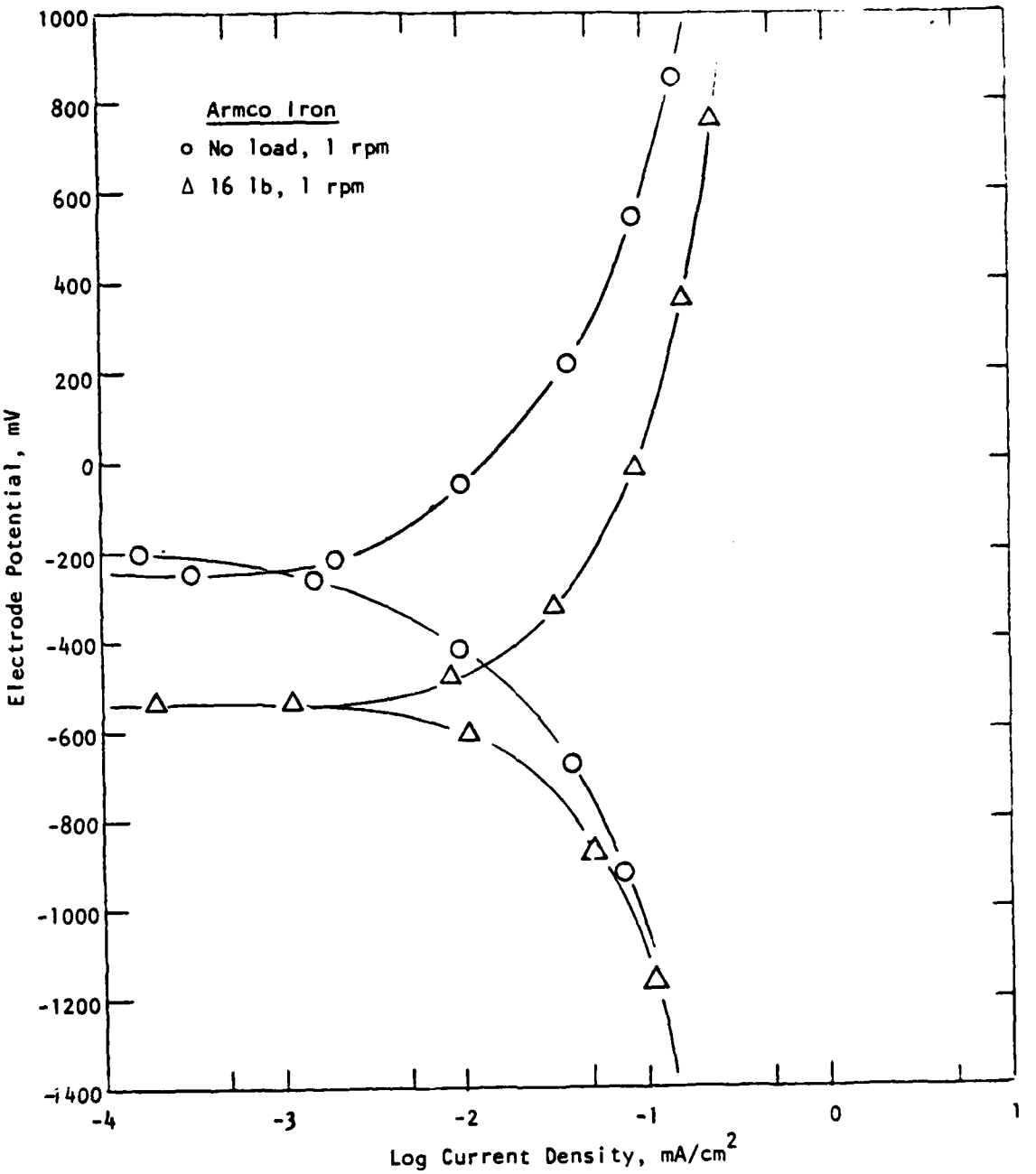

Figure B-7. Polarization behavior of Armco iron in 10 ppm NaCl solution in ambient air (test 90).

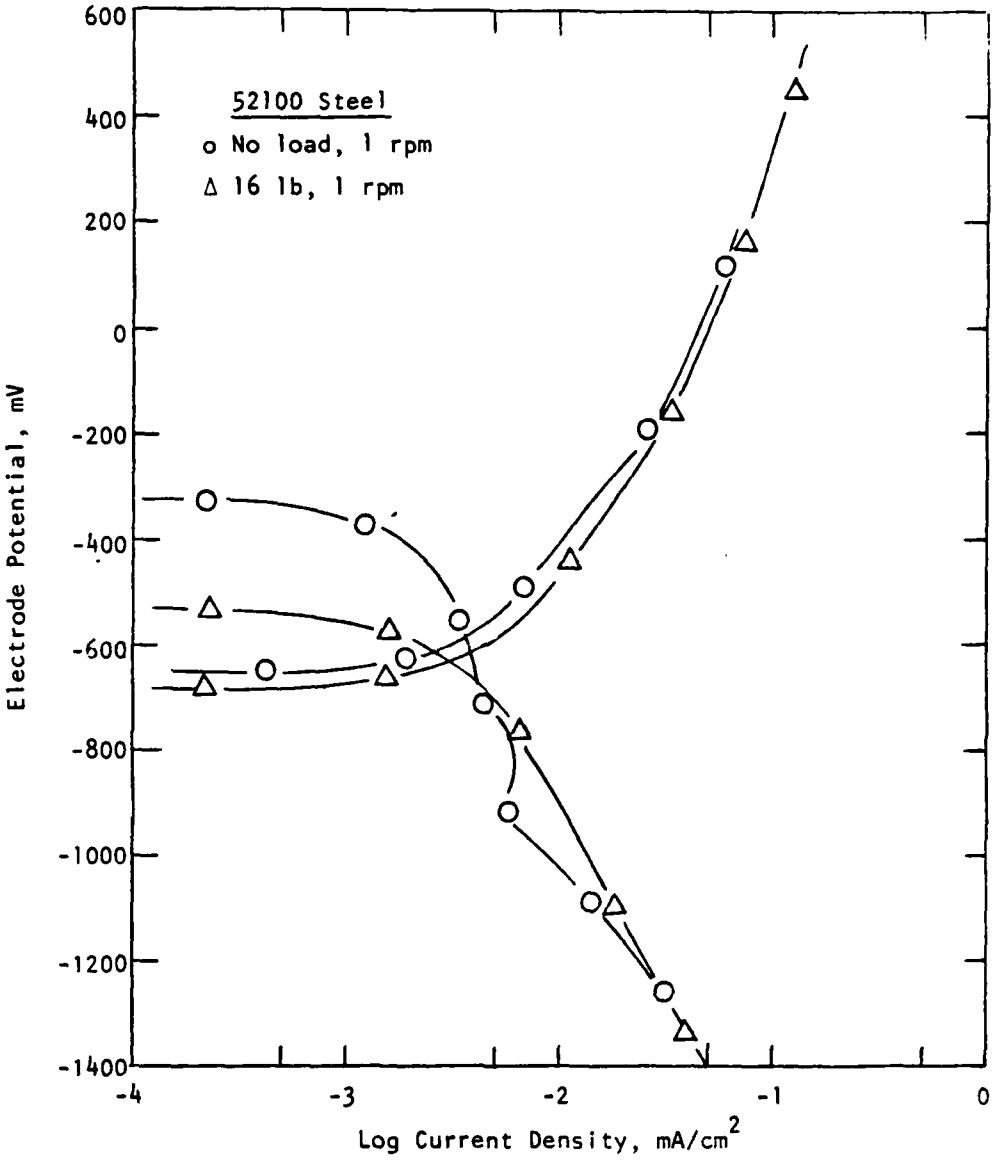

Figure B-8. Polarization behavior of 52100 steel in 10 ppm NaCl solution in deaerated condition (test 91).

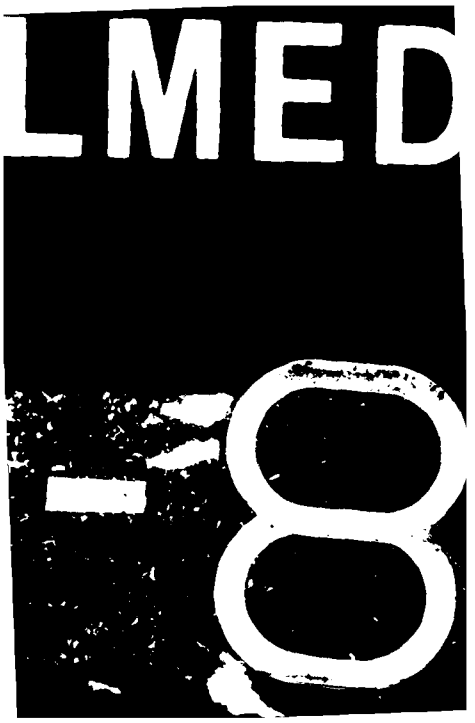
LMED
8